Modeling of Tailings Flow Following a Dam Breach Using Smoothed Particles Hydrodynamics

Poulad Daneshvar

A Thesis

in

The Department

of

Building, Civil and Environmental Engineering

Presented in Partial Fulfillment of the Requirements

for the Degree of Master of Applied Science (Civil Engineering) at

Concordia University

Montreal, Quebec, Canada

March 2010

Your file Votre référence
ISBN: 978-0-494-67122-1
Our file Notre référence
ISBN: 978-0-494-67122-1

Abstract

Modeling of Tailings Flow Following a Dam Breach Using Smoothed Particles Hydrodynamics

Poulad Daneshvar

Choosing impoundments as the method of tailings disposal for mining processes necessitates the construction of tailings dams. As various types of chemicals remaining from the mining processes are retained in the pond behind a tailings dam, a dam failure may result in environmental damages in addition to threatening lives. Therefore, the distribution and distance to which tailings would travel in the case of a dam failure is important to determine the amount of potential damage.

The aim of this research was to study the feasibility of modeling tailings following a dam breach based on the available data in the literature and reach the same distribution and travelling distance of the tailings as in the physical incidents.

The numerical tool chosen for this research would simulate tailings as a Non-Newtonian fluid using a Smoothed Particle Hydrodynamics (SPH) method. To calibrate the simulation tool a series of flume tests on two different tailings pastes from two different operation stages of Bulyanhulu gold mine (Tanzania) was modeled. The flume was created in the simulation tool and more than 30 simulations were run to calibrate the simulation tool. Through these tests the effects of changes in the values assigned to parameters related to tailings and their environment on the model were studied.

Practical application of the model was performed by using a digital elevation model (DEM) of the areas of two reported tailings dam failures in the simulation tool and repeatedly running tests with changes in the values for the terrain and tailings parameters to compare the results with the literature reported distribution of tailings outflow.

Acknowledgements

No research endeavor is ever carried out in solitude. I owe my deep gratitude to a great number of people. I would like to thank my supervisor, Dr. A. M. Zsaki, who provided invaluable academic support, and played a key role in guiding my research.

I would also like to thank my parents, Masoud and Forough, and my brother Hirad, who followed my progress with worried eyes.

Special thanks to my parents-in-law, Dariush and Nayereh, who inspired me with their concern and warmth.

My gratitude also goes to the kind staff at Concordia University who helped me throughout the research process.

Performing this research would not have been possible for me if it were not for Nassim. Nassim, you were the one I came to, whenever I was worried, frustrated or hopeless. You tolerated me when I was not myself and made me go forward. I dedicate this thesis to you, although it is not even comparable to the wings you have given me.

Table of Contents

List of Figures.....x

List of Tables.....xiii

List of Symbols.....xiv

Chapter One: Introduction.....1

1.1 Introduction.....2

1.2 Objectives.....4

Chapter Two: Production, Impoundments and Physical Properties of Tailings.....6

2.1 Introduction.....7

2.2 Production of Tailings.....7

2.3 Fate of Tailings.....15

2.4 Impoundments of Slurry Tailings.....20

2.5 Surface Impoundments.....21

2.5.1 Upstream Method.....23

2.5.2 Downstream Method.....25

2.5.3 Centerline Method.....27

2.6 Physical Properties of Tailings.....28

2.6.1 Coal.....29

2.6.2 Oil Sands.....29

2.6.3 Gold and Silver.....30

2.7 Tailings as Non-Newtonian Fluids.....33

2.7.1 Newtonian Fluids.....33

2.7.2 Non-Newtonian Fluids.....35

Chapter Three: The Smoothed Particle Hydrodynamics Method.....46

3.1 Introduction.....47

3.2 Governing Equations.....52

3.2.1 Momentum Conservation Equation.....52

3.2.2 Density and Continuity Equation.....53

3.2.3 Particle Motion.....54

3.3 Constitutive Models Implementation.....55

3.3.1 Pressure Evaluation and Equation of State.....55

3.3.2 Boundary Conditions.....57

3.3.3 Kernel Corrections for Density Reinitialization.....58

3.3.3.1 The Zero Order.....58

3.3.4 Time Stepping.....59

3.3.5 Time Step Control.....59

3.4 Algorithm for the Two Dimensional SPH Free Surface Flow.....60

Chapter Four: Numerical Simulation of Tailings Flow.....62

4.1 Introduction.....63

4.2 RealFlow.....63

4.2.1 Density.....64

4.2.2 Internal Pressure.....64

4.2.3 External Pressure.....64

4.2.4 Viscosity.....64

4.2.5 Surface Tension.....65

Chapter Five: Model Calibration....67

5.1 Variables in Calibration Tests....68

5.1.1 Density....68

5.1.2 Resolution....69

5.1.3 Viscosity....69

5.1.4 External Pressure....70

5.1.5 Friction....70

5.1.6 Roughness....70

5.2 Calibration Tests....71

5.3 Flume Test Results....82

5.3.1 Tests with Randomly Chosen Values....82

5.3.2 Test with Changes in a Single Variable....94

5.3.3 Monte Carlo Simulations....101

Chapter Six: Modeling Case Studies of Tailings Dam Failure....106

6.1 Tapo Canyon Tailings Dam....107

6.2 Merriespruit Tailings Dam....110

6.3 Considerations in Model Implementation....112

6.3.1 The Terrain....112

6.3.2 Tailing Properties....113

6.4 Model Creation....115

6.4.1 Tapo Canyon Tailings Dam Failure....115

6.4.2 Merriespruit Tailings Dam Failure....117

6.5 Results and Discussion....119

6.5.1 Tapo Canyon Tailings Dam Failure....120

6.5.2 Merriespruit Tailings Dam Failure.....124

Chapter Seven: Conclusion and Recommendations.....135

7.1 Conclusion.....136

7.2 Recommendations.....137

References.....139

Appendix.....147

List of Figures

Figure 1. Water retaining dam for tailings storage, after Vick (1983).....22

Figure 2. Upstream method of tailings embankments raising, after Vick (1983).....25

Figure 3. Downstream method of raising tailings embankments, after Vick (1983)....26

Figure 4. Centerline method of raising tailings embankments, after Vick (1983).....27

Figure 5. Velocity profile for Non-Newtonian flow between parallel plates, after Graebel (2001).....34

Figure 6. The relationship between viscosity and shear stress for mayonnaise, after Barnes (1999).....38

Figure 7. The relationship between viscosity and shear stress for toothpaste, after Barnes (1999).....38

Figure 8. The relationship between yield stress and pulp density for gold paste tailings, after Henriquez (2008).....40

Figure 9. Uniform Bingham flow after Rodriguez-Paz and Bonet (2003).....50

Figure 10. Sample scene from RealFlow 4.....66

Figure 11. The side view of the flume used in the tests.....72

Figure 12. The diagram representing Monte Carlo simulation.....81

Figure 13. Diagrams of distance and velocity versus time for Test A.....84

Figure 14. Diagrams of distance and velocity versus time for Test B.....86

Figure 15. Diagrams of distance and velocity versus time for Test C.....89

Figure 16. Diagrams of distance and velocity versus time for Test D.....90

Figure 17. Diagrams of distance and velocity versus time for Test E.....91

Figure 18. Diagrams of distance and velocity versus time for Test F.....92

Figure 19. The run out distance and angle of repose versus density for the tests with variable density (Test 1).....96

Figure 20. Angle of repose and run out distance versus viscosity for the tests with variable viscosity (Test 2).....98

Figure 21. Angle of repose and run out distance versus friction and roughness for the tests with variable friction and roughness (Test 3).....100

Figure 22. Angle of repose versus run out distance for each test performed using Monte Carlo simulations.....102

Figure 23. Diagram demonstrating the frequency of the obtained values for angle of repose and the mean value.....102

Figure 24. Diagram demonstrating the frequency of the obtained values for run out distance and the mean value.....103

Figure 25. View of Tapo Canyon tailings dam from above (Google Earth, 2010)....109

Figure 26. The Flow Path of Merriespruit from Van Niekerk and Viljoen (2005)...111

Figure 27. View of Merriespruit city and the tailings dam in the south from above (Google Earth, 2010).....111

Figure 28. Sample of a DEM of South Africa (NASA).....114

Figure 29. Diagrams demonstrating run out distance and velocity versus time for Tapo Canyon tailings dam failure modeling.....123

Figure 30. Scenes of modeling Tapo Canyon tailings dam failure demonstrating tailings at 25m, 120m and 180m distance from the dam.....124

Figure 31. Diagrams showing run out distance and velocity versus time for Merriespruit tailings dam failure modeling.....127

Figure 32. Scenes of modeling Merriespruit tailings dam failure showing tailings at 80m, 1650m and 1960m distance from the dam.....128

Figure 33. Prespective views of the Merriespruit and Tapo Canyon tailings dams failure model demonstrating the tailings at a 1960m (Merriespruit) and a 180m (Tapo Canyon) distance from the dam.....132

Figure 34. The result of Merriespruit tailings dam failure modeling projected on the map (Google Earth, 2010) of the area.....133

Figure 35. The result of Tapo Canyon tailings dam failure modeling projected on the topographic map of the area.....134

List of Tables

Table 1. Properties of different tailings (Vick, 1983).....32

Table 2. Input data for the first set of calibration tests.....83

Table 3. Values for Test 1 of tests with changes in a single variable.....94

Table 4. Values for Test 2 of tests with changes in a single variable.....97

Table 5. Values for Test 3 of tests with changes in a single variable.....99

Table 6. Data regarding Tapo Canyon tailings dam.....115

Table 7. Data regarding Merriespruit tailings dam.....117

Table 8. Data for Tapo Canyon tailings dam failure modeling.....120

Table 9. Data for Merriespruit tailings dam failure modeling.....125

Table 10. Values assigned to the parameters in Monte Carlo simulation.....148

List of Symbols

English Letters

$\hat{a}_i$	Bagnold's empirical constant
c	speed of sound, m/s
c_0	speed of sound at initial density, m/s
D	domain in SPH method; rate of deformation tensor
d_m	number of dimensions in a kernel function
d_s	diameter of particle, m
e	void ratio; friction and restitution coefficient
F_r	Froude number
f_s	force per unit area, N
G_s	specific gravity
g	gravitational acceleration, m/s^2
H	bed elevation, m
H_T	sum of the height of flume and the height of tailings in reservoir, m
h	smoothing length in SPH method, m; thickness of flow, m

h_y	height above which plug flow occurs, m
l_m	mixing length, m
m	mass, kg
N	time step
n	fluid behavior exponent in Bingham model
P	pressure, Pa
P_{ref}	artificial compressibility modulus
R	minimum distance between approaching fluid particle and boundary particles, m
R_e	Reynolds number
r	distance between two particles, m
u	velocity in Bingham model, m/s
v	velocity of particle, m/s
V	velocity, m/s; volume, m^3
V_i	volume associated to a certain point in SPH method, m^3
W	width of flume, m
$W(x, h)$	kernel function
Z	distance between approaching fluid particle and boundary particles, m

x, y, z	distance in different directions, m

Greek Letters

α	consistency condition factor
ρ	density, kg/m^3
ρ_o	initial density, kg/m^3
ρ_m	density of mixture, kg/m^3
ρ_s	density of sediment, kg/m^3
η_p	viscosity in Reynolds number equation, $Pa{\cdot}s$
Θ	diffusive terms in momentum conservation equation
θ	angle of inclined surface, *degree*
θ_r	angle of repose, *degree*
μ	viscosity, $Pa{\cdot}s$
μ_f	dynamic friction coefficient
τ	shear stress, Pa
τ_y	yield stress, Pa
τ_y'	dimensionless shear stress
ζ	combined dispersive turbulent parameter

λ	linear concentration
λs	a Generalized Lambda distribution
∇	gradient of kernel function
Δ_a	XSPH variant
Δt_v	combination of Courant and viscous time step controls
δ_f	bed friction angle, *degree*
σ	standard deviation

Chapter One: Introduction

Introduction

1.1 Introduction

Mining has been one of the main activities for many countries to provide their industry with the necessary raw materials. Besides minerals, activities performed on a mining site result in production of tailings and as the process of mining and mineral extracting continues, the tailings produced increases in volume and therefore, a method of retaining the tailings has to be included. Disposal in impoundments, disposal as free standing piles and disposal by filling open pits are some of the methods utilized by the mining operators (EPA, 1994) among which impoundment of slurry tailings is the most common one due to economical and operational considerations (Environment Canada, 1987).

Proper consideration has to be given to potential environmental and urban-planning problems, as a failure in the embankment will probably result in considerable damages and losses. Based on the type of ore being treated in the mining and extraction process there are different types of chemicals in the tailings impoundment behind the tailings dam; therefore any leakage in the structure might result in the environment being exposed to chemicals. This, in a severe case might result in the inhabitants of the area being poisoned or the vegetation damaged. Another probable incident could be the failure of the tailings dam structure and as a result the flow of a relatively great amount

of tailings into the area facing the dam which might cause damages to structures or take lives. The risk of environmental damages is also amplified in such cases.

In relation to dam failure, cases such as flow of tailings into the city adjacent to the dam damaging buildings, causing death and covering a distance of approximately two kilometers (Van Niekerk and Viljoen, 2005) have been reported. There are also reports on cases of flow of tailings into the river nearby and thus being transported to other areas (Harder and Stewart, 1996); or flow of the tailings on the ground destroying all the structures and facilities on the way and finally coming to a rest at a twenty five kilometer distance from the dam (Van Niekerk and Viljoen, 2005). The damages in such incidents would have been reduced or would not have occurred if there could be a way to predict the tailings flow direction and length, and the area it would cover in case of a dam failure.

This study focuses on utilization of the Smoothed Particles Hydrodynamics method (SPH) in the simulations of tailings flow. The simulation tool had to be calibrated in order for the correct range of input data and its variation to be found. As a result, case studies of tailings dam failures can be simulated and the results will be compared to the data collected from the reports of the failures to indicate whether the simulation tool is a suitable one to fulfill the goal of producing a realistic model of the incident.

In general, this study, by using simulation tools to simulate the previously occurred tailings dam failures, will take a step forward to providing the engineers with the chance to predict the consequences of such failures and make decisions on the locations of future dams and the precautions to take accordingly. By modeling the failure of existing tailings dams and studying the distribution of the tailings, proper steps could be taken to reduce the potential damages and losses caused by the out flow of the

tailings. Moreover, modeling the future dams and studying the distribution of the tailings in case of a failure could help the engineers with finding the best location for the future tailings dam.

1.2 Objectives

There have been several reports, such as Van Niekerk and Viljoen (2005) and Harder and Stewart (1996), of disasters caused by tailings dam failures resulting in major losses and damages in some cases and minor damages in others. One of the methods of attempting to minimize the losses of such phenomena is predicting the run out distance of the tailings in case of a failure, and thus planning and designing the structures and performing urban planning in the perimeters of the dams or even choosing the location of future dams based on such data. Therefore, the objectives of this thesis can be summarized as follows:

1. Determining the possibility of utilizing a simulation tool to model the flow of tailings as Non-Newtonian fluids.
2. Calibrating the simulation tool based on a physical experiment performed and reported by literature.
3. Implementing the reported tailings dam failures and comparing the results with the actual incidents.

The methodology opted to achieve the abovementioned objectives was to determine the behavior of tailings by studying previous research on tailings flow and accordingly utilize the properties of tailings in the simulation tool and calibrate the program based on one of the experiments performed in previous studies by other researchers. Finally,

two case studies in which the tailings traveled a distance before coming to a rest were modeled using the simulation tool and the results of the simulations were compared to the run out distances and approximate shapes of the tailings flow in the mentioned incidents.

Chapter Two:

Production, Impoundments and

Physical Properties of Tailings

Production, Impoundments and Physical Properties of Tailings

2.1 Introduction

Vick (1983) refers to 'tailings' as a generic term used for any kind of solid mine or mill waste including rock sized stripping waste, underground mine muck, and finely ground mill waste. The EPA, The U.S. Environmental Protection Agency (EPA, 1994), defines 'tailings' as the large quantities of fine grade particles, ranging from sand sized down to a few microns in size, produced by mining due to the necessity to be able to separate metals and minerals from the ores.

Tailings are one of the principal by-products, not necessarily beneficial, of mining and milling procedures. Therefore, currently, it has become a great concern to deal with these wastes and manage them in a way to have the most economical disposal while having the least influence on the environment.

However, before introducing the disposal of tailings, its conditions and prerequisites, the way in which tailings are produced during the mineral processing will be presented.

2.2 Production of Tailings

To understand the type and properties of the tailings used in the simulation, production of tailings was studied as a part of literature review.

Tailings are produced as the ores undergo processes depending on specifications such as size and the kind of mineral they contain which in turn defines the physical characteristics of tailings. Therefore, mining processes differ from ore to ore; however, there are a few fundamental processes which are frequently used in processing different ores.

The ore cannot be sent to the grinders directly after stripping. The grinders need to be fed with ores smaller in size than the ones stripped off the mine. Different crushers are used to make the ore ready to be ground. There are usually two stages for crushing the ores, the primary stage and the secondary stage. During the primary stage, the ores are crushed to have them in sizes of approximately 254 to 305 millimeters (Vick, 1983). Applying the secondary crushing, which is the more important of the two stages, since the final output is going to be taken from this stage, reduces the size of the fragments to approximately 0.85 millimeters (Vick, 1983) which is small enough to go to the grinders. However, according to Metso Minerals, depending on the size of the feeders of the grinders, the number of crushing stages can be increased or decreased (Core Industries, 2008).

There are different types of crushers; jaw crushers and gyratory crushers are used at the primary stage while hammer mill crushers and cone crushers perform the second stage of crushing. However, a gyratory crusher is sometimes used at the secondary stage as well. Moreover, Nielsen and Kristiansen (1995) suggested that using more powerful explosives can result in better crushing and grind ability of the ores.

After the desired size for the fragments is achieved, the particles are sent to grinders. This is the last stage of size reduction of the tailings and the particles produced are the ones which are processed in the rest of the mineral processing progress.

Usually there are two different grinders to perform this process, the rod mill grinder and the ball mill grinder. In a rod mill, the rock particles are ground in a rotating drum being plunged and crushed by heavy metal rods. This will reduce the size up to approximately smaller than 2 millimeters (Vick, 1983). In order for the resizing process to be complete, the output of the rod mill will be sent to the ball mill where the same process as the rod mill will occur with the exception that there are heavy metal balls inside instead of rods. This final process will reduce the size of the particles to smaller than sieve No. 20 (Vick, 1983).

There are more modern types of grinders, autogenous and semi-autogenous grinding mills, which facilitate the process of grinding by having the ability to be fed by relatively larger particles than the ones previously mentioned. Rock fragments can be directly sent to these grinders even after the primary crushing which gives these types of grinders the potential of replacing the rod mill.

In a semi-autogenous mill, grinding takes place by means of rocks and metal balls. As the rolling drum rotates, the plates which are placed on the inner wall of the drum lift the material which then falls from a higher elevation. This plunge causes the input material to become finer and the larger rocks get broken up. Some examples of using semi-autogenous mills are in gold mining (Bartrum, Bowler, Butcher, 1986), copper (Carter and Russel, 2005) and platinum (Knecht and Patzelt, 2004).

An autogenous mill also uses the same method. The only difference is that there are no metal balls in the drum anymore and the crushing is done by only using rocks.

Other types of grinding mills are pebble mills and high pressure grinding rolls. In a pebble mill (rock pebbles are used in the system) both friction and crushing are used to grind the material. This method may be used where product contamination by iron from

steel balls must be avoided. It also raises the capacity of the mill as a result of utilizing pebbles which occupy almost 40% less volume than the balls in total (Lynch and Rowland, 2005). In a high pressure grinding roll two cylindrical rollers are pushed towards each other while the ores are passing through the space between them in the opposite direction. The exerted pressure brakes and crushes the ores into finer particles (Lynch and Rowland, 2005).

The degree to which the particles are ground is related to the mineral extraction method which is subsequently going to be used and the so related efficiency expected from the method. It usually takes detailed mineralogical and metallurgical examination as the key to choose the most efficient and suitable method of extraction. If leaching is going to be the primary extraction method, then high specific surface area is sometimes what it is looked for to get to the maximum efficiency; whereas finer particles may lead us to the maximum efficiency where flotation is considered as the primary extraction method.

Due to the force exerted on the ores during crushing and grinding, the produced tailings particles are highly angular (Pettibone and Kealy, 1971). Even particles which can be categorized as silt sized material show angularity such as broken glass (Hamel and Gunderson, 1973). Ores principally consisted of shale and also the ones with high clay contents are exceptions to this kind of categorization. Crushing and grinding such ores results in tailings' having particles shape and hardness reflecting the silt and clay particles in the parent material (Vick, 1983).

When the grinding process is finished, as mentioned before, depending on the efficiency of the process and based on detailed examinations the best method of extraction of

minerals will be chosen. The three most common options are concentration, leaching and heating (Vick, 1983).

The content of minerals in the ground ore differs from ore to ore. By concentration, the ores with greater amount of mineral will be separated from the ones containing negligible amounts, which will form the "tailings", to have the mineral extracted. The method chosen for concentration depends on the type of the mineral which is going to be extracted. However, according to Vick (1983), there are three major and common ways used for concentrating the ores which are gravity separation, magnetic separation and froth flotation.

When there is a considerable difference between the specific gravity of a type of mineral and the rock holding it, then using the gravity separation is a beneficial method. Gold, iron, coal and tin have much lower specific gravity than the rock itself; therefore gravity separation is a useful way to extract them (Vick, 1983). Water is usually the means to perform gravity separation. One way to do this is by a spiral classifier (Vick, 1983) or concentrator (Matthews et al., 1999). Spiral concentrators perform separation on the basis of particle density and size. They are consisted of a central axis about which an open trough twists downward vertically and thus separates a thin-film slurry of mineral and waste material in a radial format (Matthews et al., 1999). A pinched sluice can also be used to perform concentration; however, this device is not as efficient as the other devices. Therefore, regarding the fact of sluice being an economical device in both capital and operating expenses and the operator having the benefit of manufacturing it locally, in the cases where the capacity is low and flexibility is needed, sluices are still used. In order to overcome the efficiency problem, in contrary to the other devices' processes this process is performed in several stages. The sluice is fed with the slurry of

50% to 65% solids and as the path becomes narrower the height of the slurry will increase and gradually, as the result of heavy and light minerals getting separated and going together, segregation will happen. Subsequently, the heavy and light parts are separated into two flows by splitters to either proceed to the next stage or repeat the same procedure once again (Ergun and Ersayın, 2002). The concentrating process can also be done using a jig. Through jigging process particles are stratified with respect to density by water and particles' moving regularly with pulse air. The motion and stratification of the particles in a jig are affected by water motion (Kuang, Xie and Ou, 2004).

Magnetic separation is used for separating iron from magnetic ores such as magnetite (Vick, 1983). In some cases there is a rolling belt rolling around a permanently magnetized core which separates the magnetic particles as it moves and rolls. In some other cases a magnetic field is provided to attract the magnetic particles inside a drum separator and sticks them to the body of the drum. In "open gradient" separators the "falling curtain" method is used where a stream of mixed particles is run and magnets will deflect the magnetic particles among the stream of ores (Watson, 1998).

Froth flotation is one of the widely used methods in mineral concentration and Vick (1983) believes that its one of the most complicated procedures through which concentration takes place. As a result of using different reagents ores containing considerable amounts of minerals will become water repellent and will be willing to receive air bubbles. Therefore, these ores will stay on top of the suspension and will be skimmed while the rest of the ores remain in the suspension as tailings. In fact flotation is the first stage of extraction process where a chemical reagent enters the process and

therefore, it is also a critical stage since this entrance may have serious effects on the effluent in the mill and in the impoundment in the future which might be problematic.

The reagents used in the froth flotation process depend on the mineral or minerals which are going to be extracted. As a result there is usually no specific reagent with the ability to be used as a general reagent. Moreover, the reagent acts in different ways, some reagents will coat particles to become water repellent and some will change the pH in a way to promote flotation (Vick, 1983).

Finally; the concentrate is ready to either be delivered to the consumer, in case of coal, or to be transported to the refinery for the minerals to be extracted. Nevertheless, in some cases some other processes are used either alongside or in preference to concentration. Two frequently used processes of this kind are leaching and heating.

Leaching is a process where the minerals are separated from the ground particles by directly being exposed to strong acid or alkaline solutions. Choosing either one of the solutions depends on the type of the ore being treated. According to Vick (1983) the most common acid reagent used in this process is sulfuric acid (H_2SO_4) and the most common alkaline reagents are hydroxides and carbonates of sodium or ammonium. Leaching may have some effects on the physical condition of tailings and might also cause some changes in it. While physical breakdown and alteration of rock fragments has been caused by acid leaching of rock waste dumps, much less physical breakdown of this kind probably occurs in tailings' case (Vick, 1983). One way of performing the leaching process is in situ leaching or ISL which has been used by some countries such as the United States, Uzbekistan, Kazakhstan, Australia and some European countries (Dobrzynski, 1997).

This method can have some harmful consequences and has to be operated with great attention, accuracy and supervision since there is a great chance to contaminate the ground water and also the rest of the environment if the mining area is flooded (Taylor et al., 2004). In this method acid or alkaline solutions are injected directly into the ground water through boreholes (wells). The solution strips uranium (this method is mostly used for uranium) off the rocks and dissolves it into the ground water. Usually in the center of these wells there is a pipe through which the ground water is pumped and sent to the plant where the ground water is treated to separate the uranium and the rest will be pumped away. While the uranium is being stripped off the rocks, other radioactive materials and other products of leaching such as aluminum, iron and manganese are solved into the ground water (Shatalov et al., 2001). If a proper way to treat these elements is not considered in the process, then there is a great environmental danger awaiting the area.

Heating is a process through which some minerals will be extracted from the ores. It can be performed on both ground ores and also slurry suspensions. Heating is also known as "calcining" and the most frequent example for heating is the extraction of oil from oil sands (Vick, 1983). Calcining is usually performed by heating the ore (ground ore or the slurry suspension) in a confined container until the desired changes are achieved. These changes can be either chemical or physical depending on the material. There is more than one way to perform calcination and the best way is chosen concerning the required temperature, the size of ores, resistance of the material to changes and other special physical and chemical characteristics the material might have. Calcination is usually performed with a heat between 1800° F and 2200° F; however, this temperature range is sometimes changed to between 400° F and 3200° F (EPA, 1995).

The final stage of mining process is dewatering. From the word itself it might be incorrectly assumed that the process of dewatering is performed to produce dry tailings, however, the goal of this stage is to reduce the amount of water in the tailings and also reuse this excess amount water in the mining process if possible. There are some tailings such as the ones containing acid leach uranium (Vick, 1983) from which water is taken but this water contains some contaminants which lower the efficiency of the process of extraction if reused. Such cases cause some concerns for the disposal stage of running a mine.

One of the most common methods of dewatering which is not only used in mining but also in some other activities such as sewage management and recycling is the use of thickeners. The slurry suspension is conducted into a huge pot, and then the settled tailings are pushed towards the center of the pot by usually two rotating arms where they will be collected and pumped to the disposal point. Vick (1983) mentions that hydro cyclones are sometimes used instead of thickeners, however, some old fashioned devices such as drum, disc and belt filters which perform the dewatering process by vacuum suction of water through screens or clothes can also be used. Moreover, Zhang and El-Shall (2003) have tried methods such as sedimentation thickening, filtration, centrifugation, dewatering on screens, seepage induced dewatering and consolidation in their experiment to dewater the suspension.

2.3 Fate of Tailings

When the mining and mineral extraction processes are finished the tailings have to be transported to the impoundment. The tailings at such moment are usually in a slurry

suspension form most probably inclusive of 40% to 50% water (Vick, 1983). Almost all the tailings that are collected from the thickeners are in slurry suspension form since further dewatering of the tailings is economically unreasonable (Vick, 1983).

Historically, convenience and cost effectiveness were two important factors of choosing the location of tailings disposal and thus, tailings were often disposed of in flowing water or directly into drainages. As concerns arose regarding downstream sedimentation, water use and such matters the method of forming impoundments behind earth dams, which were often built using tailings and other waste material, was chosen by mine operators. Moreover, in some regions besides containing tailings, the impoundments also served the purpose of reusing the water in the impoundment due to the lack of water resources in the area (EPA, 1994).

The transportation of the tailings is sometimes done through flumes (EPA, 2001) and troughs (Rubinstein, 1995); however, the most common transportation system in this case is through pipes. Slurry is generally abrasive with high viscosity and its water content usually reaches up to 50%, and therefore, designing piping systems for slurry is not as simple as designing for water systems. High concern and attention is needed to consider a minimum flow rate since if the slurry suspension's running speed falls below a certain amount or even if the pipe is designed too large (Abulnaga et al., 2002) the system might face slurry settlement in the pipes which may result in a blocked system. On the other hand, a maximum flow rate should also be calculated and considered in the process since too high speed might result in head loss in addition to damages to the pipe itself and eventually lowering the durability of the system (Vick, 1983).Where necessary, pumps should be used according to the difference in the elevation of the impoundment and the thickener to keep the slurry moving. On the contrary, in some

cases, such as steep down slopes, there is a necessity to reduce the flow rate by means of energy dissipating points to prevent the pipes and the system from being damaged. Moreover, a discharge system should also be planned to provide the operator with the chance of emptying the pipes from tailings in case the system shuts down in order not to let the tailings settle down and harden in the pipes (Vick, 1983).

In the case of a tailings dam, the common tailings disposal method usually used is the above water disposal method where the tailings are disposed around the perimeter of the tailings dam. This method can be performed in two ways; single point discharge and spigotting (Vick, 1983).

As for single point discharge method there is only one outlet for the tailings pipe on the perimeter of the dam. This means that in different intervals the place of the outlet has to be changed along the perimeter to let the tailings form similar deltas next to and connected to each other in order not to let the tailings be distributed unevenly along the dam and to prevent pile ups (Vick, 1983).

When the spigotting method is used there are several spigots placed in the pipe located in equal distances from each other. When the tailings are passing through the pipe, they will be disposed through spigots along the embankment. Using this method there is no need to relocate the spigots as frequently as the former method and also usually each spigot has a separate valve so the operator would be able to control the disposal of the tailings through each spigot separately (Vick, 1983). There are various particle sizes in the tailings and as a result the same gradation exists in the pond behind the dam. As the tailings pour out of the spigot, the coarser particles settle in the area closer to the dam itself and the finer ones are thrown and taken farther than the dam where they will settle in the stationary water.

Cycloning is also another method of tailings disposal for tailings dams where the finer particles and the water will be discharged from the top of a cyclone into which the tailings enter under pressure and the coarser particles (usually sand) will be discharged from the bottom to be used in the further construction of the dam (EPA, 1994).

If necessary, some amount of the water behind the dam in the tailings pond might be taken back into the system to be reused for the mining process (Vick, 1983) or to protect the dam from overtopping (Babaeyan-Koopaei, 2002). There are usually two ways to do this, pumps or siphons and decant towers.

Pumps or siphons are floated on the water surface using barges and pontoons (Vick, 1983). Water is pumped and goes through pipes over the dam to the mill. A decant tower is made of a hollow concrete column which extends vertically from the bottom of the pond to the water surface. There are some ports on the column to take the water in; however, the ports located in the elevation range of the tailings are closed. Water runs through the column and it flows into a conduit which is extended perpendicular to the dam and goes beneath the dam toward the mill (Vick, 1983).

The decant tower system is usually less preferable than the floating pump method. The conduit for the decant tower is subject to settlement and rupture which might result in internal erosion and the collapse of the dam. The decant tower is made of concrete and concrete having the possibility of being affected by different acids and sulfates that might be in the tailings suspension is one reason this method is not as popular as the other one. Moreover, the pond might be divided into different parts in order for each segment to be handled individually. In such cases the pump or the siphon can be pushed to each segment very easily whereas an individual decant tower must be built for each segment (Vick, 1983).

As the U.S. Environmental Protection Agency (1994) states there are several other disposal methods besides disposal of tailings slurry suspension in impoundments such as disposal of dry or thickened tailings in impoundments where the tailings are thickened or dried before disposal which minimizes the seepage and the area of the land needed for the impoundment in addition to providing the chance of simultaneous tailings deposition and reclamation of the mixed water. However, it is an expensive method since considerable amount of energy and equipment are needed. Other methods are disposal as free standing piles and disposal by backfilling underground mines which is used to provide ground or wall support and stabilize the mined out area which will greatly decrease the occupied above ground area. It should be noted that only that part of the tailings which has high permeability, is less compressible and has the quality of getting dewatered rapidly (the sand fraction) is used underground. Cement can be added to this part of tailings in order to achieve even more satisfactory results. In this method the slimes are deposited above ground. Disposal by filling open pits is another method where the tailings are deposited into an abandoned pit or a part of an active pit which the former is a bit unusual to find because an embankment has to be built in the pit in order not to let the tailings go toward the active pit and also the seepage might affect the embankment and cause problems. There is also subaqueous disposal which is limited to coarser tailings which can settle quickly where the tailings are disposed in deep lakes or oceans which will prevent the process of oxidation of sulfate from taking place resulting in inhibiting acid generation. This method is used for areas with steep terrain, high precipitation and high seismicity. Ripley et al. (1982) stated that unless the proper way of disposal is organized, the tailings could cover large areas of the ocean or lake floor and cause turbidity. This method can be performed as depositing the tailings in

pits or impoundments permanently which can almost have the same benefits. However, the water level and the effect of seepage on ground water have to be monitored constantly. Nevertheless, the most suitable method should be chosen based on the situation and the location.

2.4 Impoundments of Slurry Tailings

Impoundment of slurry tailings is the most common method of tailings disposal and the reason for this, as Environment Canada (1987) states is the method's, in comparison to the other methods, being economically preferable and also easier to operate. According to Environment Canada (1987) designing a tailings impoundment is also to take care of a number of treatment functions such as removal of suspended solid by sedimentation, separation of heavy metals by forming hydroxides, containing of the settled tailings permanently, equalization of waste water quality, stabilizing some constituents that are prone to oxidization, stabilization and storage of the recycled water from the suspension and balancing the incidental flow caused by storm. There are some disadvantages as well, which are having difficulty maintaining a well distributed flow and draining water from the uncontaminated parts. Reclamation is generally difficult but in presence of acid generating tailings because of the material characteristics and large surface area it becomes more difficult. Since the bio-oxidation process is exposed to seasonal changes and its efficiency is therefore variable, the treatment process is inconsistent. Moreover, it takes great expense and difficulty to collect the seepage through the structures and finally, unless the surface is stabilized by vegetation, chemical binders or rock cover, the finer part of the tailings material is seriously prone to wind dispersion.

2.5 *Surface Impoundments*

There are generally two major types of surface impoundments; water retention dams (Figure 1) and raised embankments. Based on topography of site, site situation, availability of materials and economic situation impose each of these major types of impoundments can be designed as ring dikes, in pits, specially dug pits and a variety of valley designs (EPA, 1994).

The amount of fill affects the cost of construction of a dam; therefore it is beneficial to be able to reduce the size of the dam and also to use local material, in this case tailings, to build the dam.

The water retention dam is constructed with its full height which will not give the operator a chance to change the height in the future. According to Vick (1983), the internal zoning of a water retaining dam which is used for tailings is very similar to a conventional earth dam's technology; however, since a water retaining tailings storage dam does not experience draw-downs as rapid as a normal water retaining dam, therefore, its upstream slope can be built steeper.

Whenever there is a need for a high quantity of water storage, a water retaining dam is preferable, for instance, where the constituents in the processed effluent prevent the operator from recycling water, which will require larger evaporation areas and water storage (Vick, 1983).

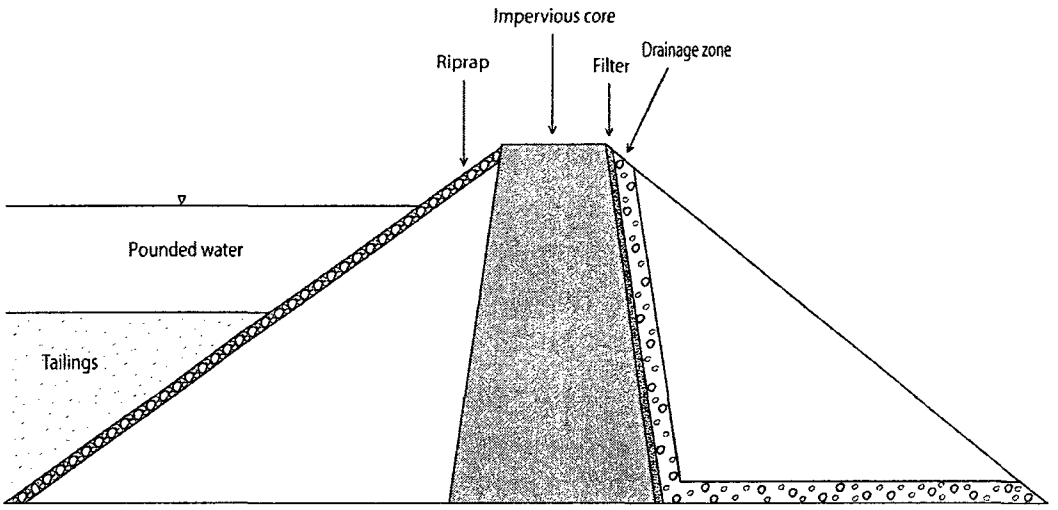

Figure 1. Water retaining dam for tailings storage, after Vick (1983)

Raised embankments are built in stages depending on the need of the site and the increase in the amount of produced tailings and effluent needed to be impounded. Construction starts with a 'starter dike' usually constructed with natural soil which is a type of retention structure and will be developed later on as time passes and needs grow. As a result of the construction and development taking place in stages, by constructing a raised embankment the operator undergoes a lower initial cost and since it starts with a starter dike which needs less material than a water retaining embankment, it is a more economical choice. Moreover, according to Vick (1983), as a result of a smaller quantity of material being used for construction of a raising embankment at the starting point, choices are available to choose from as construction materials. This means that while natural soil is used for construction of a retaining dam, one has the choices of natural soil, sand tailings or waste rock to choose from. Using a combination of the above mentioned materials is also possible.

Due to the raised embankments' staged method of construction, the operator has the opportunity to remedy the possibly occurring problems without having to have a great deal of materials or tailings moved or put the embankment out of service.

Starter dikes are usually constructed for the first couple of years in order to keep the processed effluent and the volume of possible flood in the first couple of years of mining activities. The upcoming raises in the embankment should be in a way that can stand the pace of rise in volume of the tailings plus the storage allowance for a possible flood.

A wide range of materials such as natural borrow soils, pit mine waste, underground development muck, hydraulically deposited tailings, or cyclone sand tailings might be used in order to build embankment raises (Vick, 1983).

There are three methods of raising the embankment regardless of the type of materials used in the construction of each model and they are recognized by the position of the crest in relation to its position on the starter dike as the embankment is raised higher and higher. Each method has its own advantages and disadvantages and they are known as upstream, centerline and downstream methods.

2.5.1 Upstream method (Figure 2): The construction of the embankment commences with a starter dike and a beach is formed by the tailings being squirted from the top of the crest by a spigot. The second dike is built on the beach upstream, and so the construction goes on with the next dike. Vick (1983) mentions that as a general rule, the amount of sand in the discharged whole tailings should not be less than 40% to 60% and thus, for tailings in soft rock or fine categories the option of using upstream method is eliminated. This also applies to tailings from which the sand fraction is removed for use as underground mine backfill. The most significant advantages of choosing the upstream method are the simplicity and the low cost of the process. The dikes are built

on the beach upstream the starter dike, therefore, there is usually very little amount of fill needed to be added mechanically to the new dike and as a result the embankment can go higher and higher with a low cost.

Although the upstream method has the mentioned benefits it also has some very critical and challenging restrictions. The location of the phreatic surface is a critical issue in the upstream embankments and the important factors to control this location are the permeability of the foundation in relation to the tailings, the grain-size segregation degree and lateral permeability variations within the deposit and the location of the pond behind the embankment. When the pond gets closer to the face of the embankment, it boosts the phreatic zone to a higher level and the stability of the dam will be endangered.

In fact, the only factor that can be controlled during the operation is the pond encroachment on the beach which can be done by increasing the spigotting action in the areas where the distance between the face and the pond has become critical and also by increasing the decanting speed. However, this pond control is very difficult when a flood or great inflows are gathered behind the embankment. Consequently, an upstream embankment is not generally built for the use of water accumulation and storage. Moreover, an upstream embankment's low density and high saturation degree result in its being vulnerable to seismicity which makes the upstream embankment unsuitable for the locations with high seismicity.

As an important consideration, the rate of raising an upstream embankment should also be controlled since the higher the rate, the higher the excess pore pressure in the embankment will be (Vick, 1983).

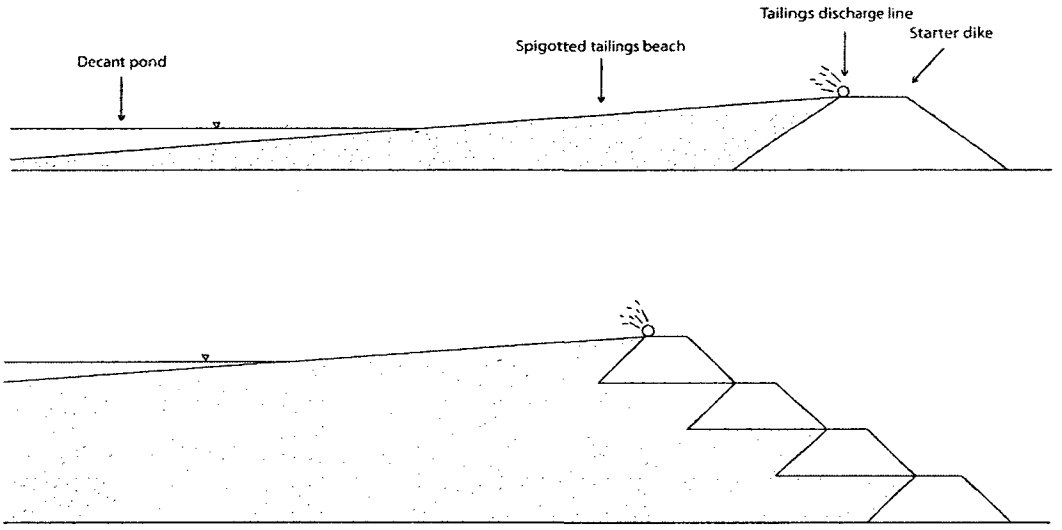

Figure 2. Upstream method of tailings embankments raising, after Vick (1983)

2.5.2 Downstream Method (Figure 3): In this method, construction starts with a starter dike, however, in order to raise the embankment the fill will be deposited on the downstream face of the dike. The raised embankments are equipped with internal drains and impervious cores, therefore, the location of the phreatic surface is kept low and also by having the fill compacted, water storage behind the embankment can be possible in addition to the structure's being highly seismicity tolerant.

The raising rate in an upstream embankment is a critical factor in its stability. This factor, however, is not of importance in a downstream embankment since its method of construction makes it independent of the beach and the tailings on the upstream side. The fill on which the embankment is raised, as previously mentioned, can be compacted in addition to the existence of the internal drains and impervious cores. Vick (1983) states that regarding structure soundness and behavior, dams constructed with downstream raising method and water retention type dams have the same value.

In spite of all the mentioned benefits, construction of a downstream embankment requires some preplanning since as the embankment rises, the toe of the dam moves outward and as a result the dam will occupy more space. To prevent this procedure from interfering with or crossing roads, piping systems and other facilities, sufficient planning has to be done before the construction commences. Moreover, construction using this method needs a great amount of fill which makes the method costly and also if the mine waste and the tailings are used as the fill since their production rate is usually constant and the demand for the fill goes higher as the embankment rises, material shortage might be faced as the construction process advances.

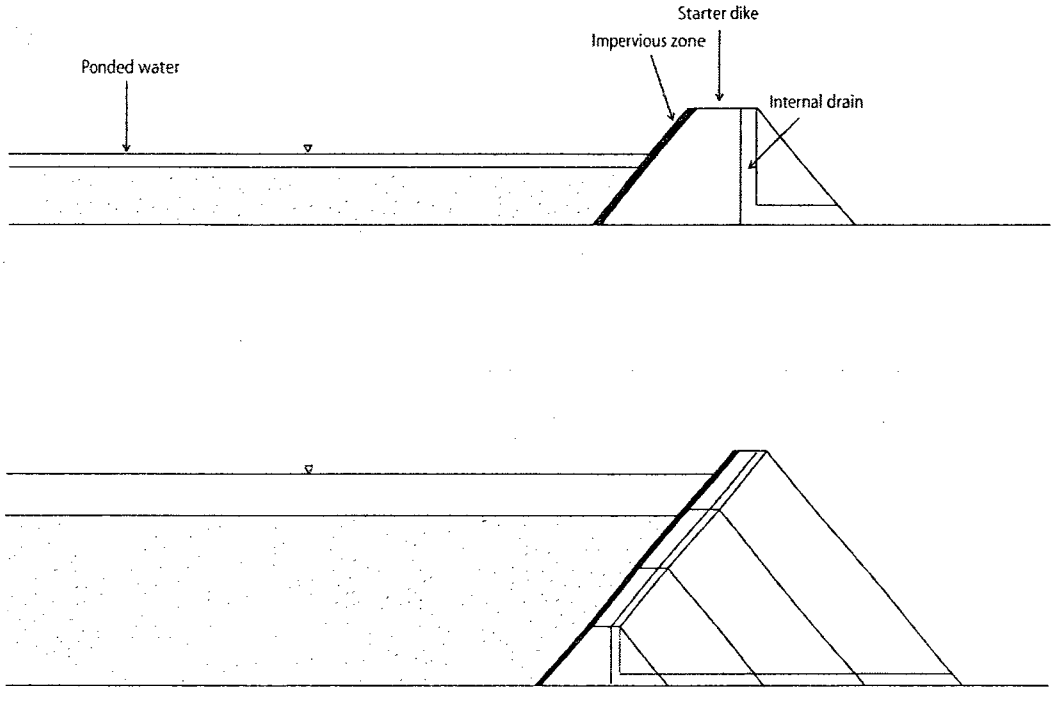

Figure 3. Downstream method of raising tailings embankments, after Vick (1983)

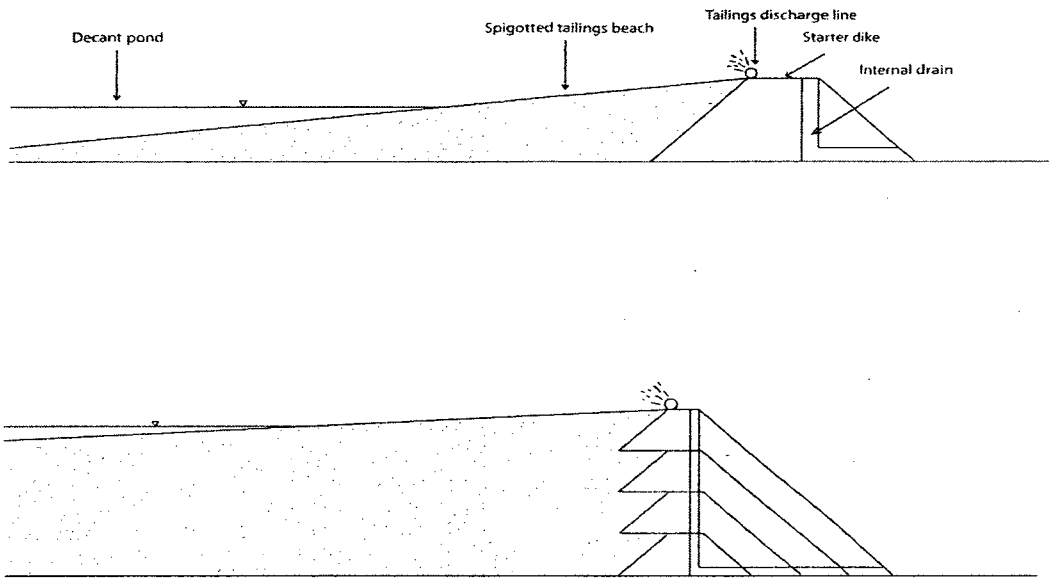

Figure 4. Centerline method of raising tailings embankments, after Vick (1983)

2.5.3 Centerline method (Figure 4): This is a method in-between the previous two methods, which means that it has some benefits that others have and also some of the disadvantages present in the previous methods have been shrunk or minimized in this method. In the centerline method, as well as the other ones, the construction starts with a starter dike and the waste and tailings are spigotted behind the dike and a beach is formed, however, the raise is performed differently. In this case, the structure is raised by putting the fill on the beach and the downstream face of the dike simultaneously keeping the center of all the dikes on a vertical line which passes through all of them. By using this method the amount of fill needed to raise the embankment would be something in between the upstream and the downstream methods by which a lower cost of embankment raise is provided. Fewer problems regarding the fill production and its demand will be faced performing the centerline method. Due to the existence of internal

drains in the embankment there should be no concerns about the distance of the beach and the embankment face regarding the phreatic zone.

While spigotting and forming a beach is not necessary in the downstream method, it is necessary for a centerline embankment to have a beach since it is needed for the embankment to be raised on.

An embankment built using this method is not suitable for retaining water for a long time. It is possible to keep water behind the dam for a while but for a long term program this method is not the one functioning well. As Vick (1983) has mentioned, the rate of raising the dam is not affected by the pore pressure dissipation but the undrained shear strength of the beach material should be considered. As a result of the internal drainage being present and the fill in the body being compacted, this kind of embankment should have good seismic resistance. In case of liquefaction, the upstream might be damaged, however, as long as the center and the downstream parts are not affected and the effluent is not ponded directly at the upstream face of the embankment, the structure is considered as stable and unaffected.

2.6 Physical Properties of Tailings

There are various types of tailings based on the ore type which is being processed at the mill. Amongst several existing tailings types, physical properties of coal tailings, oil sands and gold tailings are included in this thesis.

2.6.1 Coal

It is not always needed for coal to be processed. The procedure of processing ores is sometimes done in order to improve the quality of the coal and the burning process. Processing coal is also done to decrease the amount of the sulfur in the coal by removing the pyrites from it. Gravity separation is used in the mill in order to process coal by which coarse refuse is produced, which is handled dry. However, when wet cleaning or froth floatation methods are applied, the produced tailings are called fine refuse or sludge (Vick, 1983).

According to Vick (1983), tailings produced from coal wash generally consist of fine grained materials; mostly clay and silt particles from the existing shale and also coal particles which result in a low specific gravity for the tailings. This composition, for the amount of its clay content, also results in the tailings having some plasticity. As an example from the same source and reported by Wahler (1973), the specific gravity of fine coal refuse in Buffalo Creek, W.V. is between 1.4 and 1.6, the liquid limit is between 20% and 40% and the plasticity index is in the range of 2% to 12%.

2.6.2 Oil Sands

For oil sands or tar sands, such as in Athabasca Tar Sand region in northern Alberta, Canada, the ore usually does not need to be ground and therefore, a considerable portion of tailings is coarse material. However, clay, silt and oil residue, mostly as bitumen, consist a small part of the tailings (Vick, 1983).

The sludge reacts poorly to consolidation and sedimentation therefore the void ratio in this type of tailings is high. Vick (1983) mentions it can reach up to 10 in some cases.

Such a high void ratio will result in the tailings' occupying a large volume in the impoundment. In addition, production of oil sand tailings is in a very high pace; therefore, there are rapid increases in the height of tailings dams which in turn affect the stability of embankments.

Using Hot Water Process (HWP) in commercial oil sands operations results in the coarse tailings effluent's being produced in a form of slurry which is a mixture of sand particles, dispersed fines, water and residual bitumen. The slurry, which is hydraulically transported to and deposited in the tailings ponds has approximately 50% (by weight) solids. The solids portion consists of sand (82% by weight), fines smaller than 44 mm (17% by weight) and residual bitumen (1% by weight). When the tailings are deposited in the pond, a beach is formed due to quick segregation of sand particles. The remaining fine tails (6% - 10% by weight) accumulate in the pond and settle quickly to 20% (by weight) solid content and in a few years to 30% (by weight) solids with a stable slurry structure which is called mature fine tails (MFT). The MFT has a very slow consolidation rate and as a result keeps its fluid state for decades (Chalaturnyk et al., 2002).

2.6.3 Gold and Silver

Gold and silver are usually extracted in combination. The size of the particles of the tailings depends on the amount of the metals in the ore. The richer the ore, the coarser the tailings might be. As a result of the amount of clay present in gold-silver ores, the produced tailings are usually low or non plastic (Hamel and Gunderson, 1973). Specific gravity of 2.6-2.7 is reported by Soderberg and Busch (1922) and 3.1 by Hamel and

Gunderson (1973). As Vick (1983) mentions, higher specific gravities are probably due to the presence of pyrites in gold tailings reported by several investigators such as Hamel and Gunderson (1973) and Blight and Steffen (1979).

Vick (1983) has summarized the physical properties of the tailings and has classified them as Soft-rock tailings, Hard-rock tailings, Fine tailings and Coarse tailings. As for the previously introduced tailings, the fine refuse of the coal wash consists of both sand and slimes; however, since the clay is present in the slime part, the latter may be the dominant part; therefore, it falls into the soft rock tailings class. Gold-silver tailings may include both sand and slime fractions. There is usually low amount of clay in them and as a result, there is usually low or no plasticity and sand is the dominant part in the physical properties and that is the reason this kind of tailings belongs to the hard rock tailings group. As for tar sands, they have either sands or non-plastic silt sized particles which generally behave like sand and therefore, they fall into coarse tailings. However, the slimes from the tar sand tailings do not usually contain the sand fraction and the behavior is dominated by silt-clay particles and therefore, as mentioned before, may cause consolidation. The slime therefore, belong to the fine tailings group. In Table 1, Vick (1983) summarizes typical in-place densities and void ratios for different kinds of tailings. The higher void ratios and lower dry densities show the tailings which are closer to the surface and are newly deposited whereas the higher dry densities and lower void ratios belong to the tailings in deeper parts.

Table 1. Properties of different tailings (Vick, 1983)

Tailings Type		Specific Gravity G_s	Void Ratio e	Dry Density (kg/m³)	Source
Fine Coal Refuse	Eastern U.S. Western U.S. Great Britain	1.5 – 1.8 1.4 – 1.6 1.6 – 2.1	0.8 – 1.1 0.6 – 1.0 0.5 – 1.0	2.8 – 3.4 2.8 – 4.4 3.4 – 5.3	Busch, Baker, Atkins and Kealy, 1975 Baker, Busch, and Atkins, 1977 Wimpey, 1972
Oil Sands	Sands Slimes	—— ——	0.9 6 – 10	5.44 ——	Mittal and Hardy, 1977
Lead-Zinc	Slimes	2.9 – 3.0 2.6 – 2.9	0.6 – 1.0 0.8 – 1.1	5.81 – 7.1 5 – 6.4	Mabes, Hardcastle and Williams, 1977 Kealy, Busch and McDonald, 1974
Gold-Silver	Slimes	——	1.1 – 1.2	——	Blight and Steffan, 1979
Molybde-num	Sands	2.7 – 2.8	0.7 – 0.9	5.75 – 6.2	Nelson, Shepherd and Charlie 1977
Copper	Sands Slimes	2.6 – 2.8 2.6 – 2.8	0.6 – 0.8 0.9 – 1.4	5.8 – 6.9 4.4 – 5.6	Volpe, 1979
Taconite	Sands Slimes	3.0 3.1 3.1 – 3.3	0.7 1.1 0.9 – 1.2	6.9 5.7 6.1 – 6.6	Guerra, 1973 Klohn, 1979a Guerra, 1979
Phosphate	Slimes Gypsum	2.5 – 2.8 2.4	11 0.7 – 1.5	0.9 3.7 – 5.6	Bromwell and Raden, 1979 Vick, 1977
Bauxite	Slimes	2.8 – 3.3	8	1.2	Samogyi and Gray, 1979

When the tailings are dewatered or thickened, the finer particles are retained which makes the tailings have a somewhat homogeneous amount of fine material throughout their mass (Kwak, 2004). According to the same source, if further dewatering takes

place, a paste like condition is reached, which will reduce the risk of the impoundment failure, lower the amount of seepage in the ground, and lessen acid generation. Furthermore, the capillary action which is caused by the fine material in the paste and the low permeability of the paste as a result of its nature reduces the possibility of water infiltration. In addition, the shear strength of paste will increase as time passes which will result in more stable tailings in the impoundment.

2.7 Tailings as Non-Newtonian Fluids

Rheology, the study of deformation and flow of matter, classifies fluids into two categories based on their flow pattern: Newtonian and Non-Newtonian. One of the methods of tailings deposition is to deposit tailings in a concentrated 'paste like' state which is achieved by dewatering and pumping the tailings to the extent at which it behaves as Non-Newtonian material (Henriquez and Simms, 2009). Industrial tailings and concentrated mineral tailings often demonstrate Non-Newtonian behavior (Sofra and Boger, 2002a).

2.7.1 Newtonian Fluids

As Chhabra (2007) discussed using a hypothetical example of a layer of fluid between two plates and a steady horizontal force is applied to the top plate, the shear stress is proportional to the shear rate with a constant of proportionality "μ", known as viscosity, which is dependent on temperature and pressure and independent of the shear stress.

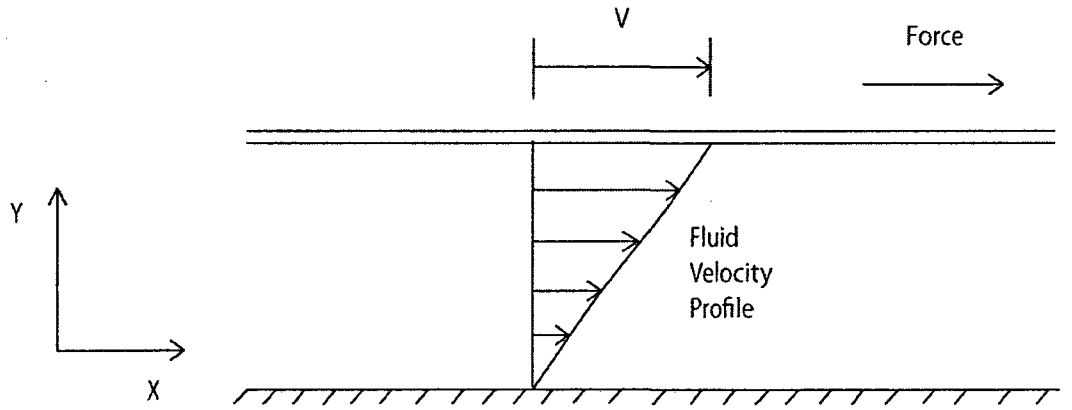

Figure 5. Velocity profile for Newtonian flow between parallel plates, after Graebel (2001)

The example above is the case where the force is applied in the horizontal direction (X) and it results in linear velocity changes in the vertical direction (Y). In case of a three dimensional flow, there are vertical and shear stresses on different sides and planes. In such case, there are two shear stresses (yz and yx for y plane as an example) and a vertical stress (one of Pxx, Pyy or Pzz) for each plane. This vertical stress is composed of the isotropic pressure and the deviatoric normal stress (Chhabra, 2006).

The definition of a Newtonian fluid implies that this kind of fluid is the one having a constant viscosity (in order to maintain a linear velocity change) meaning that it is not a function of time and the viscosity will be the same if the stress is applied after a resting period; and also having the three deviatoric normal stresses [for the three main dimensions, (X, Y and Z)] equal to zero since deviatory reflections are not usually of the properties of Newtonian fluids.

2.7.2 Non-Newtonian Fluids

In contrast to Newtonian fluids, a Non-Newtonian fluid is defined as a fluid to which the previous equation for Newtonian fluids is not applicable meaning that the proportion of applied shear stress to the shear rate is not constant under a specific pressure and temperature anymore and therefore, μ is not the constant of proportionality. The value of viscosity for Non-Newtonian fluids depends on the flow conditions such as the shear stress, which is developed through the fluid or shear rate, duration of shearing and geometry of the flow. He also lists that the Non-Newtonian fluids are divided into three groups.

First, the fluids for which the shear stress (or the shear rate) solely depends on the shear rate (or the shear stress). These fluids are commonly known as purely viscous, time independent or generalized Newtonian fluids.

This group is also divided into three sub categories:

1. Shear thinning or pseudoplastic fluids, for which an apparent viscosity is defined as the shear stress divided by the shear strength. The higher the shear rate, the lower the viscosity will be. The reason, as Sofra and Boger (2001) mentioned, is that the network between the particles will develop, as the shear stress increases, to be in the same direction as the shear stress which decreases the resistance against flow.
2. Shear thickening fluids or dilatant fluids are usually the type of fluids such as a concentrated suspension of solids where the viscosity increases with the increase in shear rate. At low shear rates, since the liquid part is almost filling most of the voids in the suspension, it facilitates the movement of the particles on each other;

however, as the shear rates increases, the structure breaks, the material expands or dilates and the solid parts are pushed over each other and the resulting friction causes a rapid increase in the apparent viscosity. The term 'dilatant' is generally used for the fluids which have the same reaction towards the increase in shear rate even if they do not expand with the change of conditions.

3. Visco-plastics in which there is a resistance against the shear stress (yield stress), therefore the shear stress needs to exceed the resistance in order to make deformations or a flow. This kind of fluid is also known as Bingham Plastic Fluid. Tailings have been considered as Bingham fluids in such works as of Henriquez (2008), Rodriguez-Paz and Bonet (2003) and Kwak et al. (2005) and therefore, it is considered the same in this thesis. Henriquez (2008) mentions that considering Herschel-Bulkley model a constitutive equation can be described for the visco-plastic fluids:

$$\tau = \tau_y + (k\gamma^m) \qquad \text{where} \qquad \tau \geq \tau_y \qquad \text{(eq. 1)}$$

τ_y is the yield stress and m and k are constants. The fluid is a dilatant when $m > 1$, shear thinning when $m < 1$ and is a Bingham in case of $m = 1$.

Second, the fluids for which not only the shear stress and the shear rate have the relationship they have in the first group, but the relationship also depends on aspects such as the duration of shearing which are usually called time-dependant systems.

Finally, there are the visco-elastic fluids which will react elastically and have a recoil reaction when deformed and generally have the properties and characteristics of both an elastic solid and a viscous fluid.

Larson (1999) describes the yield stress present in the visco-elastic fluids the transition zone between the elastic behavior and the viscous behavior of the fluid. The solid parts in the suspension tend to make bonds with each other forming a network or flock in the suspension. To make the suspension flow, breaking this structure is necessary and if the shear stress is smaller than the yield stress the fluid will act as an elastic material and will recoil after the shear stress is applied. When the shear stress exceeds the yield stress the material acts as a viscous fluid and starts to flow. Cements, soils, paints, pastes, printing inks, greases, pharmaceutical creams and ointments, and a large variety of food products such as dressings, sauces and spreads are among the materials having a yield stress (Lidell and Boger, 1996). Examples of yield stress material from Barnes (2000) mayonnaise and toothpaste for which the relationship between the viscosity and the applied shear stress are plotted in Figures 6 and 7. The sudden fall in the viscosity after being quite constantly a high value, can be explained by the idea of the yield stress. In the range of low shear stress values the material resists against the shear stress and later when the yield stress is overcome by the shear stress the material starts to flow and it experiences a fall in viscosity.

Rheological factors like yield stress and viscosity in turn, can be influenced by factors such as physical conditions, zeta potential and temperature (Henriquez, 2008). For tailings at a specific solids concentration, changes in the particle size distribution affect the yield stress for that type of particular tailings. A study performed by Sofra and Boger (2002b) on several types of tailings revealed that the more concentrated the tailings are, the higher the yield stress becomes. As an example, it is shown in the same study that the yield stress for a gold tailings sample with almost 67 percent of weight

concentration is approximately 50 Pa and the same factor for a gold tailings sample of almost 76 percent of weight concentration is 1600 Pa.

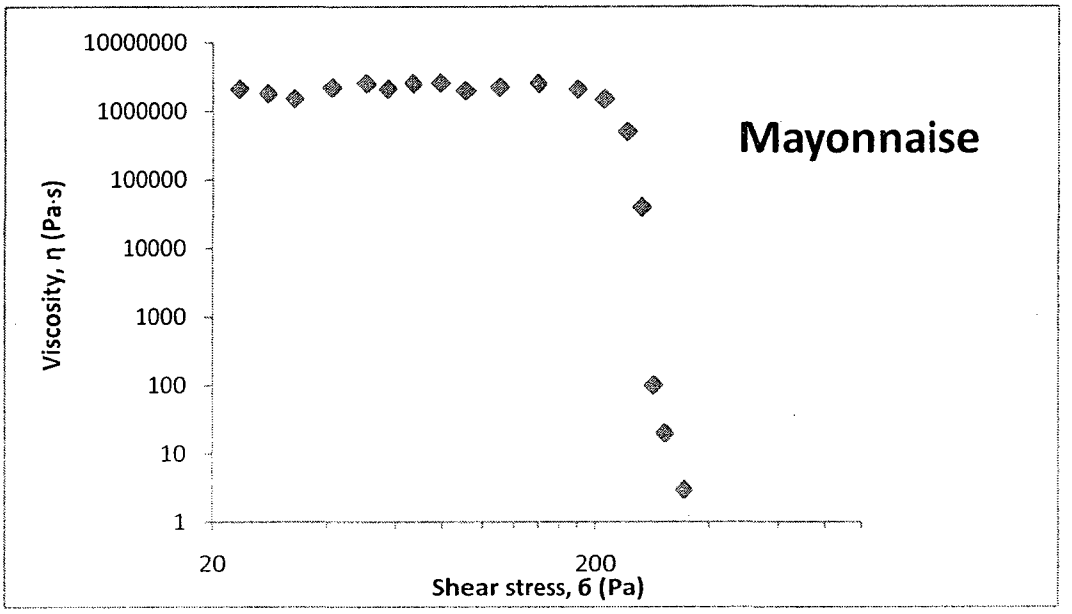

Figure 6. The relationship between viscosity and shear stress for mayonnaise, after Barnes (1999)

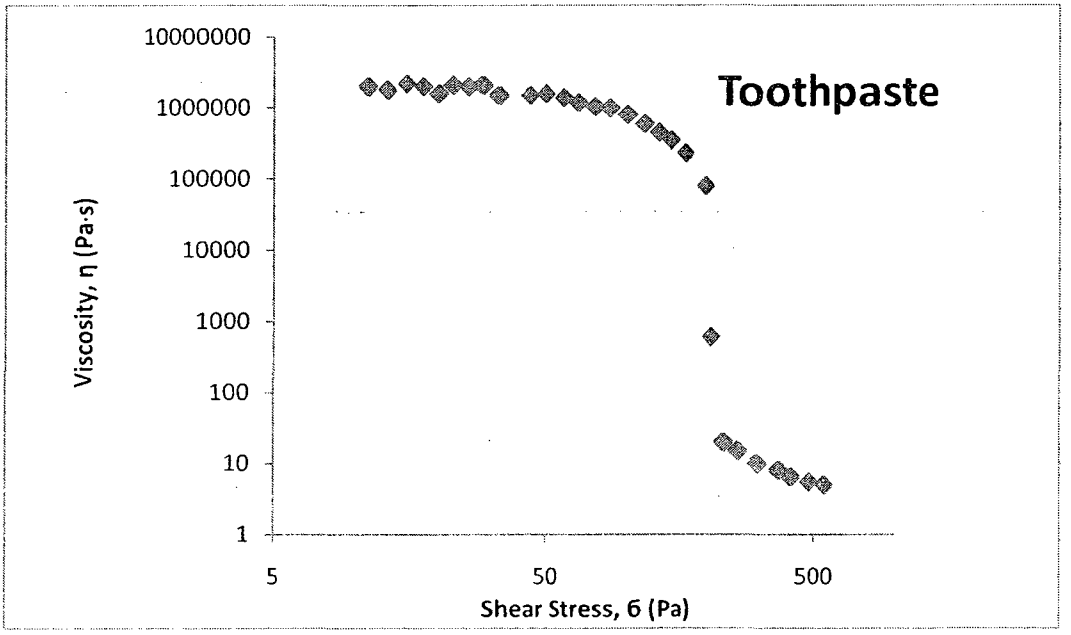

Figure 7. The relationship between viscosity and shear stress for toothpaste, after Barnes (1999)

As a result, tailings with higher concentration and therefore higher yield stress will settle closer to the discharge point or if there is a gate and flume closer to the gate.

On the other hand, tailings with lower concentration which have lower values of yield stress will spread over the site or through the flume (Kwak, 2005). Tailings are mostly consisting of 70% to 80% solids by weight (Henriquez, 2008) and according to the definition of yield stress when the distance between the particles decreases the interaction between them increases and as a result the value of yield stress rises. Finally, according to Kwak (2005), if a tailings paste consists of a minimum of 15 percent of its mass of particles smaller than 20μm it will be able to flow through a pipe without segregation and also keeps enough water to prevent bleeding.

A negative or positive electrical charge exists on the surface of a particle in a medium like water (Henriquez, 2008). Kwak (2004) mentions that when a particle under the effect of an electrical field moves with some ions, there will be a boundary between the particle and moving ions together and the stationary ions. This is called the shear plane. Since the charge cannot be measured, the potential at the slip plane is measured which is called the zeta potential. In other words it is the magnitude of repulsion or attraction between the particles. If there is attraction between them, aggregates will form in the slurry and consequently there will be an increase in the viscosity in comparison to when there is repulsion. Mpofu, et al. (2003) have shown that the yield stress is affected by the variations in the zeta potential.

Temperature also affects the rheological properties of the fluid. Viscosity is affected by temperature in both Non-Newtonian fluids (Pinarbasi and Imal, 2005) and Newtonian fluids (Wright, 1977).

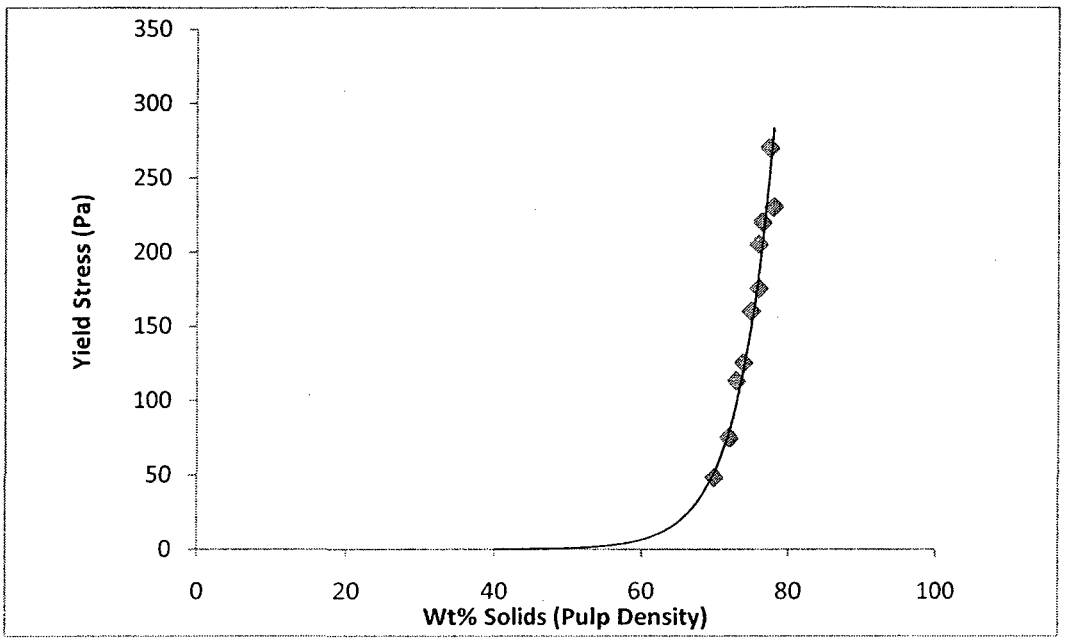

Figure 8. The relationship between yield stress and pulp density for gold paste tailings, after Henriquez (2008)

Kwak (2004) has concluded from the previous studies on rheological behavior of mineral suspensions and slurries that their rheological behavior is influenced by the measurement technique and also by their physical and chemical environments.

In an experiment on dewatered tailings including two-dimensional parameters performed by Sofra and Boger (2001), it was observed that after the dam or the obstacle retaining the movement was taken away, the tailings flowed from the reservoir into the flume connected to it. Bingham model was used to get an approximation of the flow behavior in this study. It was observed that the velocity increases from zero to a maximum and eventually declines to zero. They defined the maximum velocity as:

$$V = (2gH_T)^{1/2} \qquad \text{(eq. 2)}$$

where V is the maximum velocity, g is gravitational acceleration and H_T is the sum of the height of the flume and the height of tailings in the reservoir.

When the tailings came to rest, the depth at toe and the depth at gate were measured in addition to the length of tailings to determine the angle with which the tailings had come to rest. Moreover, they observed that the volume of tailings in the reservoir and also the angle of the flume's floor influence the flow of fluid from the reservoir into the flume. In order to explain this influence, they introduced τ_y' as a yield stress without dimension which depends on the maximum velocity, the yield stress and the density of tailings.

$$\tau_y{}' = \frac{\tau_y}{V^2\rho} = \frac{\tau_y}{2gH_T\rho} \qquad \text{(eq. 3)}$$

where V is the maximum velocity, τ_y is the yield stress and ρ is the density of the fluid. They also developed a relationship between the angle of repose (the angle to which the tailings come to rest at the toe) and other dimensionless parameters such as Reynolds and Froude numbers which is:

$$\theta_r = f\frac{\tau_y{}' F_r}{R_e} \qquad \text{(eq. 4)}$$

Having defined Reynolds number as:

$$R_e = \frac{WV\rho}{\eta_P} \qquad \text{(eq. 5)}$$

where W is the width of the flume, V is the velocity of the fluid, ρ is the density of the tailings and η_p is the kinematic viscosity and Froude number as:

$$F_r = \frac{V^2}{Wg} \qquad \text{(eq. 6)}$$

the above mentioned relationship for the repose angle can be written as:

$$\theta_r = f\frac{\tau_y \eta_P}{\rho^2 W^2 g V} \qquad \text{(eq. 7)}$$

This yields that the angle of repose is affected by the balance between the parameters resisting flow, which are the yield stress and viscosity, and those contributing to flow, which are the fluid density, flume width, gravitational acceleration and the maximum velocity (Kwak, 2004).

Sofra and Boger (2001) after performing the tests on tailings, kaolinite, titania and Laponite, "Laponite is a synthetic hectorite [soft, greasy clay mineral], which forms exfoliated silicate layers when dispersed in water." (Daniel et al., 2008), reached the conclusion that the mentioned relationship for the repose angle is a linear relationship. In other words, approximately all the values resulted performing the test for all four materials fall on a straight line if the angle of repose is plotted versus the right side of equation 7.There are several techniques to simulate a Non-Newtonian fluid such as MAC (Marker and Cell), which uses finite difference equations with the variables of velocity, pressure and divergence. MAC breaks the area into several cells which have their own pressure and velocity. The Marker-and-Cell (MAC) method uses a grid to evaluate the dynamics of an incompressible viscous fluid in which variables of pressure and velocity are employed. This method has particular application to the modeling of fluid flows with free surface (Tome and McKee, 1994).

Another method is SPH (Smooth Particle Hydrodynamics), in which a group of particles with associated properties like mass, position, velocity and density, discretize the continuum of the flow. The governing equations are constructed in a Lagrangian form considering that the particles move with the material velocity of the continuum (Rodriguez-Paz and Bonet, 2003).

In addition to the aforementioned methods, Henriquez (2008) describes that there are other methods which have simplified the procedure by applying simplifying assumptions to the Navier–Stokes equations and basically solve the reduced form of the equations. The same source also mentions the Lubrication Theory as an example of reduced Navier-Stokes equations with the assumption of slow spreading of a thin layer of liquid. The continuity and momentum equations for lubrication theory are simplified assuming that the ratio of the thickness of the flow to its length is small. Moreover, it is assumed that the Reynolds number is small and as a result the flow is laminar. In other words, the velocity is so slow that the ratio of the inertial forces to viscous forces in the momentum equation will be omitted (Henriquez and Simms, 2009). For instance, Liu and Mei (1989), applying the Bingham model, used the Lubrication Theory and the mentioned assumptions to study the flow of fluid mud. The momentum equation became:

$$\frac{\partial P}{\partial x} = \rho g Sin\theta + \frac{\partial \tau}{\partial z} \qquad \text{(eq. 8)}$$

where P is the pressure, the 'x' axis is the direction of the inclined plane, ρ is the bulk density, g is the gravitational acceleration, θ is the angle of the inclined surface, τ is the shear stress and the 'z' axis is normal to the surface of the plane.

If in the above mentioned study the pressure is assumed as hydrostatic, then the equation will change to (Henriquez and Simms, 2009):

$$P = \rho g(h - z)Cos\theta \qquad \text{(eq. 9)}$$

where h is the height of the free surface or the thickness of the flow at a particular 'x'.

If the equation is solved for shear stress (τ) depending on depth (z), the following equation results (Henriquez and Simms, 2009):

$$\tau = \rho g(h - z)Cos\theta(tan\theta - \frac{\partial h}{\partial x}) \qquad \text{(eq. 10)}$$

As for a flat bed θ can be set to zero and if the steady state of the fluid or the tailings is considered z should be set to zero. In this case, noting that the shear stress is smaller than the yield stress ($\tau < \tau_y$), the following equation will be achieved (Henriquez, 2008):

$$h^2 - {h_0}^2 = \frac{2\tau_y}{\rho g}(x - x_0) \qquad \text{(eq. 11)}$$

where h_0 is the height at x_0.

Deriving from the previous equation, according to Yuhi and Mei (2004) the equation for the steady state flow profile of a flow from the top of a hill might be (Henriquez and Simms, 2009):

$$h' - h'_0 + \ln(1 - h') = x' - x'_0 \qquad \text{(eq. 12)}$$

where

$$h = h'(\frac{\tau_y}{\rho g Sin\theta}) \qquad \text{(eq. 13)}$$

and

$$x = x' Cot\theta(\frac{\tau_y}{\rho g Sin\theta}) \qquad \text{(eq. 14)}$$

Henriquez (2008) reports that comparing the results achieved from the aforementioned equations with field measured profiles, Simms (2007) has confirmed the applicability of

the equations for a flat bed and the flow from top of a hill to the in situ physical condition in the field.

Yuhi and Mei (2004) studied the spreading of fluid mud over a surface with a small angle for the slope. Bingham model was assumed and the Lubrication Theory was applied. They introduced an equation for depth integrated flow for one dimension for constant mass (Henriquez and Simms, 2008):

$$\frac{\partial h}{\partial t} = \frac{g\rho}{\mu}\frac{dh}{dx}\frac{1}{6}(3h - h_y - 2H)(h_y - H)^2 \qquad \text{(eq. 15)}$$

where h is the vertical height of flow, μ is the dynamic viscosity, H is the bed elevation and h_y is the depth above which plug flow occurs.

Henriquez (2008) reports the depth integrated law of mass conservation for one dimensional limit equation in a different arrangement of variables:

$$\frac{\partial h}{\partial t} + \frac{\rho g}{\mu}\frac{\partial}{\partial x}\left[\left(-\frac{\partial h}{\partial x}\right)F\right] = 0 \qquad \text{(eq. 16)}$$

where

$$F = \frac{1}{6}(3h - h_0 - 2H)(h_0 - H)^2 \qquad \text{(eq. 17)}$$

and

$$h_0 = h - \frac{\tau_y}{\rho g}\left(\frac{\partial x}{\partial h}\right) \qquad \text{(eq. 18)}$$

where h is the free surface height and h_0 is the yield surface height and H the channel bottom height.

Chapter Three: The Smoothed Particle Hydrodynamics Method

The Smoothed Particle Hydrodynamics Method

3.1 Introduction

The ability of mesh free methods, among which is the Smooth Particle Hydrodynamics (SPH) method, to treat large deformations without dealing with difficulties of a twisted mesh has made such methods popular in the recent years. SPH is a method relying on conservation laws in which some clearly separate particles are followed in the continuum and kernel functions are used for the physical quantities to be interpolated (Rodriguez-Paz and Bonet, 2003). According to Rodriguez-Paz and Bonet (2003), in the SPH method particles having properties such as mass, velocity, density and position are used to discretize the continuum. Assuming that the particles move with the material velocity of the continuum, results in the construction of Langrangian type governing equations for this method. The partial differential equations are transformed into integral equations as a result of reproducing kernel approximation being used to assess the spatial derivatives of the sample points and particles.

The main purpose of this method is the interpolation of a certain function such as $f(x)$ based on equation 19 where it is evaluated by a kernel function $W(x, h)$:

$$f(x) = \int_D f(x')W(x - x', h)dx', \qquad \text{(eq. 19)}$$

which in terms of discrete particles will be:

$$f(x) = \sum_b^N f(x_b) W(x - x_b) V_b = f_h(x), \qquad \text{(eq. 20)}$$

where h is the smoothing length – a significance of the area around a particle in which the dynamics of the first particle are considerably affected by a second particle - and V_b is the volume associated with point b; or as Crespo et al. (2008) state:

$$f(x) = \sum_b^N m_b \frac{A_b}{\rho_b} W_{ab} \qquad \text{(eq.21)}$$

where m and ρ are the mass and density for particles 'a' and 'b' respectively and the kernel function is:

$$W_{ab} = (x_a - x_b, h) \qquad \text{(eq.22)}$$

On account of a kernel function being used to interpolate the values resulted for the sample particles, in addition to Crespo et al. (2008), who suggest the kernel function having to satisfy consistency, positivity and being monotonically decreasing, Swegle et al. (1995) also mention that the chosen kernel function has to satisfy the following requirements:

a. having delta function behavior, meaning that

$$\lim_{h \to 0} W(x, h) = \delta(x) \qquad \text{(eq.23)}$$

b. being normalized

$$\int W(x, h) dx = 1 \qquad \text{(eq.24)}$$

c. being zero everywhere except in the smoothing are

$$W(x, h) = 0 \quad \text{for} \quad |x| \geq 2h \qquad \text{(eq.25)}$$

While a general form for a kernel function is:

$$W(x,h) = \frac{\alpha}{h^{d_m}} f(\xi); \qquad \xi = \frac{\|x\|}{h} \qquad \text{(eq. 26)}$$

where d_m is the number of dimensions and α is a factor that ensures the satisfaction of the consistency condition $\int_D W(x)dx = 1$, Rodriguez-Paz and Bonet (2003) used the following form of the kernel equation to simulate debris flows:

$$(x,h) = \frac{3}{64h}\begin{cases}(2-\xi)^5 - 16(1-\xi)^5 & if\ 0 \le \xi < 1 \\ (2-\xi)^5 & if\ 1 \le \xi < 2 \\ 0 & if\ \xi \ge 2\end{cases}; \quad \xi = \frac{\|x\|}{h} \qquad \text{(eq. 27)}$$

where h is the smoothing length which would be an equivalent for an element in methods such as FEM. All the mentioned functions have a compact support of radius $2h$ which would be equal to the elements next to the sampled one.

Alternatively, Monaghan and Lattanzio (1985) developed the following spline kernel:

$$W(x,h) = \frac{1}{\pi h^3}\begin{cases}1 - \frac{3}{2}q^2 + \frac{3}{4}q^3 & if\ \ 0 \le q \le 1 \\ \frac{1}{4}(2-q)^3 & if\ \ 1 \le q \le 2 \\ 0 & otherwise\end{cases} \qquad \text{where} \quad q = \frac{r}{h} \qquad \text{(eq.28)}$$

r being the distance between the sample particles a and b.

A debris flow which is widely considered to perform as a Non-Newtonian Bingham plastic flow in a certain regime, it is comprised of two layers; the first and the upper layer is the plug layer where the material forming the debris are transported and the lower layer known as the shear layer where the other portion of the same material experiences shear (Rodriguez-Paz and Bonet, 2003).

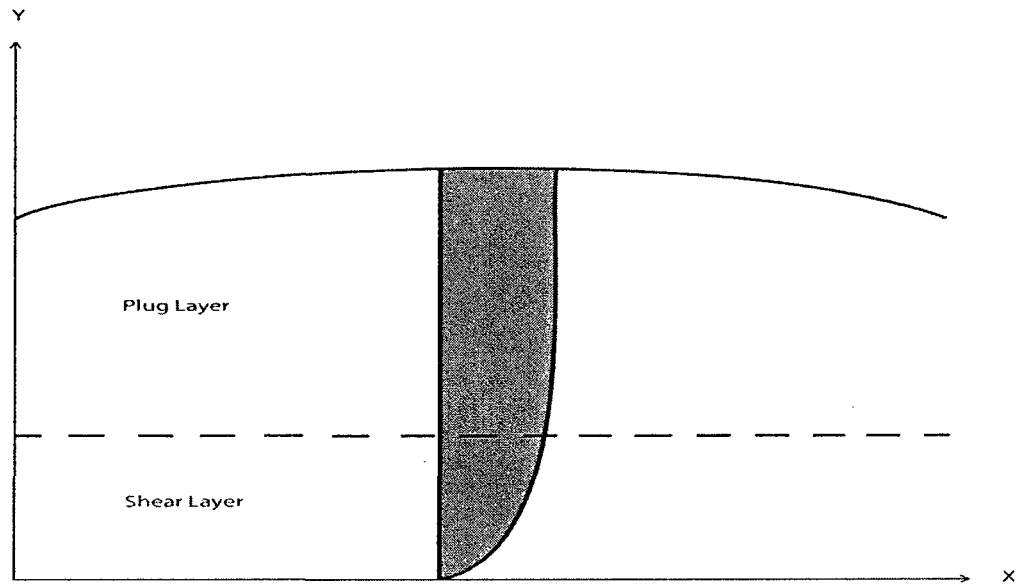

Figure 9. Uniform Bingham flow (Rodriguez-Paz and Bonet, 2003)

The Bingham model, which is shown in figure 9 and as mentioned before is:

$$\tau = \tau_y + \mu \frac{\partial u}{\partial x} \qquad \text{(eq. 29)}$$

τ_y being the yield stress, μ the viscosity and u the velocity in the 'x' direction. In a three dimensional case the same model would be:

$$\sigma = -p1 + \Phi_1 D \qquad \text{(eq. 30)}$$

where

$$\Phi_1 = \frac{\tau_y}{\sqrt{II_D}} + 2\mu \qquad \text{(eq. 31)}$$

and 1 in "$-pI$" being the unit tensor, D the rate of deformation tensor and Φ is the scalar function of the three principal invariants of $D(I_D, II_D, III_D)$ (Rodriguez-Paz and Bonet, 2003).

Pastor et al. (1999) expressed an equation derived from the original Bingham model introducing an exponent 'n' which covers the behavior of the fluid providing the ability to also cover some other types of Non-Newtonian fluids:

$$\tau = \tau_y + \mu\left(\frac{\partial u}{\partial x}\right)^n \qquad \text{(eq. 32)}$$

where for $n = 1$ the original Bingham model is described, for $n < 1$ a pseudo plastic behavior and for $n > 1$ a dilatant fluid behavior are described. As for its three dimensional equation it would be:

$$\Phi_1 = \frac{\tau_y}{\sqrt{II_D}} + 2\mu|4II_D|^{(n-1)/2} \qquad \text{(eq. 33)}$$

According to Rodriguez-Paz and Bonet (2003), more advanced equations have been introduced by adding a second order to the term D, as ζ which is the combined dispersive turbulent parameter, adding the turbulence and the inertial impact of the particles into the considerations:

$$\tau = \tau_y + \mu\frac{\partial u}{\partial x} + \zeta\left(\frac{\partial u}{\partial x}\right)^2 \qquad \text{(eq. 34)}$$

with

$$\zeta = \rho_m l_m^2 + \hat{a}_i \rho_s \lambda^2 d_s^2 \qquad \text{(eq. 35)}$$

ρ_m being the density of the mixture, l_m the mixing length, ρ_s density of the sediment particles, $\hat{a}_i$ Bagnold's empirical constant, d_s diameter of the particles and λ linear concentration which demonstrates particle size and concentration affecting the turbulent parameter.

3.2 Governing Equations

The equations in the SPH method are used to simulate the motion of interpolating points in the fluid, which are assumed as particles, using the properties of each particle such as mass and velocity.

3.2.1 Momentum Conservation Equation: A general form for the momentum conservation equation is as follows:

$$\frac{Dv}{Dt} = -\frac{1}{\rho}\nabla P + \boldsymbol{g} + \boldsymbol{\Theta} \qquad \text{(eq.36)}$$

where $\boldsymbol{\Theta}$ stands for the diffusive terms. Among different diffusive equations used to reach a momentum equation, the 'Artificial Viscosity' approach has been used by Monaghan (1994) and Crespo et al. (2008) which results in the following equation for particle '*a*' in SPH method:

$$\frac{dv_a}{dt} = -\sum_b m_b \left(\frac{P_a}{\rho_a^2} + \frac{P_b}{\rho_b^2} + \Pi_{ab}\right)\nabla_a W_{ab} + g \qquad \text{(eq.37)}$$

where $g = <0, -9.81, 0>$, P is the pressure and ∇ is the gradient of the kernel and

$$\prod_{ab} = \begin{cases} \frac{-\alpha \overline{c_{ab}} \mu_{ab} + \beta \mu_{ab}^2}{\overline{\rho_{ab}}} & v_{ab} x_{ab} < 0 \\ 0 & v_{ab} x_{ab} > 0 \end{cases} \qquad \text{(eq.38)}$$

and

$$\mu_{ab} = \frac{h v_{ab} x_{ab}}{x_{ab}^2 + \eta^2} \qquad \text{(eq.39)}$$

where 'x' and 'v' present the position and the velocity of the particle, $x_{ab} = x_a - x_b$, $v_{ab} = v_a - v_b$, $\eta = 0.01h^2$, 'c' is the speed of sound:

$$\overline{c_{ab}} = \frac{c_a + c_b}{2} \qquad \text{(eq.40)}$$

Monaghan (1994) suggests taking β = 0 and states that the phrase containing α in equation 38 contains both bulk and shear viscosity, however since there are such low changes in the density value as a result of the fluid being considered incompressible, the phrase almost totally represents shear viscosity. While Rodriguez-Paz and Bonet (2003) mention that 'α' typically has a value between 0.001 and 0.1, Monaghan (1994) states that it is commonly taken as 0.01.

Moreover, the rate of change in the thermal energy for each particle or the thermal energy per unit mass becomes:

$$\frac{du_a}{dt} = \frac{1}{2} \sum_b m_b \left(\frac{P_a}{\rho_a^2} + \frac{P_b}{\rho_b^2} + \Pi_{ab} \right) v_{ab} \nabla_a W_{ab} \qquad \text{(eq.41)}$$

3.2.2 Density and Continuity Equation: The SPH method is based on laws of conservation. According to conservation of mass law:

$$\frac{d}{dt} \int \rho dV = 0 \qquad \text{(eq. 42)}$$

The objective of using the SPH method is to reach a rate of change for density, find smoothed density for each particle and sum over the particles in the effective radius of a sample point.

$$\rho = \sum_b m_b W_{ab} \qquad \text{(eq.43)}$$

Since the fluid is considered incompressible, or to be easier to solve the problem, slightly compressible and for fluids such as water the density on a surface falls to zero (not continuously), to be able to avoid this artificial density decrease near the interfaces and have correct pressure values and make the calculations easier, Crespo et al. (2008) suggested using the following equations which assigns the same initial density to all the particles which only changes when they are in motion (Monaghan, 1994):

$$\frac{d\rho_a}{dt} = \sum_b m_b v_{ab} \nabla_a W_{ab} \qquad \text{(eq.44)}$$

3.2.3 Particle Motion: The rate of changes in the position of a particle '*a*' can be shown by:

$$\frac{dx_a}{dt} = v_a \qquad \text{(eq.45)}$$

However, in order to avoid particle penetration and keep the order of particles especially in a high speed flow, Monaghan (1989) proposed an XSPH variant 'Δ_a' which is used in other works such as Monaghan (1992) and Crespo et al. (2008) and will be added to the right side of equation 45:

$$\frac{dx_a}{dt} = v_a + \epsilon \sum_b \frac{m_b (v_b - v_a)}{\overline{\rho_{ab}}} W_{ab} \qquad \text{(eq.46)}$$

where 'ε' is suggested to be taken as 0.5 (Monaghan, 1989).

3.3 Constitutive Models Implementation

In order to be able to model a debris flow or a free surface flow adopting a proper constitutive model is necessary. In the corrected SPH (CSPH) method which is presented by Rodriguez–Paz and Bonet (2003), a constitutive model is needed to have the internal forces equation as well. For Non-Newtonian fluids with no memory, the same reference states the following general form:

$$\sigma = -p1 + \Phi_1(II_D, III_D)D + \Phi_2(II_D, III_D)D^2 \qquad \text{(eq. 47)}$$

Although this equation needs the fluid to be incompressive, some of the most accepted debris flow models are based on such a model (Rodriguez-Paz and Bonet, 2003).

Applying the corrections mentioned previously, the gradient of velocity can be evaluated using:

$$\nabla v_a = \sum_{b=1}^{N} V_b v_b \otimes \tilde{\nabla} \widehat{W}_b(x_a) \qquad \text{(eq. 48)}$$

Since the rate of the deformation tensor is:

$$D = \frac{1}{2}(\nabla v + \nabla v^T), \qquad \text{(eq. 49)}$$

therefore, having the value of the gradient of velocity, yields the deformation rate. Knowing the value of rate of the deformation tensor, a desired constitutive model such as Bingham model can be utilized.

3.3.1 Pressure Evaluation and the Equation of State: Despite the fact that pressure should be evaluated assuming the fluid being incompressible, assuming the fluid being

water and slightly compressible allows time integration and the evaluating equation will be (Rodriguez-Paz and Bonet, 2003):

$$p = P_{ref}\left[\left(\frac{\rho}{\rho_0}\right)^{\gamma} - 1\right] \qquad \text{(eq. 50)}$$

where ρ and ρ_o are the current and initial densities for any particle, P_{ref} is an artificial compressibility modulus (high enough to ensure realistic simulation) and for water 'γ'is equal to 7 (Monaghan, 1994) and therefore according to Crespo et al. (2008), 'ρ_o' is taken as 1000 ($kg{\cdot}m^{-3}$).

To determine the value of P_{ref} both Rodriguez-Paz and Bonet (2003) and Monaghan (1994) have suggested using the speed of sound in the fluid:

$$P_{ref} = \frac{\left(\frac{v_{max}}{\alpha}\right)^2 \rho}{\gamma}; \qquad v_{max} = \alpha c \qquad \text{(eq. 51)}$$

where 'α' has a value between 0.001 and 0.1 [0.01 suggested by Monaghan(1994)] and the speed of the sound 'c' for such equation of state is:

$$c = \sqrt{\frac{\gamma P_{ref}}{\rho}} \qquad \text{(eq. 52)}$$

According to Crespo et al. (2008), it is also possible to calculate P_{ref} from the following equation:

$$P_{ref} = \frac{c_0^2 \rho_0}{\gamma} \qquad \text{(eq.53)}$$

where 'c_o' is the speed of sound at the reference (initial) density.

3.3.2 Boundary Conditions: For the boundary friction to come into account the boundary is discretized into line segments and using algorithms, the penetration of particles into the boundary and the forces interacting on each particle during the contact are detected (Rodriguez–Paz and Bonet, 2003). According to a restitution coefficient a force normal to the boundary affects the normal velocity of a particle. There is an impulse to a particle, which is a tangential drag force proportional to the dynamic friction coefficient μ_f.

$$\mu_f = \tan \delta_f \qquad \text{(eq. 54)}$$

where δ_f is the bed friction angle.

The tangential and the normal velocities of a particle are affected by the mentioned tangential and normal forces. The penetrating particle's position in the boundary is calculated according to its normal distance from a boundary. Then it is assumed that the particle will bounce back from a rigid boundary and an energy loss is calculated according to the friction and restitution coefficients 'e'. The particle will bounce back with a momentum which is defined by the new velocity which is the result of the impact. The normal velocity is calculated according to 'e' and μ_f (Rodriguez-Paz and Bonet, 2003).

Crespo et al. (2007) have applied a Dynamic Boundary condition in which the governing equations for fluid particles must be applied and satisfied by the boundary particles. The only exception to this condition is the equation of motion with the XSPH correction since the boundary particles are considered to be fixed and stationary unless external forces exist. According to this method when a particle approaches a wall of boundary particles in an order that the distance between the fluid particle and the boundary

particles becomes smaller than 2h, the density of that part increases (continuity equation: eq.44) and therefore, the pressure will be increased (equation of state: eq.50). To calculate this pressure a 'Normalized Pressure Term' is introduced:

$$NPT_Z = \frac{\left(P/\rho^2\right)_Z}{\left(P/\rho^2\right)_R} \qquad \text{(eq.55)}$$

where 'Z' is the distance between the approaching fluid particle and the boundary particles and 'R' is the minimum distance between them.

3.3.3 Kernel Corrections for Density Reinitialization: The aforementioned conditions and equations result in fluctuations in the pressure value. To correct such inaccuracy in the data, several corrections have been made to the kernel function by different scholars. Colagrossi and Landrini (2001) applied two correction orders to the kernel by re-assigning density values to each particle in different time steps; the Shepard filter and the Moving Least Squares approach.

3.3.3.1 The Zero Order: The zero order actually applies a filter (Shepard Filter) over the density to help re-assign new values to the density field in specific periods. This is done by applying a correction to the original kernel every 30 time steps:

$$\rho_a^z = \sum_b m_b \acute{W}_{ab} \qquad \text{(eq.56)}$$

where ρ_a^z is the new density for particle 'a' and $\acute{W}_{ab}$ is the corrected kernel which is calculated by:

$$\acute{W}_{ab} = \frac{W_{ab}}{\sum_b W_{ab} \frac{m_b}{\rho_b}} \qquad \text{(eq.57)}$$

3.3.4 Time Stepping: In order to apply a time stepping to the governing equations, the Verlet algorithm is used in this work. The algorithm is written in two parts for the position of the particles, one for the next step and one for the previous step:

$$v_a^{n+1} = v_a^{n-1} + 2\Delta t F_a^n \qquad \text{(eq.58)}$$

$$\rho_a^{n+1} = \rho_a^{n-1} + 2\Delta t D_a^n \qquad \text{(eq.59)}$$

$$x_a^{n+1} = x_a^n + \Delta t V_a^n + 0.5\Delta t^2 F_a^n \qquad \text{(eq.60)}$$

$$u_a^{n+1} = u_a^{n-1} + 2\Delta t U_a^n \qquad \text{(eq.61)}$$

where $F_a = \frac{dv_a}{dt}$, $D_a = \frac{d\rho_a}{dt}$, $V_a = \frac{dx_a}{dt}$ and $U_a = \frac{du_a}{dt}$.

To stop the time integration diverging, variables are calculated in the following way every N time step:

$$v_a^{n+1} = v_a^n + \Delta t F_a^n \qquad \text{(eq.62)}$$

$$\rho_a^{n+1} = \rho_a^n + \Delta t D_a^n \qquad \text{(eq.63)}$$

$$x_a^{n+1} = x_a^n + \Delta t V_a^n + 0.5\Delta t^2 + F_a^n \qquad \text{(eq.64)}$$

$$u_a^{n+1} = u_a^n + \Delta t U_a^n \qquad \text{(eq.65)}$$

and N is a time step on the order of 50 (Gesteira et al., 2008).

3.3.5 Time Step Control: The suggested variable time step is calculated according to the equations Monaghan and Kos (1999) proposed and depend on the Courant-Friedrichs-Lewy (CFL) stability condition, the force terms and the viscous diffusion term (Crespo et al., 2008):

$$\Delta t = 0.3 min(\Delta t_f, \Delta t_{cv}) \qquad \text{(eq.66)}$$

where

$$\Delta t_f = min\left(\sqrt{\frac{h}{|f_a|}}\right) \text{ (eq.67)} \quad \text{and} \quad \Delta t_{cv} = min \frac{h}{c_s + max\left|\frac{h v_{ab} x_{ab}}{x_{ab}^2}\right|} \qquad \text{(eq.68)}$$

In the above equations Δt_f is based on the force per unit mass f_a where the forces are all the forces acting on particle 'a' following the momentum equation and Δt_{cv} combines the Courant and the viscous time step controls (Crespo et al., 2008).

3.4 Algorithm for the Two Dimensional SPH Free Surface Flow

Rodriguez-Paz and Bonet (2003) presented the following algorithm for SPH free surface solver:

1. Evaluate initial values: $\rho_{0,a}$, m_a, h_a.
2. Find the new density for current time step (eq.44, eq.59 and eq.63).
3. Evaluate the pressure using equation of state (eq.50).
4. Find internal forces based on constitutive behavior (eq.30, eq.34 and 46).
5. Evaluate external forces such as self weight and boundary forces.
6. Assemble equation of motion.

   Newton's second law is used in this step which can be written as:

$$F_a - T_a = m_a a_a \qquad \text{(eq. 69)}$$

where F represents the external forces and T represents internal forces due to current state of the material.

7. Update particle positions and find new velocities.
8. Output results for current time.
9. Repeat steps 2 to 8 if $t \leq t_{max}$.

Chapter Four: Numerical Simulation of Tailings Flow

Numerical Simulation of Tailings Flow

4.1 Introduction

The simulation task required a modeling solution which could simulate liquids. It also had to take tailings properties into consideration and more importantly could simulate a Non-Newtonian fluid such as tailings. It had to have the capacity of simulating particle movements in the continuum and demonstrating the effects of changes in key parameters engaged in the flow of the fluid being simulated. Therefore, RealFlow 4 was chosen to be used as the simulation tool. It could also provide the user with an option of defining and simulating the fluid in both three and two-dimensional environments.

4.2 Real Flow

Real Flow is a fluid flow and general dynamics simulation software. It consists of a standalone program and a set of plug-ins by which the data can be imported and also exported to some other graphical software. It can be used to simulate fluids, water surfaces, fluid-solid interactions, rigid bodies and soft bodies and provides the option of adding meshes to the model meshes. In order for the user to increase the program's capabilities, overcome some possible limitations and to have more control on different aspects of the program the creators have used Python as the scripting language.

As used in RealFlow4, the SPH method assigns various properties such as density and mass to the particles to control the continuum and develops the simulations based on particle interaction. It also does not require a predefined mesh to calculate properties and movement of the continuum. Common material properties can be assigned to particles and the governing equations of SPH stated in the previous chapter apply to them:

4.2.1 Density: A change in the density (kg/m^3) of the fluid affects the density of a particle proportionally and therefore the behavior of a continuum can be influenced and controlled in this way.

- **Resolution and Mass:** A parameter that directly cooperates with the density in RealFlow is resolution. The higher the resolution is, the lower is the mass (kg) of particles and the lighter are the particles, while an increase in the density has an opposite effect.

4.2.2 Internal Pressure: The forces between a group of adjacent particles are represented by internal pressure. The higher the internal pressure is, the higher is the interaction between the particles and as a result the distance between the particles increases and the volume occupied by the mass of particles becomes greater.

4.2.3 External Pressure: In order to keep the particles together and prevent the flowing fluid from expanding, RealFlow uses external pressure. This is a force which is exerted on the model. The force increases as the value of external pressure increases.

For both pressure types above the values are between 0 and 1.

4.2.4 Viscosity: Viscosity is a dimensionless parameter in RealFlow. Thin fluids such as water are represented by values between 1 and 5. The thicker the fluid is the higher the

value for viscosity will be. However, these values do not represent the physical viscosity of such fluids.

4.2.5 Surface Tension: Adding surface tension to a simulation in RealFlow will result in an increase in the cohesion between the particles in the fluid skin and will also be an asset in simulating high viscous fluids.

The most basic and fundamental components of a RealFlow model are emitters and daemons. Emitters which come in a range of different shapes generate fluid particles and the basic behavior of the fluid is actually controlled by them (Botella et al., 2006). The fluid is generated by producing particles for which the properties are defined by aforementioned parameters. The maximum number of particles emitted can be defined to reach the desired simulation result.

"Daemon" is a term used to define forces in RealFlow. Adding a daemon to the simulation model will result in exerting a force on all or a part of the particles which are included in the model (Botella et al., 2006). A gravity daemon, as an example, will add the gravity force to the forces which have to be computed for each particle. One other kind of daemon which is called a killer daemon uses boundaries for the simulation model to eliminate the particles which do not have the desired condition or location. It in other words "kills" them and as a result there is no more computation or graphical results for these particles (Botella et al., 2006).

A 'view from above' scene from RealFlow 4 is shown in Figure 10. It demonstrates flow of tailings in a flume after the gate to the reservoir (vertical line in the middle) was lifted. The numbers at the bottom of the figure represent the simulation time (ST) up to this specific scene and the corresponding actual time (TC) for the physical flume test which is modeled.

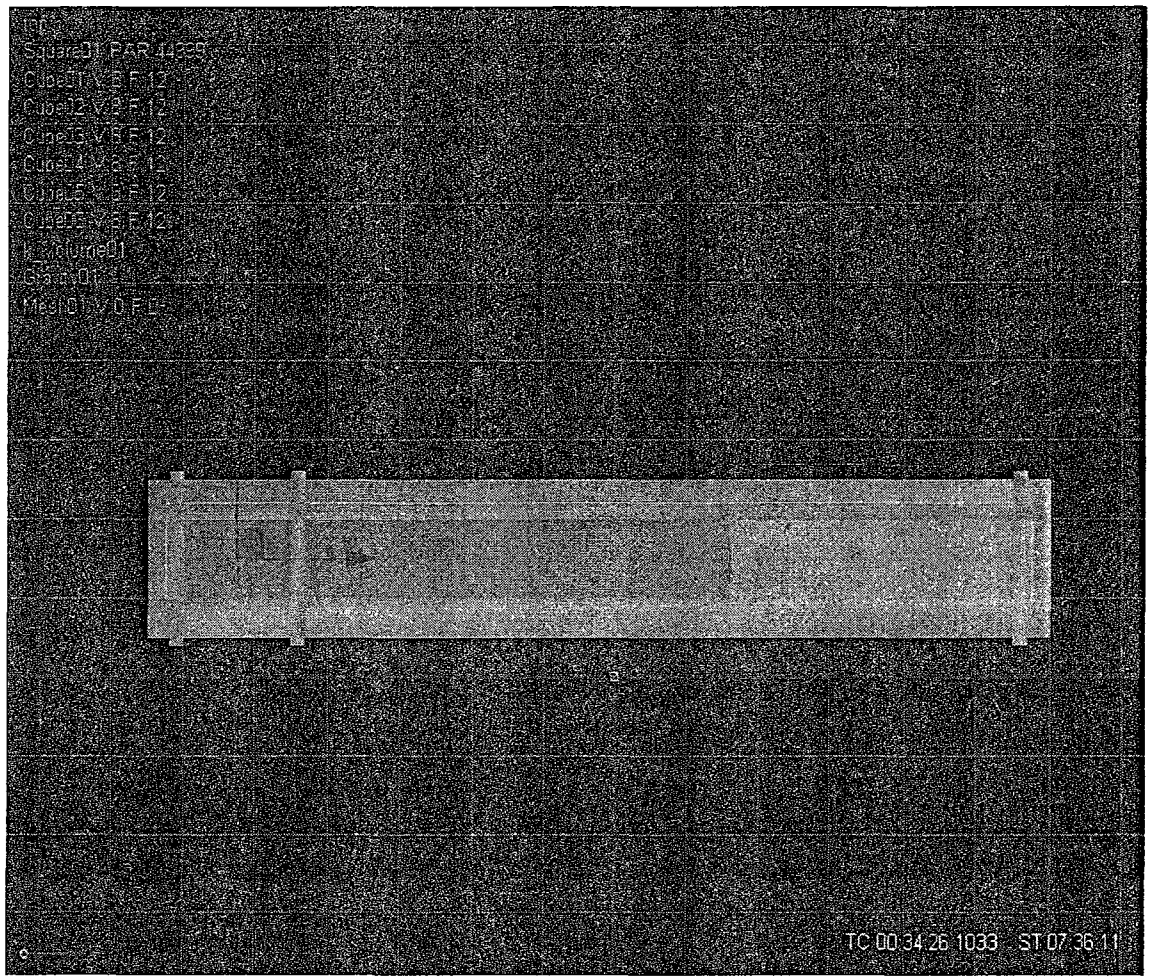

Figure 10. Sample scene from RealFlow 4

Chapter Five: Model Calibration

Model Calibration

Several tests were run in RealFlow with the target of becoming familiar with the program's environment and studying the effects of changes in the values assigned to terrain and fluid properties, with fluids not necessarily having tailings properties. It was concluded that the values assigned to some key characteristics of flow such as viscosity are not very realistic or the changes in values such as density do not show the expected physical results. This fact emphasizes the necessity of performing a program calibration.

5.1 Variables in Calibration Tests

As there are some properties which play key roles in the movement of fluids, in this case tailings, and there are also a few of them which are effective in the simulation process in RealFlow, the following properties were chosen as the variables in the program calibration:

5.1.1 Density: One of the most important aspects in the movement of the fluid which can have a behavioral control is the density. Density is the proportion of mass over volume. For a constant volume as the number of particles increases in the fluid and it becomes denser the interaction between the particles also increases in number. Density in RealFlow is one of the few parameters that has the physically accurate value and dimensions. Since the default value for density in RealFlow is for water, and the tailings have higher values, knowing that there are several types of tailings with

different densities a range of values for the density which represents the density of tailings had to be found. As a result density was chosen to be one of the variables in order for the effects of changes in the density to be studied.

5.1.2 Resolution (Spatial Resolution): As mentioned in the previous section, resolution and density have a close relationship in RealFlow. The higher the density is the higher the resolution should be in order to achieve better results. In situations where there is a great difference between the density and the resolution, especially where the resolution appears to be lower than the expected value in coordination with density the result of the simulation could be rather vague.

Density and resolution have opposite effects on the mass of the particles. The higher the density is the heavier is the particle, however, if the resolution increases the particles become lighter.

In addition, there is a parameter called ***Maximum Particle*** in the program by which the number of the particles and as a result, in relation with the density and the resolution, the volume of the fluid can be controlled.

5.1.3 Viscosity: Viscosity is the resistance of the fluid against flow or deformation which is normally caused by shear stress. Viscosity is a type of internal resistance of the particles in the fluid against flow which has a direct effect on the behavior of the fluid. The degree of liquidity of the substance is higher and its movement is easier if the viscosity is low. Since RealFlow is a particle based simulation program this parameter plays a key role in the results of the simulations.

The default value for viscosity in the program which is assumed for water is not representative of the real viscosity of water and the value is an arbitrary chosen value and is therefore considered dimensionless. Therefore, it was important to test a range of

values for the viscosity to reach a value or a range of values which provide the closest result to the real world processes for the simulations.

5.1.4 External Pressure: External pressure is a parameter used only in RealFlow which represents a force which is exerted on the whole system and collection of particles in order to keep them closer to one another. Raising the value of external pressure results in the particles being more attached to one another and prevents splashes from happening frequently. Due to the fact that the simulated fluid was tailings, and tailings are closer to a paste like substance rather than water, having an external pressure value greater than the internal pressure, which causes interactions between the particles resulting in the easiness in the particles being separated from the continuum, to keep the particles closer to one another produces the simulation of a material closer to tailings.

5.1.5 Friction: Friction is a force which prevents two surfaces from moving on each other easily and smoothly which acts in the opposite direction of the movement. This parameter is a property of the terrain in the case studies or one of the properties of the plane on which the fluid is moving on or is in contact with in RealFlow. This property of the environment has a direct effect on the speed at which the tailings move forward in the simulation or surge after a dam break and also on the distance up to which the tailings move forward and the distance they reach.

5.1.6 Roughness: One of the other properties of the terrain is the roughness which represents the unevenness of the surface or the heterogeneity of the material the terrain is consisted of. Roughness not being a force itself, affects the fluid by causing friction forces to be created. Therefore the result of the effects of the roughness on the fluids movement or the distances it covers is similar to the ones produced by friction. The

main effect roughness has on the particles, which makes it different from friction, is making a slight variation in the direction of the particles when they collide with the surface for which roughness has been defined. This provides the option of avoiding perfect and symmetrical collisions.

One other parameter which was not kept at the default value assigned by RealFlow and was changed was the ***stickiness.*** This parameter is also one of the properties of the terrain or the plane the fluid runs on and determines the extent to which the fluid particles become attached to the surface of the terrain or are slowed down as a result of the surface being sticky. The value of stickiness in RealFlow can be chosen between 0 and 1. Since the odds of having a sticky terrain where the tailings flow are low therefore a low value (0.1) was assigned to stickiness in all the performed simulations.

5.2 Calibration Tests

To apply correct values to the abovementioned parameters in order to have a realistic simulation, a suitable real life project or phenomenon by which the simulation program, RealFlow, could be calibrated had to be utilized. The research had to be on the characteristic of tailings related to the purpose of this study such as the 'angle of repose' or the 'covering distance'. Utilizing a reference project a form of a simulation would be created that could provide useful calibrating information regarding the changes in the values of the parameters such as density and viscosity by changes in the simulation results. The reference project was chosen to be the flume test for tailings which was performed by Crowder (2004). Several tests were performed by Crowder on three different tailings pastes, retrieved from Bulyanhulu gold mine, in order to examine their

characteristics. The first paste, or paste A, was made using the ores taken from the mine during the first developing stages of the mine. The second paste, or paste B, was taken from the mine's paste plant at a later time and the third paste, or paste C, was taken from the same place as paste B a year later.

Among the test performed on the pastes, a number of flume tests were performed on pastes A and C and paste B was left out due to insufficient amount of paste available. The flume tests were performed on two different states of the tailings pastes, 'As Received Paste' and 'Deflocculant Added Paste'. The tests were run in a flume shown in Figure 11 which consisted of a box with the length of 2.30m where the first 0.30m was used as the reservoir and was separated from the 2m run out length with a lift gate.

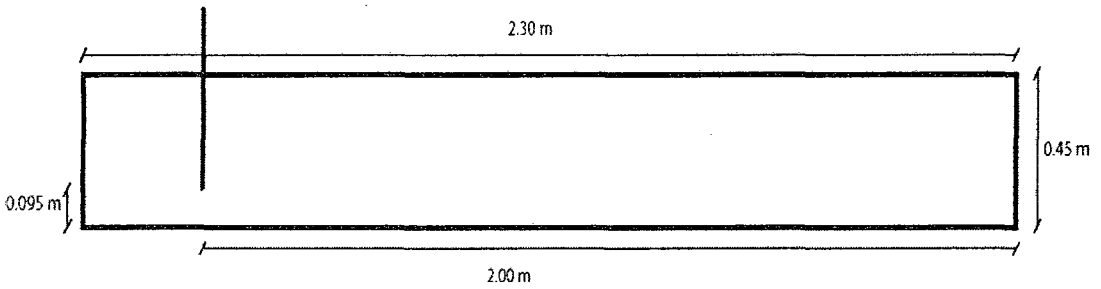

Figure 11. The side view of the flume used in the tests

The tests would start by filling the reservoir with the tailings sample up to the height of 0.20m. It was then when the vertical lift gate was lifted to the height of 0.095m quite rapidly in order for the whole freed plane to be able to react at the same time. While the tailings paste was running along the run out length of the flume the distance covered, the angle of the tailings stack with the horizontal plane and the speed at which the stack

was moving were monitored and finally at the end of the test, where the paste would come to a rest, the angle of repose, the height and the run out distance were measured. To calculate the angle of repose for the material at rest the data collected from each test was put into an equation introduced by Sofra and Boger (2001) with the assumption of the surface profile being linear:

$$\theta_r = tan^{-1}\left(\frac{H_1 - H_2}{L}\right) \qquad \text{(eq. 69)}$$

where θ_r stands for the angle of repose for the material at rest, H_1 and H_2 are the heights of the material at the beginning of the run out length which is the gate and the toe of the flowing material when it comes to rest respectively and L is the distance the paste has covered from the gate to come to a stop. Since Crowder's flume test where performed with different water contents for the tailings paste, therefore a sample of the paste was also taken from the toe after each test was finished.

Based on Crowder's research, a similar flume was created in RealFlow in order to perform the same tests to calibrate the program by comparing the results obtained from the tests with the ones in the reference research. It has to be mentioned that due to the program's using the SPH method to calculate the interactions between particles and also between the particles and the surface of the container, the higher the values for the aforementioned variables, as the main RealFlow and physical calibrating parameters, are the longer the simulation time will be. Therefore, the majority of the tests run in this program took long time (from 7 hours to even a week) in order to let the paste come to a rest and the simulation finish completely. Therefore, lack of time was an important parameter which prevented having as many runs as possible and reduced the number of simulations.

Moreover, the arbitrary essence of most of the parameters in the program such as viscosity, results in using some assumptions and unrealistic values for the paste characteristics to define the fluid.

The calibrating tests were performed in three different ways. In other words, three different assumptions were made to perform three series of simulations:

1. The first series of simulations were run with the aim of achieving an overall understanding of the general regime of changes in the angle of repose or the covered distance with the fluctuation in aforementioned core parameters of the fluid and the program. Considering this goal some ranges of values were chosen for the parameters. According to the program's instructions about the resolution stating that the ideal resolution for the simulations without changing the scales in the platform is a value between 1 and 10, the value of 5 was chosen for this series of simulations. It was not too high to take plenty of time for the program to process each simulation and it was not too low not to serve the goal of simulation correctly and vividly.

   As the value of the density of water being 1000 kg/m^3 was actually correct in the program therefore the assumed values from tailings started from 3500 kg/m^3 and units of 500 kg/m^3 were used to increase the value for the next tests. This value was selected due to the general definition and combination of tailings presented in the first part of this work in comparison to the standard density value for water.

   External pressure was another factor considered in this series. The value is by default set to 1 as the minimum value and equal to the internal pressure in RealFlow. In addition to this value some higher values were also tested in this

part of simulations with the goal of exerting more pressure on the particles as a whole and keep the particles together and have fewer chances to get separated from the whole body of particles as in a tailings-like rather than a water-like movement.

Viscosity is one of the parameters in RealFlow which has not been assigned a realistic value. As most of the example simulations shown in RealFlow using the default values are performed to simulate water, therefore it is assumed that the default value 3 is for water with the actual viscosity of 1.002×10^{-3} N·s/m^2. Therefore, the minimum value taken for viscosity was 20 which corresponded to a viscosity value of approximately 7×10^{-3} N·s/m^2 and it was increased in units of 5.

As for friction and roughness of the terrain, the default arbitrary values assigned were 0.001 and 0.0001 respectively. Since the type of surface in the final simulations was going to be the land behind a tailings dam, the values assigned to these parameters were decided to be increased. The minimum value for friction was decided to be 0.2 and the value of 0.1 was assigned to roughness.

Bounciness is a factor that does not have a large value with regards to the terrains that tailings pastes were going to move on. As a result, the default arbitrary value of 0.25 was decreased to 0.1 to create a potentially realistic simulation model.

To simulate the flow with the correct amount of tailings paste in the reservoir a specific number of particles had to be chosen for each simulation to which the density and the resolution are directly proportional.

When the reservoir was filled with the tailings paste with the desired properties and the simulated material would come to rest, the gate was lifted to allow the paste to flow in the created flume under gravity. Finally, when as a result of the interactions between all the forces it would come to rest, the distance covered, the height of the paste at the gate and the height of it at the toe were measured and after that using equation 69 the angle of repose would be calculated for each simulation.

2. Having performed the first series of tests and understanding the general behaviour of changes in the simulation results as a matter of random factors in the previously defined range, the second series of simulations were run with the goal of finding the effect of changes in the individual parameters on the result of the tests. In this case, the effect of these changes, such as increases in the value of density or viscosity, on the angle of repose or the distance covered by the tailings whether the value increases or decreases can be studied and analyzed.

   To serve the purpose of the test the value of one of the individual parameter was considered as variable and the values for the rest of parameters were taken as constant. In this way, as the variable parameter would change, its effect on the angle of repose and the distance would be observed. The second series of test were performed in three sections to study the effect of changes in a single variable.

   a. The first section was performed with the density being the variable. Having an assumed range for density of tailings made it necessary to be taken as one of the major variable parameters. Thus, the behavior of the paste under different values of density and the effect of the particles having different

weights and being slightly different in numbers in various tests could be observed. Due to the paste-like characteristic of the type of tailings being simulated the range of values chosen for density was 3000 kg/m^3 to 4500 kg/m^3.

b. Taking viscosity as a variable parameter was the second section of these series of tests. Different types of tailings have different viscosity values. Therefore, the effect of the paste changing from being a bit more viscous to being far more viscous than water was necessary to be observed. The values assigned to variable density and viscosity were integers ranging from 10 to 35 increasing steadily with the same pattern from the lowest to the highest one.

c. As friction and roughness are both related to the terrain and the surface the paste is running on and they both almost have the same effect on the paste and its movement, since roughness will also affect the paste by exerting a friction force, it was decided to take the same values for both friction and roughness. In other words, the two similar parameters were considered as one. Since it was observed that changes in the roughness or friction of the terrain is directly proportionate to the time the paste takes to advance in the running length and the ease of the movement of the paste on the surface, it was decided to take the two mentioned parameters together as the third variable parameter in the third section of these series of the simulations. The tests started with lower values (starting from 0.2 which was yet higher than the default values) being assigned to the parameters and continued with

regular steady increases in the values with the maximum friction and roughness of 0.7.

As for bounciness the default value of 0.25 was decreased to 0.1 to create a more realistic simulation model.

Having assigned the desired values to the parameters, the second series of tests was performed using the same procedure as the first series.

3. The third series of the tests were conducted while the previous test results on how individual parameters affect the flow of the tailings paste were observed. Since the goal of all the performed tests was to be able to calibrate the program and gain the knowledge of simulating samples of tailings with various properties, the data which had been collected so far was not sufficient. The already obtained data and results were only taken by deliberately changing the values by adding or deducting predefined equal units or by keeping the rest of the parameters constant. This approach would not provide a complete control over the fluctuation of the values assigned to the parameters. For this problem to be solved the risk of taking any random numbers within the aforementioned specific defined range of input data (values) for the parameters had to be taken. This means that if the input data range for the density was between 3000 kg/m^3 and 5000 kg/m^3, starting the tests with the lowest value and adding 500 kg/m^3 or such units to the data for the next tests would also be considered as having control over the input data and does not cover all the values in the range.

   A suitable solution to overcome the stated problem was to utilize a Monte Carlo simulation method. "A Monte Carlo method consists in formulating a game of chance or a stochastic process which produces a random variable whose expected

value is the solution of a certain problem" (Bauer, 1958). To utilize the Monte Carlo method, a range or domain of input data has to be defined. An equation is then used to generate random values and consequently the effect of changes in the values of parameters and its distribution and sensitivity in the result of the simulations, the angle of repose at rest and the distance covered by the tailings, is achieved.

The following equation was used to obtain the random values for the variables:

$$x_i = \mu + \sigma(y_i^{0.1349} - (1 - y_i)^{0.1349})/0.1975 \qquad \text{(eq. 70)}$$

where 'y_i' is a random value and is confined as: $0 \leq y_i \leq 1$.

The abovementioned equation is a form of Generalized Lambda distribution (GLD) which is useful in performing a series of Monte Carlo simulations (Fournier et al., 2006). It has the general form of:

$$x = \lambda_1 + (p^{\lambda_3} - (1 - p)^{\lambda_4})/\lambda_2 \qquad \text{(eq. 71)}$$

'x' as a function of 'p' and 'λs' is a GLD when $p \in [0,1]$. Having the values of the 'λs' provides the data with which a histogram of the simulated values can be obtained which facilitates achieving a general knowledge of the population under study. 'λ_1' and 'λ_2' are parameters which define location and scale, 'λ_3' defines the asymmetry or skewness and 'λ_4' the kurtosis or flatness of the histogram (Headrick and Mugdadi, 2005). It is rather challenging to reach correct data for the 'λs' and therefore there are computer programs such as LambdaFinder to facilitate data collection (Fournier et al., 2006).

Due to the fact that the aim of performing the third series of tests was to observe the results of simulations with random values for tailings properties, the ranges for the values assigned to the properties of tailings were chosen to be the same

as the second series of tests to have the same set of data for both series of tests. The mean values were selected as the average of the extremes of the ranges since the extremes were selected as the maximum and minimum of the possible values for the properties therefore the values between the extremes were more representative of the possible values. The standard deviation for the values assigned to the properties, which represents the possible existing variation of the values from the mean, was selected to be half of the difference between the extreme value and the mean due to the fact that the values for properties of the tailings are expected to be closer to the mean values than to the extremes.

Having determined the mean values and the standard deviations of the simulated tailings properties, equation 70 was applied to all the parameters included in each of the tailings paste movement simulations and random values within the range defined for each parameter was generated. Each of the obtained values from the equation was then used as input data with the random values obtained for other parameters and eventually run out distance and angle of repose values representative of each series of random values were obtained.

For random values to be calculated for each parameter using the above mentioned equation 'μ' is the mean value of the parameter such as 22.5 for the viscosity and 'σ' is the standard deviation of the values assigned to the same parameters such as 6.25 for viscosity.

These defined values represent a frequency versus value diagram for each parameter which is similar to a parabola with the focus on the top known as a Gaussian function. The peak of the diagram is the value of the parameter which most frequently occurs and the distance from the axis of symmetry to the point

where there is a significant change in the slope of the bell curve at either side is twice the value of standard deviation (Figure 12). Due to the fact that the third series of tests were performed by assigning random values to parameters to find the mean value and the distribution of other values around the mean, based on Gaussian distribution, the values showing the frequency of the calculated values obtained for angles of repose and run out lengths were expected to form a diagram with the same pattern as well.

In these series of tests density, viscosity and resolution as fluid and program parameters and friction and roughness as terrain characteristics were taken as variables and relative credible ranges of input data were assigned to them.

Friction and roughness were given the same values and the two similar parameters were considered as one and bounciness was set to 0.1 to create a more realistic model.

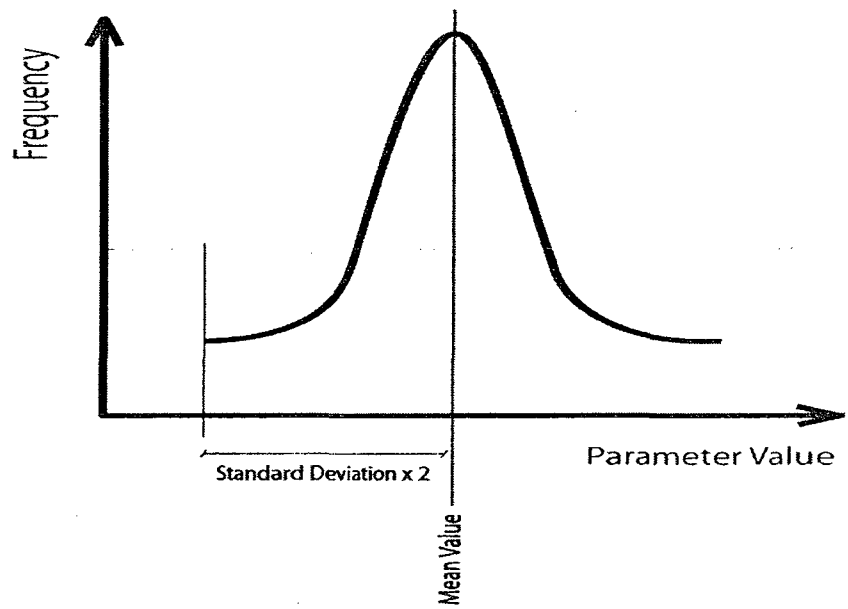

Figure 12. The diagram representing Monte Carlo simulation

Similar to how the first and second series of simulations were run, when the appropriate number of particles was chosen and the reservoir was filled with the tailings paste with the desired properties and the simulated material would come to rest, the gate was lifted to allow the paste flow in the created flume under the gravity force and finally when as a result of the interactions between all the forces it would come to rest, the run out distance, the height of paste at the gate and at the toe were measured and after that, using equation 69, the angle of repose would be calculated for each simulation.

5.3 Flume Test Results

5.3.1 Tests with Randomly Chosen Values

The first series of tests were performed with random numbers for the major parameters in RealFlow with predefined equal increases in the values in order to examine how differently the program simulates tailings with different properties. The followings are the input data:

Table 2. Input data for the first set of calibration tests

Test	Resolution	Density (kg/m^3)	Viscosity	External Pressure	Friction	Roughness	Bounce
A	5	4500	25	3	0.4	0.2	0.1
B	5	4000	20	2	0.4	0.2	0.1
C	5	4500	25	1	0.4	0.2	0.1
D	5	4500	20	1	0.3	0.15	0.1
E	5	4000	20	1	0.3	0.15	0.1
F	5	3500	20	1	0.2	0.1	0.1

The high values for density, viscosity and external pressure suggested that the speed at which the paste would advance would decrease as the time passed. The followings are the diagrams obtained in the tests:

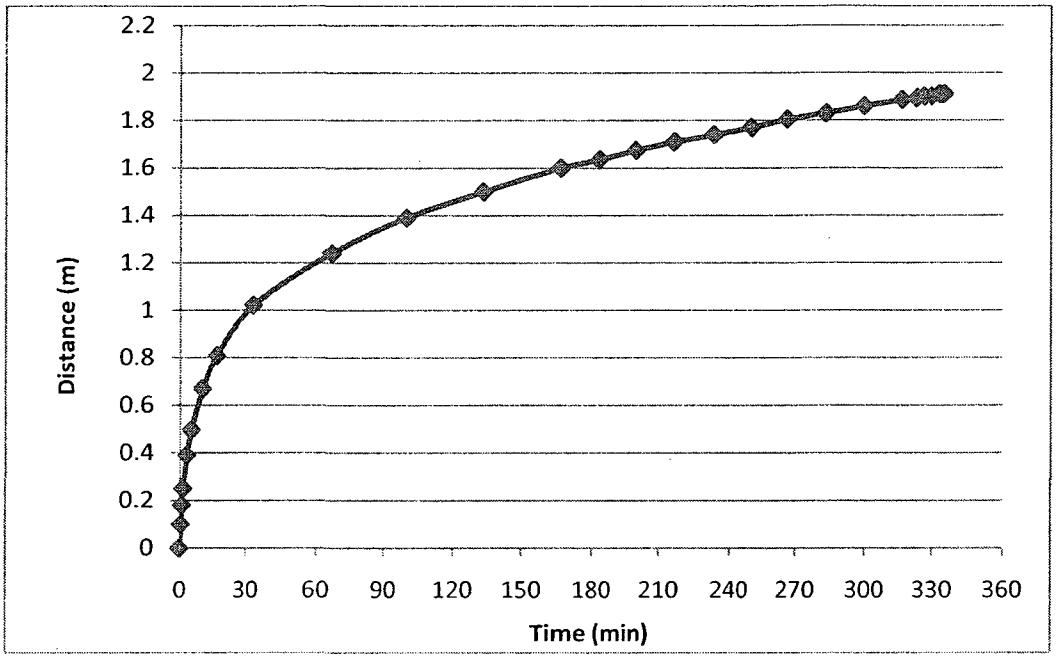

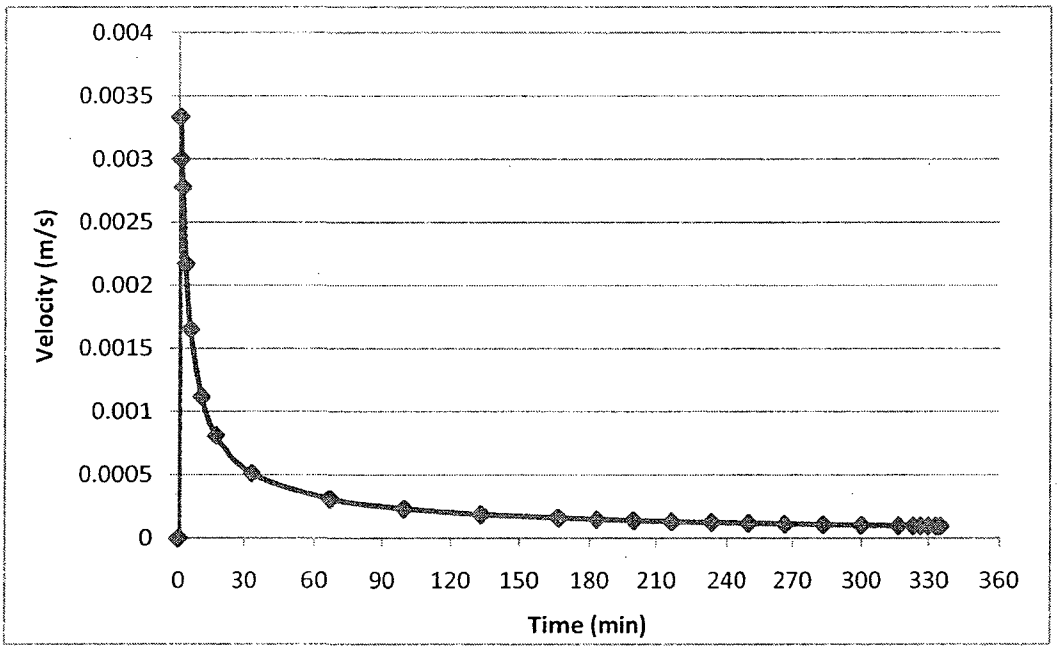

Figure 13. Diagrams of distance and velocity versus time for Test A

It was observed that during the initial moments of the simulation gravity has a significant effect and drives the paste out of the reservoir and forces it to run on the flume surface. The slope of distance versus time diagram for the first 10 minutes and the

fact that the paste travelled for almost half of the flume length in a half hour confirms that the resisting forces such as friction and the viscosity of the paste were not as influential in the first stages of the test. As time passes, the effect of resisting forces are more visible than before and as it is seen in the velocity versus time diagram as gravity, which lets the paste advance wears out, the sudden fall in velocity is finished and the value of the velocity falls to a slow, but almost constant value. The same pattern was observed in the rest of the tests for this part.

As time passed the corresponding data was collected in shorter intervals in all the tests to observe the changes in the velocity and density as the tailings moved closer to the end of the flume. Therefore, an accumulation of data is visible in the diagrams for the last minutes of the experiments. It has to be mentioned that in all the diagrams the corresponding time for velocity and density is the time it will take for the tailings to travel the distance to the end of the flume in the physical experiment and is not representative of the simulation time. Since the tailings selected for the experiment had a paste-like characteristic, the time taken for it to travel the distance to the end of the flume, as is shown in all the diagrams, is much greater than a fluid with low density or viscosity.

Figure 14 shows the diagrams obtained from Test B in which the values for viscosity, density and external pressure were decreased.

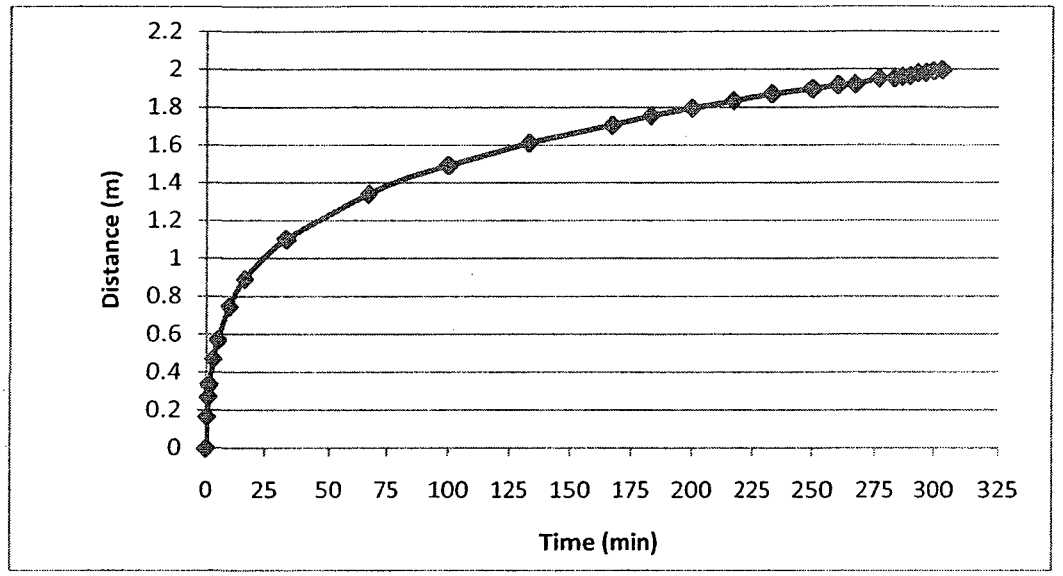

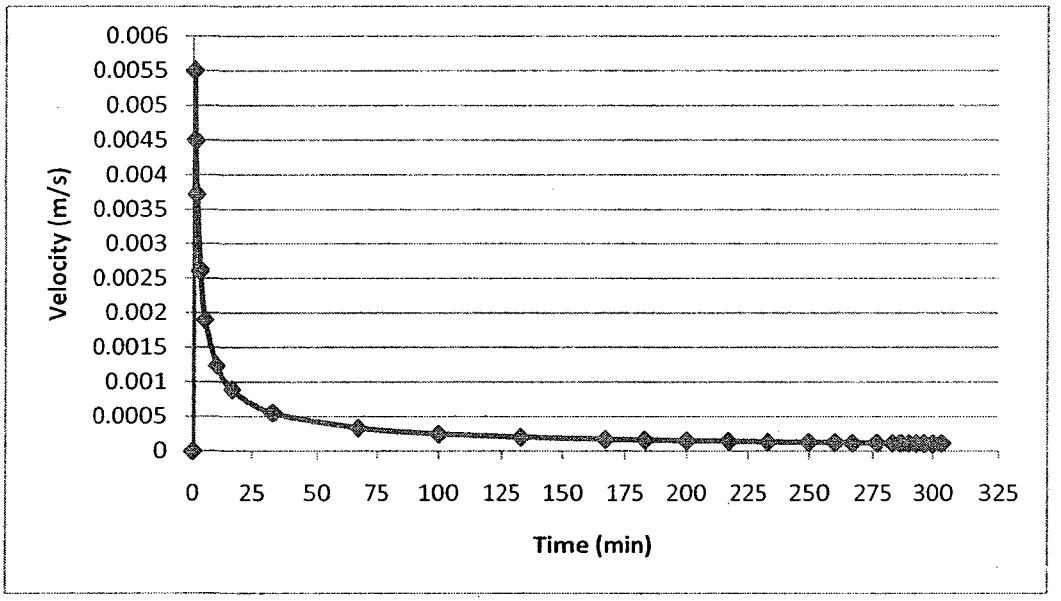

Figure 14. Diagrams of distance and velocity versus time for Test B

The effect of the resisting forces, which is the decrease in velocity, can be observed in the diagrams. While the diagrams show a trend similar to the one presented in test A, comparing the diagrams from both tests, it can be observed that the run out time for test B is slightly shorter which is due to the lower value of density and viscosity which allow the tailings to move more easily than in the previous test.

This is also noticeable in the values for the maximum velocity and the velocity at which the tailings reach the end of the flume, which are slightly greater for Test B.

Figure 15 presents the diagrams resulted from Test C. The values assigned to the properties of tailings in Test C are all the same as the values in Test A except the value assigned to external pressure. External pressure functions as pressure being exerted on the tailings to keep the particles together during the flow of the tailings. Having the value of 3 in Test A, the external pressure made the particles mostly remain within the enclosing body of tailings whereas in Test C this value was reduced to the default value 1, which resulted in the particles being able to leave the flow more easily. Thus, as it can be observed in the diagrams, the reduction in the value of external pressure resulted in a greater traveling time and as a result a smaller value for the velocity was observed as the tailings reach the end of flume.

In Test D, while the values for density and external pressure were not changed in comparison to Test C, the values for viscosity, friction and roughness were decreased. Selecting smaller values for friction and roughness resulted in reduction in the value of resisting forces. Hence, tailings could flow more easily in the flume which resulted in a relatively shorter time for the tailings to reach the end of the flume. In addition, when the value assigned to viscosity was reduced, a rather smaller force was needed to make the tailings flow into the flume and keep moving forward. This fact also contributed to the tailings traveling the length of the flume in a shorter time in comparison to previous tests, as it is indicated in Figure 16.

One other effect of reducing the value of the parameters, which also contributed to the tailings' run out time being shortened, was the velocity. As the friction force was decreased, the tailings could flow with a higher velocity and as a result a higher value

than the previous tests for velocity was observed when the tailings reached the end of the flume.

The results of Test E are presented in Figure 17. In Test E similar values as Test D were assigned to all the parameters except density. The decrease in density, which caused less particles being present in the tailings and hence less particle interaction in the simulation, resulted in a slightly shorter run out time for Test E. The reduction in particle interaction led to a smoother flow than Test D which in turn resulted in the tailings' traveling the length of the flume in a slightly shorter time.

Test F, the last test of this series of tests, was performed with the lowest values among the tests assigned to density, friction and roughness. As it can be observed in Figure 18, due to the reduction in values for the mentioned parameters, the traveling time for the tailings paste was significantly reduced. Lower values assigned to roughness and friction caused less resistance against the flow and thus the increase in velocity. Fewer particles were generated due to lower value of density in comparison to previous tests and therefore particle interaction was reduced and hence a smoother flow was observed which led to a significantly shorter run out time and higher velocity at the end of the flume.

Comparing the results of the test with the value assigned to external pressure equal to the default value assigned to internal pressure (1) to other tests which had higher values for their external pressures than the internal pressures, states that a higher external pressure value than the internal pressure delays the paste's reaching the end of the path and therefore provides a more realistic environment for paste-like tailings.

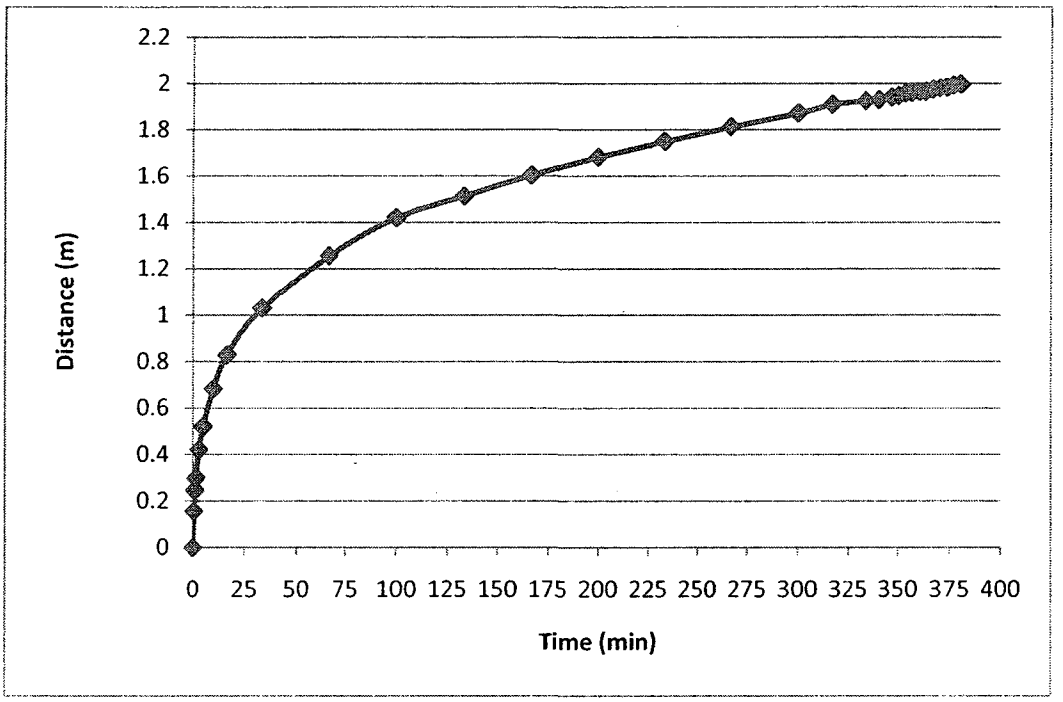

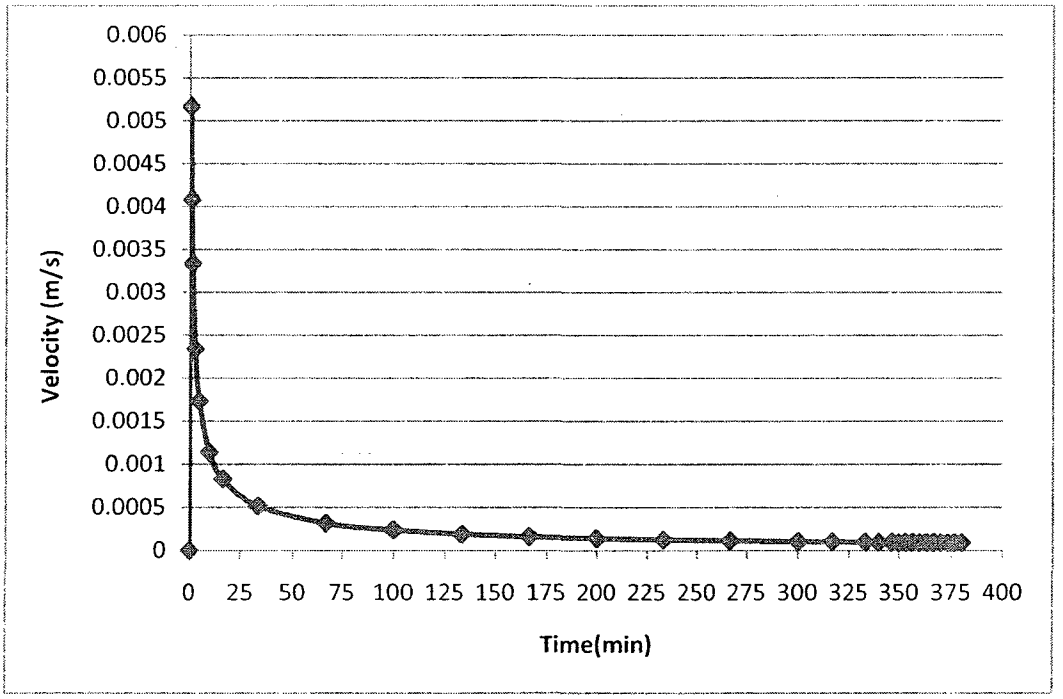

Figure 15. Diagrams of distance and velocity versus time for Test C

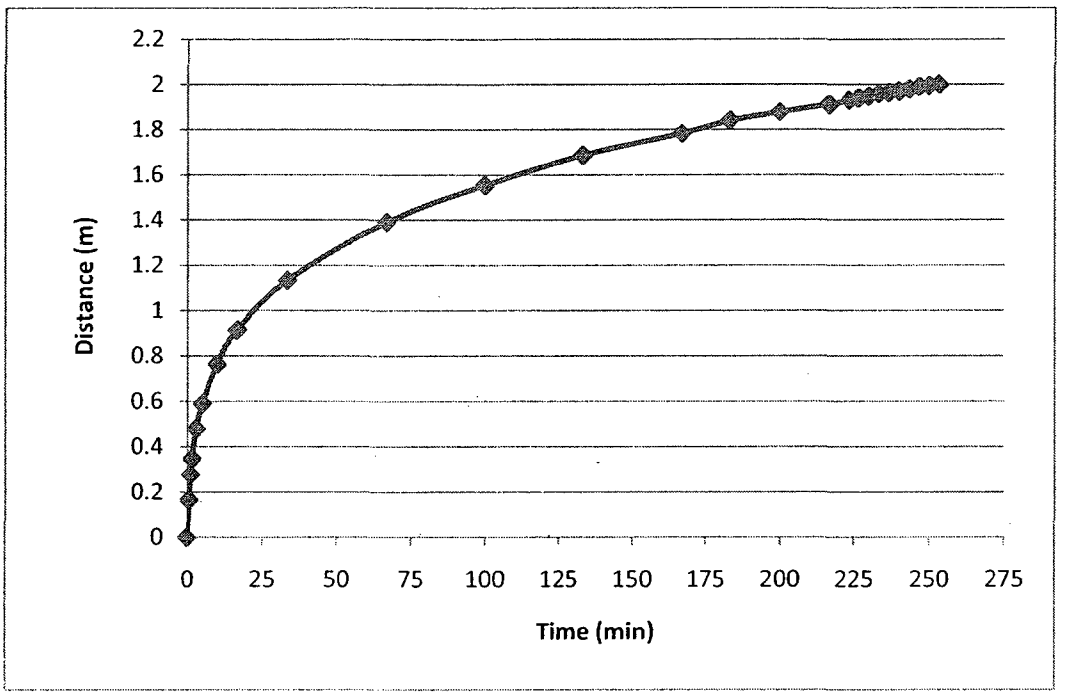

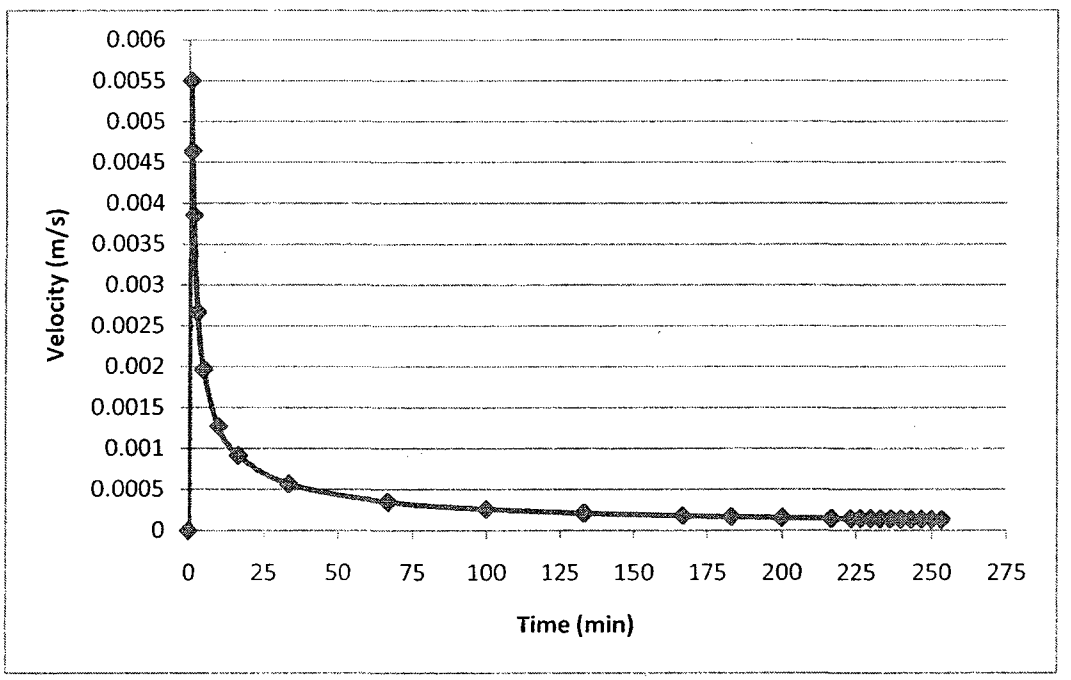

Figure 16. Diagrams of distance and velocity versus time for Test D

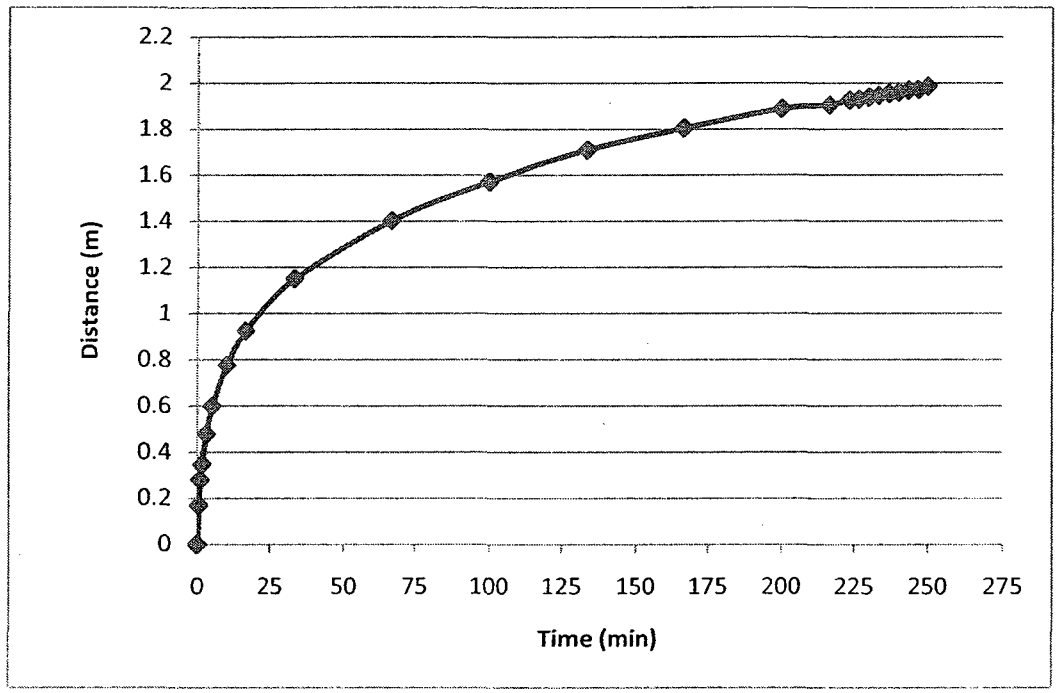

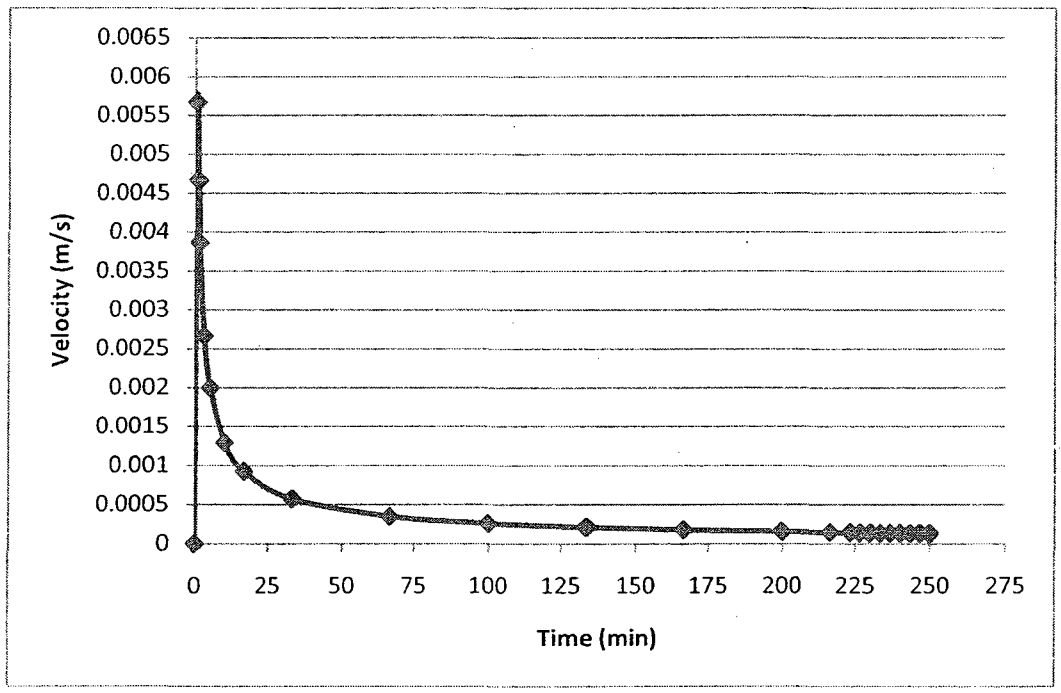

Figure 17. Diagrams of distance and velocity versus time for Test E

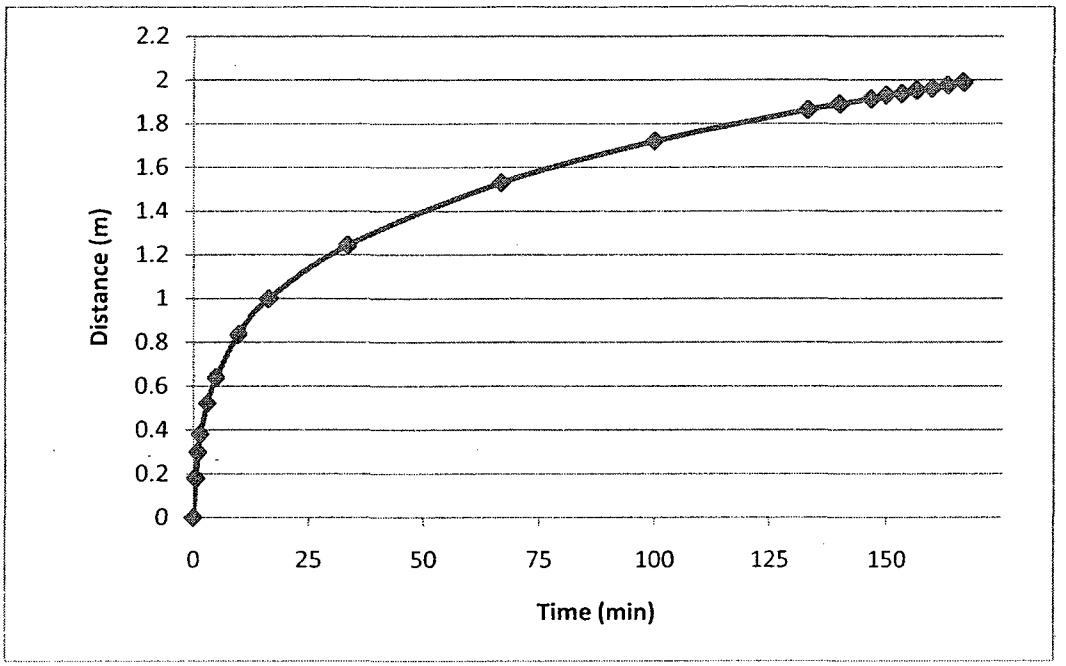

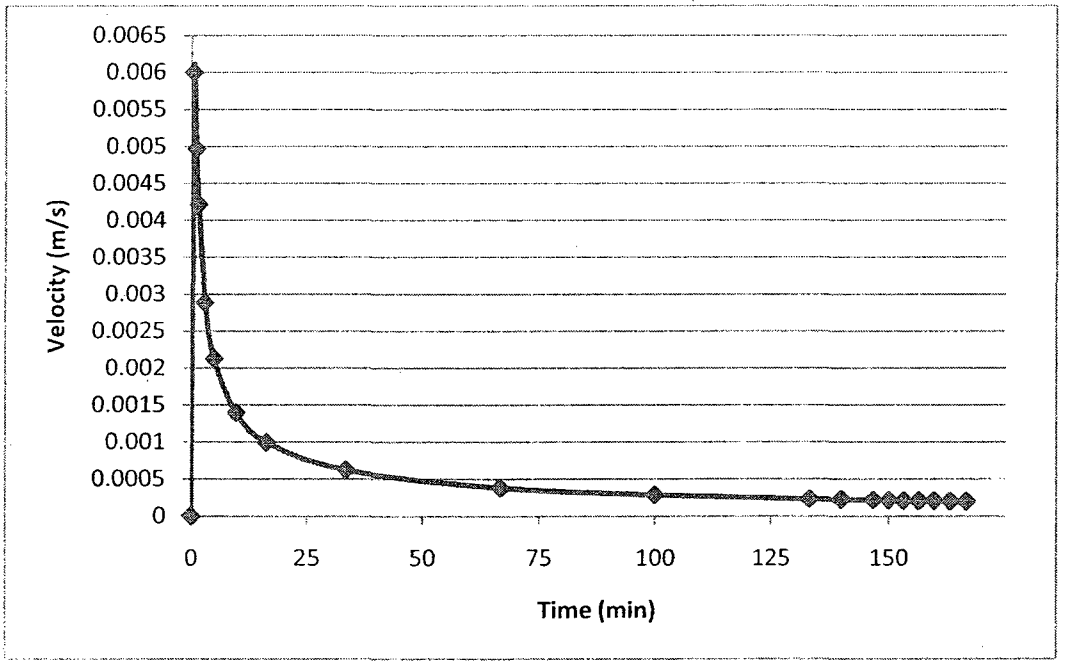

Figure 18. Diagrams of distance and velocity versus time for Test F

It was observed in the first series of the tests that none of the pastes came to a complete 'rest' prior to reaching the end of the flume and therefore an angle of repose at rest was

not observed. However, as it is shown in the velocity versus time diagrams the value of the velocity at which the paste travels along the flume falls to very low values and, as a result, it takes the paste a considerably long time to reach the end of the flume and similarly a very long time for the program to simulate the flow of paste. Nevertheless, as the diagram shows, there is a point at which there is a sudden change in the regime of velocity decrease and from this point onward the dramatic decline in the velocity switches to an almost steady velocity with much smaller deductions in the value. Comparing the distance versus time diagrams for this part of simulations reveals that the majority of the simulations reach the mentioned point at approximately halfway through the journey along the flume.

Based on the abovementioned observations and with the goal of the paste reaching a resting point, a point after which due to the significant reduction in the velocity, it took the system a considerable time to continue simulating the movement, could be determined. The velocity at which the paste moved at this particular point was chosen to be the 'at rest condition' velocity. Since most of the tests had the stated point at approximately halfway through the run out length, the velocity of 0.0005 m/s^2 was chosen to be the 'at rest condition' velocity.

It could be concluded from the first series of the tests that when the speed of the paste reached the value of the 'at rest condition' velocity the test would be considered complete and finished. Thus the angles of repose and run out distances would be taken.

5.3.2 Tests with Changes in a Single Variable

The second series of simulations were performed to observe the sensitivity of the simulations to changes in the value of a single parameter and therefore, while one of the main parameters was chosen as the variable, remaining parameters were held constant. Density, viscosity and friction and roughness were in turn chosen to be as the variable parameter.

Using the results of the first series of tests which indicated the velocity of 0.0005 m/s as the 'at rest condition' velocity, at which the test would come to an end, the flow of the tailings paste was simulated under the following circumstances.

Table 3. Values for Test 1 of tests with changes in a single variable

Resolution	Density (kg/m^3)	Viscosity	Friction and Roughness	External Pressure	Bounce
5	3000 to 4500 Increments: 500 (kg/m^3)	20	0.2	2	0.1

The values chosen for the constant parameters were relative to the default values of RealFlow, which is assigned to water. A high resolution value for the simulation will require more particles to be created which results in higher number of particle interactions to be calculated and therefore it takes RealFlow a long time to process the simulation. As a result the value taken was 5 in comparison to the default value which was 1. Due to the default assigned value to viscosity for water being 3, an average value

(20) which is representative of a more viscous material than water such as tailings paste was assigned to the paste as the constant value. The same values were chosen for both roughness and friction and the tests were not performed with each one of them having separate values.

The importance of one of the features of the simulation tool introduced as 'external pressure' was emphasized in the result of the first series of tests. Therefore, it was decided to have an external pressure exerted on the whole body of the paste with a doubled value in comparison to the internal pressure.

As previously discussed, the terrain on which the tests were performed did not have a great bounciness value. Therefore, the value for this parameter was reduced to 0.1 in the tests. The result of the simulations with the abovementioned values can be observed in Figure 19.

The existing trend in the diagrams shows that as the density of tailings paste increases there is a decline in the run out distance in an approximately linear fashion. Similarly, the density increase in the paste has a direct effect on the value of the angle of repose at rest. This shows that as the mass of the particles in the tailings paste in the same volume of material increases, the interactions between the particles increase and therefore a greater force is needed to pull the paste to a point at the same distance as before. Whereas gravity stays the same and even the change in the weight of the paste is not enough to drive the paste to the previous point. The mentioned changes will result in the paste travelling a shorter distance and therefore more material remaining at the gate than before and as a result the H_1 in equation 69 will be higher which results in a greater angle of repose.

Computed values and the diagrams presented a realistic trend in which a gradual decline in the values of run out distance and a constant increase in the values of angle of repose were demonstrated which implies the fact that RealFlow performed the desired simulation for the aforementioned set of values.

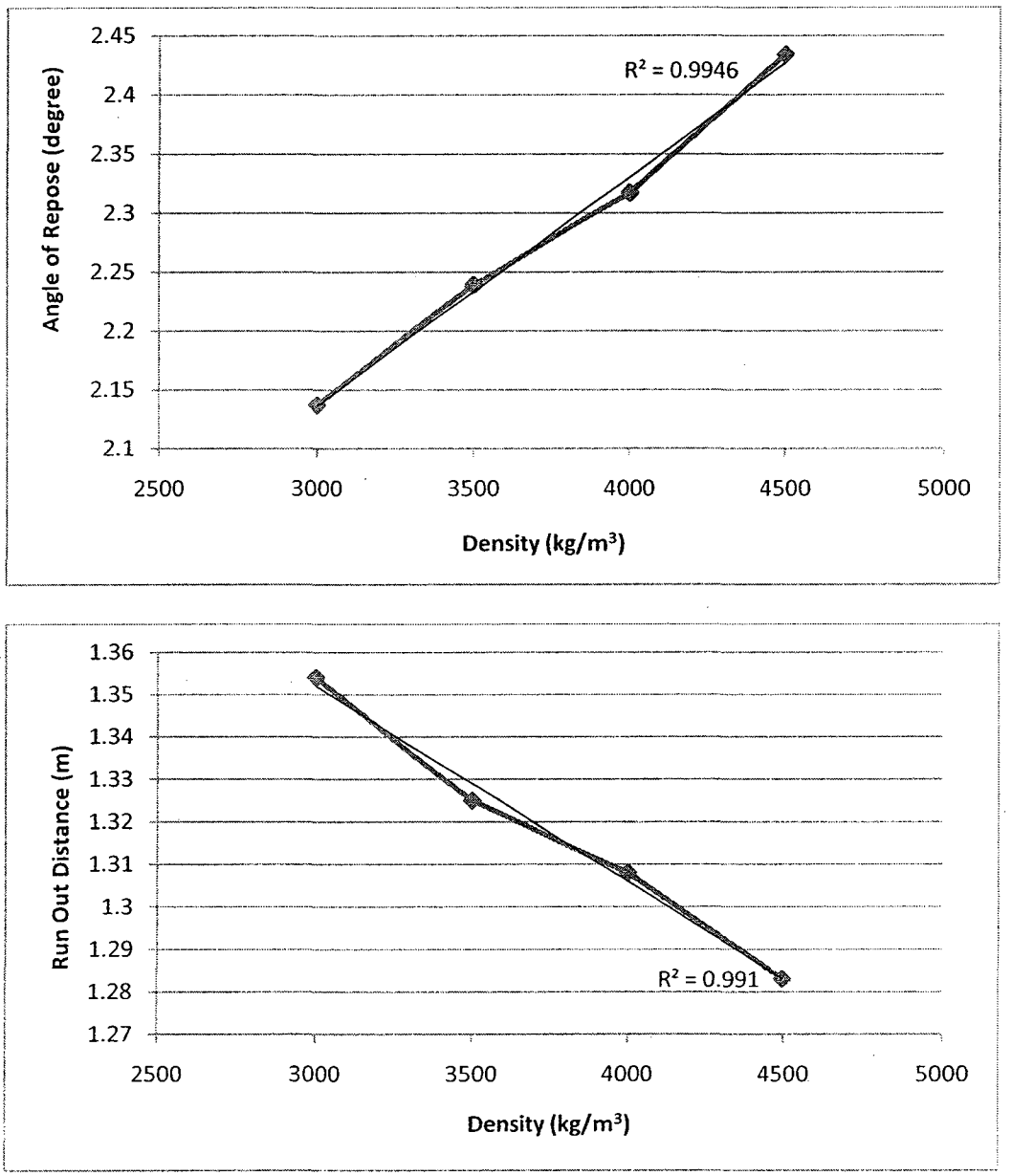

Figure 19. The run out distance and angle of repose versus density for the tests with variable density (Test 1)

Table 4. Values for Test 2 of tests with changes in a single variable

Resolution	Density (kg/m^3)	Viscosity	Friction and Roughness	External Pressure	Bounce
5	4000	10 to 35 Increments: 5	0.2	2	0.1

For the second test of the second series of simulations, while the viscosity was taken as the variable parameter the assigned value to density was 4000 kg/cm^3. This value was the mean value in the range of 3000 kg/cm^3 and 5000 kg/cm^3 which was assumed as the representative of the density domain to be applied to the program. The rest of the parameters had the same values as the previous test. The result of Test 2 is provided in Figure 20.

The angle of repose versus viscosity diagram in Figure 20 demonstrates an approximately linear regime of changes under viscosity change. As the viscosity increases the force needed to be exerted on a material to move and slide the particles on one another also increases. Thus, since the gravity, which drags the paste along the flume, was constant and did not change during the simulation, it resulted in shorter run out distances with the increase in the viscosity and therefore having the same volume of materials for all of the tests the angle of repose was increased as the distance was shortened. The run out distance versus viscosity diagram (Figure 20) suggests that up to some extent as the viscosity increases the run out distance decreases in a linear

fashion, however, as the value of the viscosity increases over a certain point a non-linear trend is observed.

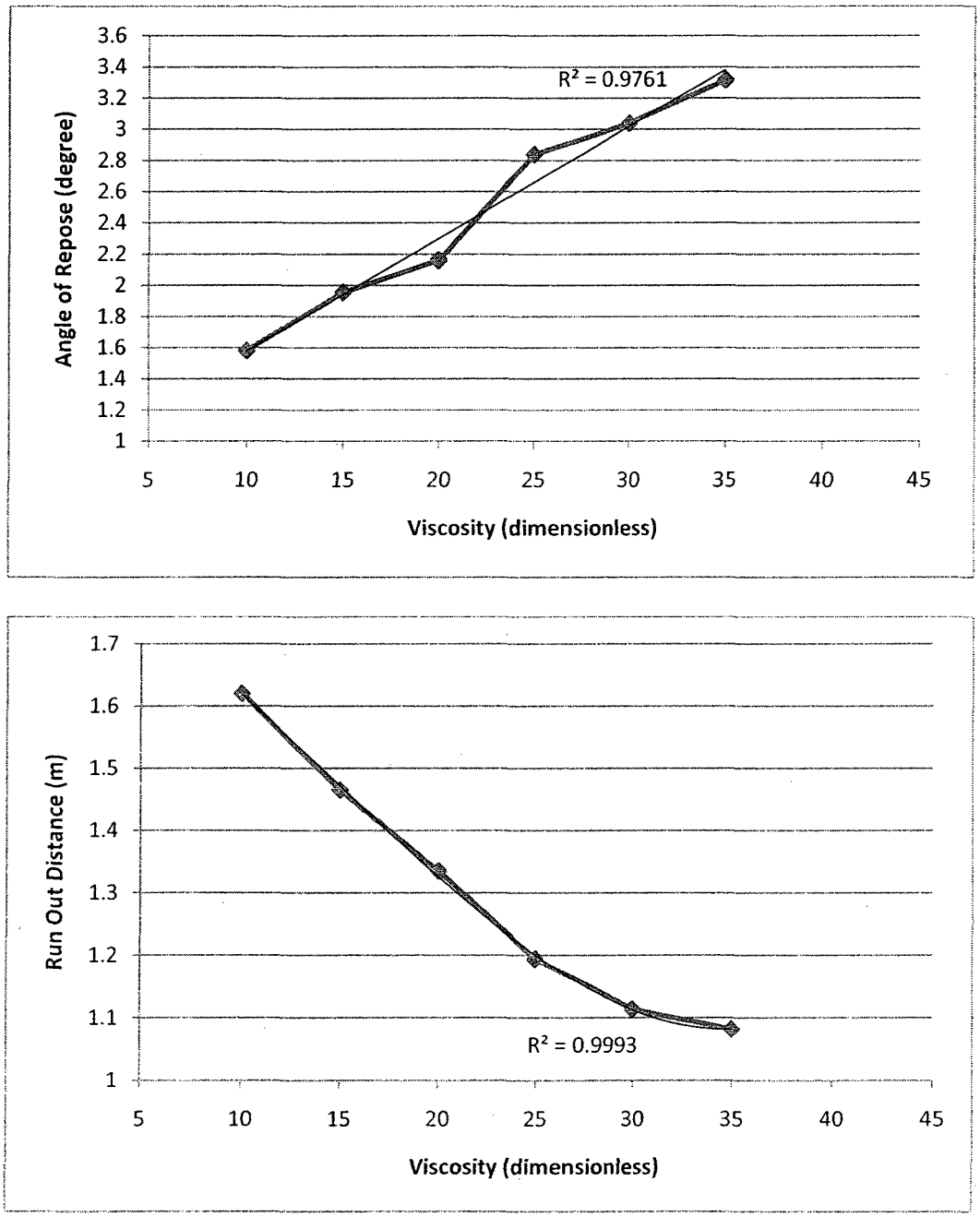

Figure 20. Angle of repose and run out distance versus viscosity for the tests with variable viscosity (Test 2)

Table 5. Values for Test 3 of tests with changes in a single variable

Resolution	Density (kg/m^3)	Viscosity	Friction and Roughness	External Pressure	Bounce
5	4000	20	0.2 to 0.7 Increments: 0.1	2	0.1

As the last test of the second series of the simulations, the effect of changes in the friction and roughness values was observed. Thus, as friction and roughness values were chosen to be the variables the value of viscosity was set as 20 again. Figure 21 demonstrates the results obtained from the simulations for constant friction and roughness.

The diagrams in Figure 21 demonstrated the effects of changes in the terrain's friction and roughness values on the tailings paste's angle of repose at rest and run out distance. According to the diagrams, as the flume surface or terrain becomes rougher the flow of the paste becomes more difficult whereas the dragging gravity force does not experience any increase. Therefore, the rise in friction and roughness values shortened the run out distance which in turn resulted in a greater angle of repose at rest. However, the diagrams demonstrate that the interactions of the mentioned parameters under such condition do not follow a linear trend. As the roughness and friction values increase, the rate of increase in the values of angle of repose at rest and decrease in the run out distance decreases due to the fact that as the value for friction and roughness increases,

the difference in the value between resisting forces and driving forces decreases and therefore the results of the experiments become closer to one another.

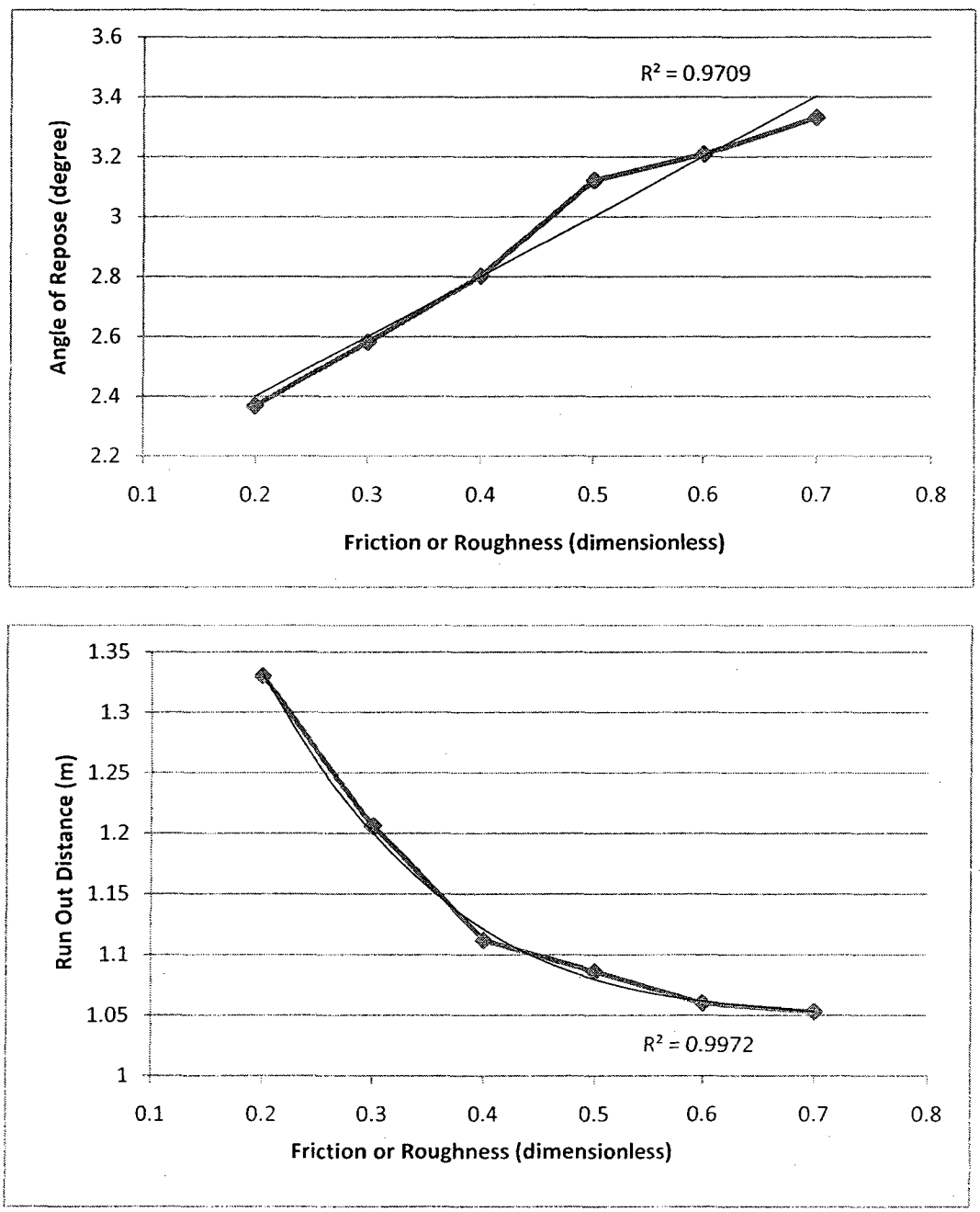

Figure 21. Angle of repose and run out distance versus friction and roughness for the tests with variable friction and roughness (Test 3)

5.3.3 Monte Carlo Simulations

Having observed the effects of changes in each one of the parameters on the flow of the tailings paste individually, Monte Carlo simulations were chosen to observe the effect of changes in all the parameters at the same time or in other words the odds of obtaining different values for the angle of repose and the run out distance by assigning random values within the defined range for each parameter to each one of them was observed. The goal of this series of tests was to reach a mean value for the angle of repose and the run out length while the data was randomly chosen from the specific predefined domain of each parameter.

To obtain a result as the mean value, the quantity of simulations was important. The more simulations were run the more accurate would the results be. On the other hand, time was a limiting factor for the quantity of the simulations. As it was previously mentioned, it would take RealFlow a great amount of time to simulate the flow of materials with characteristics like tailings paste as a result of the high values assigned to the parameters in the simulation tool. Therefore, in order to maintain the quantity and the quality of the tests as many as 30 tests were performed. The details of the performed simulations and the specifics of the values taken for equation 70 are provided in the Appendix. The run out distances and corresponding angles of repose are shown in Figure 22.

The following diagrams show the data obtained from the Monte Carlo simulations performed in RealFlow:

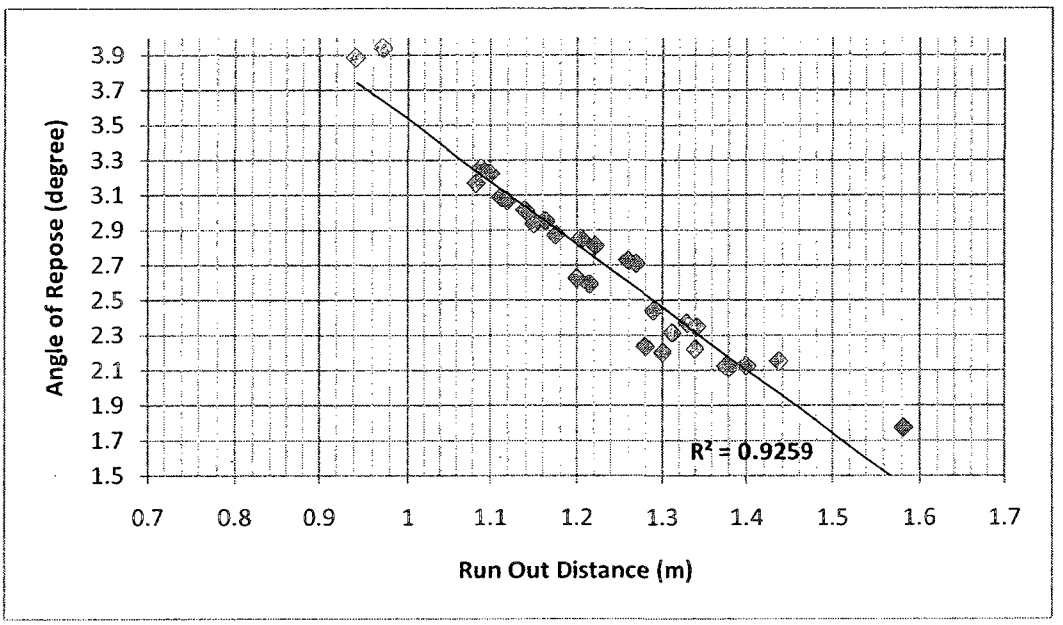

Figure 22. Angle of repose versus run out distance for each test performed using Monte Carlo simulations

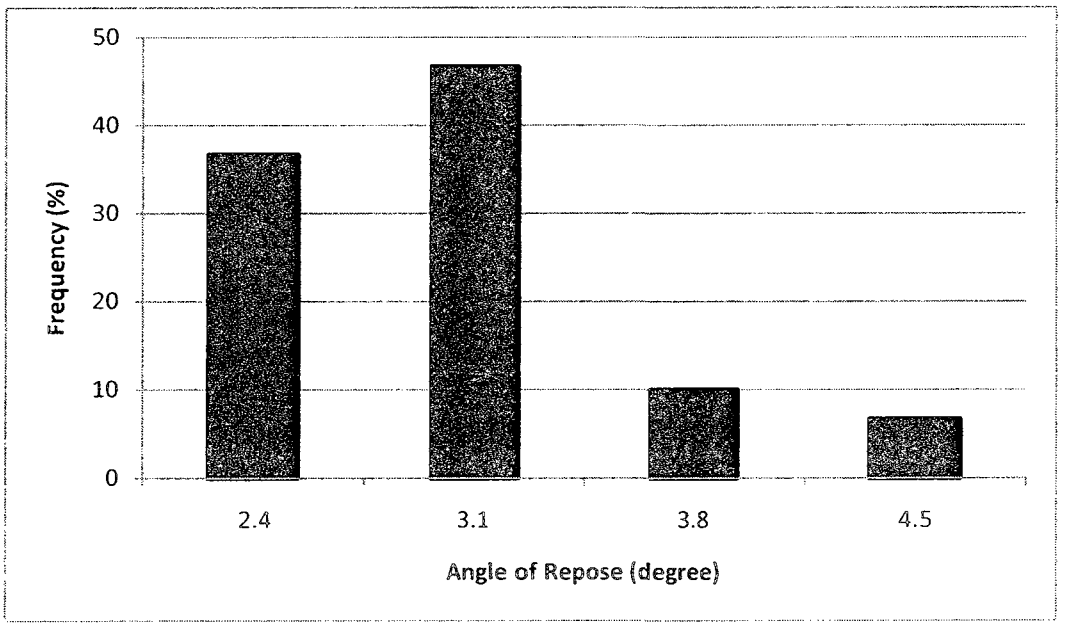

Figure 23. Diagram demonstrating the frequency of the obtained values for angle of repose and the mean value

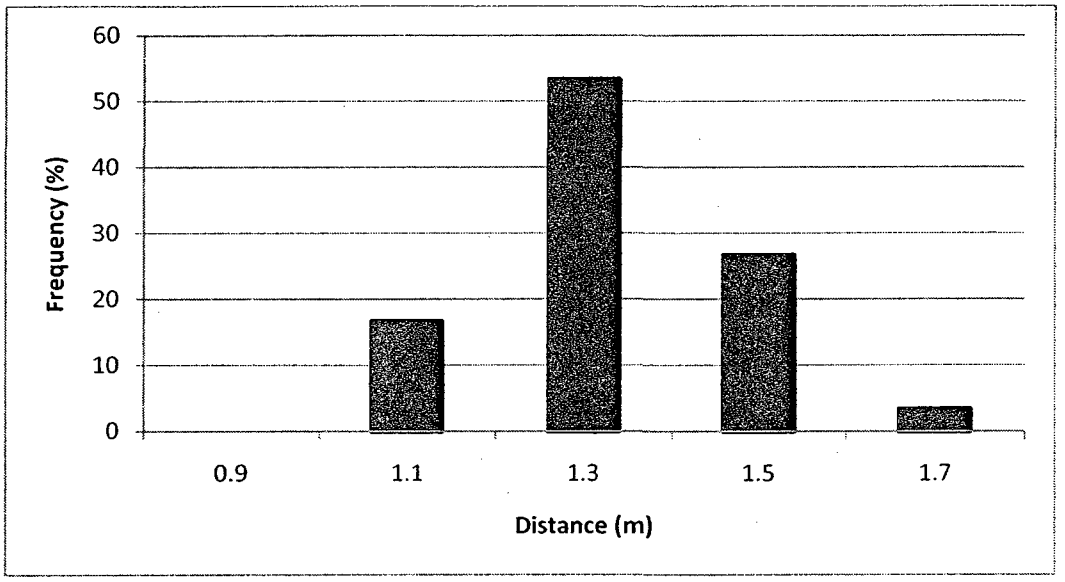

Figure 24. Diagram demonstrating the frequency of the obtained values for run out distance and the mean value

The values taken for density in the third series of tests ranged from 3000 kg/cm^3 to 5000 kg/cm^3 with the mean value of 4000 kg/cm^3 which was a credible range for a tailings paste in comparison to the density of water. The domain chosen for resolution was between 4 and 16 and the mean value of 10 which was based on the information collected from the sample RealFlow simulations and the instructions in comparison to very low numbers used with lower densities to simulate the flow of water. The values for viscosity ranged between 10 and 35 with the mean value of 22.5.

As for the friction and roughness values the mean was taken as 0.5 with the range of data between 0.2 and 0.8. The values were inputs for equation 70 and the diagrams above were produced from the simulations using these values.

The minimum and maximum values obtained for the run out distance using the random values for the parameters were 0.942 m and 1.582 m respectively. The same values for the angle of repose were 1.774° and 3.943°. For the range of data, based on the

information taken from the diagrams, the mean value for the angle of repose was approximately 3.1° and the mean value for the run out distance was approximately 1.3 m. The same data is also provided in Figure 22. It can be observed that more than 50% of the points on the diagram have a distance close to 1.3 m. Similarly for the angle of repose in Figure 23, more than 40% of the tests had an angle of repose value close to 3.1°. This shows that there is a high probability that the distance travelled by a type of tailings paste similar to the one simulated and having a characteristic with the values of its parameters in the same range as the simulated paste would be a number close to 1.3 m and the angle at which it comes to rest would be approximately 3.1°.

In Crowder's experiment (2004) which was used as the base of the simulations, two different pastes were used for the flume tests. The first paste was from the ores extracted from the initial development of the mine and the second one was taken at a later time from the paste plant.

Comparing the results from the Monte Carlo simulations with the ones obtained from Crowder's flume tests reveals that the mean value of 3.1° for the angle of repose obtained from the simulations is equal to the angle of repose for the first paste with the water content of 31.7% as the "as received" paste and 25.8% when deflocculant was added to the paste, both at the temperature of 22°C. As for the second paste 3.1° is equal to the angle of repose of the paste at 27.7% water content when deflocculant is added and 41.6% and 42.9% of water content (two different tests for the same paste) for the "as received" paste, all of them at the temperature of 22°C. This shows that the simulations produced data which fits the credible area for a tailings paste and as the real pastes performed in Crowder's tests the higher the density and viscosity was the higher the angle and the shorter the run out distances for the simulations were. Moreover, to

enhance the result of the calibration, having the mean values for run out length and angle of repose and observing the effects of changes in each of the values individually, the same pattern can be extended and applied to other data ranges and different tailings pastes according to the trend observed in the previous tests.

Chapter Six: Modeling Case Studies of Tailings Dams Failure

Modeling Case Studies of Tailings Dams Failure

6.1 Tapo Canyon Tailings Dam

Tapo dam was a 24 meter high tailings dam retaining sand and gravel-sized aggregate mining waste, located in Northridge, California which failed as a result of an earthquake on November 17, 1994 (Harder and Stewart, 1996). The pond, along which the embankment failed was constructed within a hill which had been excavated prior to the construction of the pond. Since the ground water level had made the excavation difficult, mining was stopped and this pound was converted to be used for settling out the fines washed out of the sand and gravel aggregates during the mining process. Most of the fines were smaller than the No. 140 sieve size. The tailings were composed of stratified layers of soils covering a wide range of material from fat clays with plasticity indices as high as 30 – 50 to non-plastic sandy silts and silty sands (Harder and Stewart, 1996).

From 1992 for two years the pound was used by a nearby concrete batch plant for waste concrete. The waste concrete would be washed off the trucks driven into the eastern pond. This resulted in a discontinuous layer of concrete with the depth of 1.2 to 1.8 meters on the surface of the pond. The western half still contained some water which Harder and Stewart (1996) believe to be as a result of leakage through the conveyance ditches and ponds located on the immediate northern side.

Liquefaction of the tailings and parts of the dam caused reductions in soil strength and stiffness resulted in large and relatively intact blocks of the dam sliding over 60m downstream, which caused the impounded tailings to flow out through the breach and travel several hundred meters downstream (Harder and Stewart, 1996). The failure occurred at a part of the dam where a gap was made between the hill and the dam as a result of mining activities. An approximately 60 meter long part of the dam failed and the dam broke at least into two parts and slid out. The two parts were displaced and moved for 60 and 90 meters downstream the dam respectively. The retained tailings behind the breach had shaped a slope toward the breach in a shape that Harder and Stewart (1996) describe as the tailings going through a cone. Some parts of the retained tailings passed through the breach and traveled up to 180 meters downstream. There were also up to 3 meters of settlements of the embankment close to the breach both downstream and upstream. Several cracks of the size of around 1 meter were found on the embankment as a result of displacements. The buttress and the riprap were moved to the opposite side of their original place and temporarily blocked the creek. The presence of the creek bank in the site, where the debris was stopped, had decreased the displacement of the embankment. "Downstream of the principal, relatively viscous flow slide, more "fluid" tailings were found to have splashed up across the creek and against the adjacent hillside. The splashed material appears to be composed predominantly of clayey soils. Further downstream, tailings entered the creek channel, filling much of the channel to unknown depths, and flowed hundreds to thousands of meters downstream. Trees were found in the channel surrounded by tailings with "splashes" running as much as 1 m up the upstream side of their trunks." (Harder and Stewart, 1996, p.5)

In addition to the above mentioned, there were blocks of concrete waste, typically 1.2 to 1.8 meters in thickness, 7.5 meters across and weighing 200 tons, which slid on the surface of the tailings having a mild slope and were displaced. They were stopped either at the end of the slope or by the buildup piles of tailings ahead of them.

Later, two boils were found in the site both consisting of non-plastic silty sand with one containing 47% non-plastic fines and the other containing about 15% non-plastic fines. Harder and Stewart (1996) believe that using a significant amount of slimes in that part of the embankment in the form of upstream method of raising embankments caused the flow failure. They have mentioned that saturated tailings cannot be relied on for the slope stability as a result of the low value of shear strength this material has. They believe that unless this matter is considered in the design, founding or building the structure with this material will not result in satisfactory post-earthquake performance.

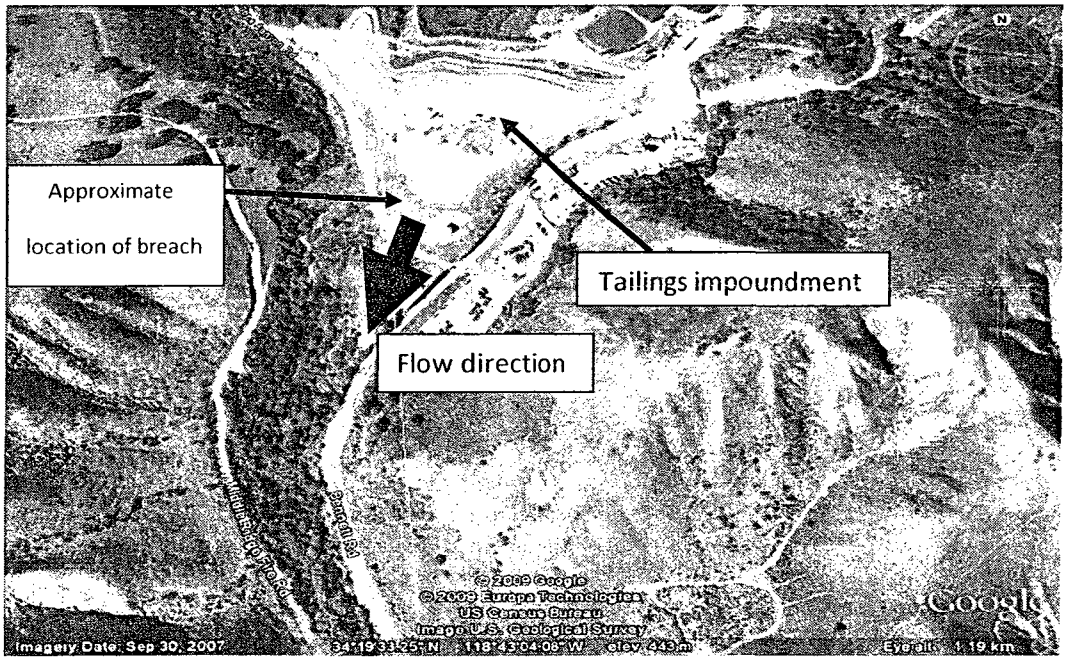

Figure 25. View of Tapo Canyon tailings dam from above (Google Earth, 2010)

6.2 *Merriespruit Tailings Dam*

The Merriespruit gold tailings dam was 38m high located 250 kilometers from Johannesburg, South Africa occupying 154 hectares. By 1978, after 16 years of operation, the embankment was retaining approximately 260×10^6 m^3 of mining waste and later the capacity was increased to 10 million tons (Van Niekerk and Viljoen, 2005). The northern wall of the dam was as close as 320m to houses nearby, which were located in the suburbs of Merriespruit. An almost north-south extending valley is located between the houses and the northern wall of the dam. This shallow drainage valley underlies the center of the northern and the center part of the dam and is located below the dam.

Later in 1993, some seepage was reported in the northern wall of the dam above the drainage exit and in addition, some time before the main incident the separating wall between the center and the northern part of the dam was broken and tailings flowed into the pond of the northern part as a result. These events, in addition to violation of the freeboard, which was recorded to be from 500mm to 150mm in some parts of the northern part of the dam, resulted in the accumulation of the tailings closer to the northern wall and farther from the decant towers (Van Niekerk and Viljoen, 2005).

Due to unexpected heavy rainfall on February 22, 1994 water started to flow over the northern wall followed by a break in the dam and a gap of 150m was formed. It took 600,000m^3 (2.5 million tons (Van Niekerk and Viljoen, 2005)) of the tailings 5 minutes to travel a distance of 1960m through the valley and into the city (Davies, 2001) which resulted in 17 deaths and some serious and minor damages to the properties (Wagener, 1997).

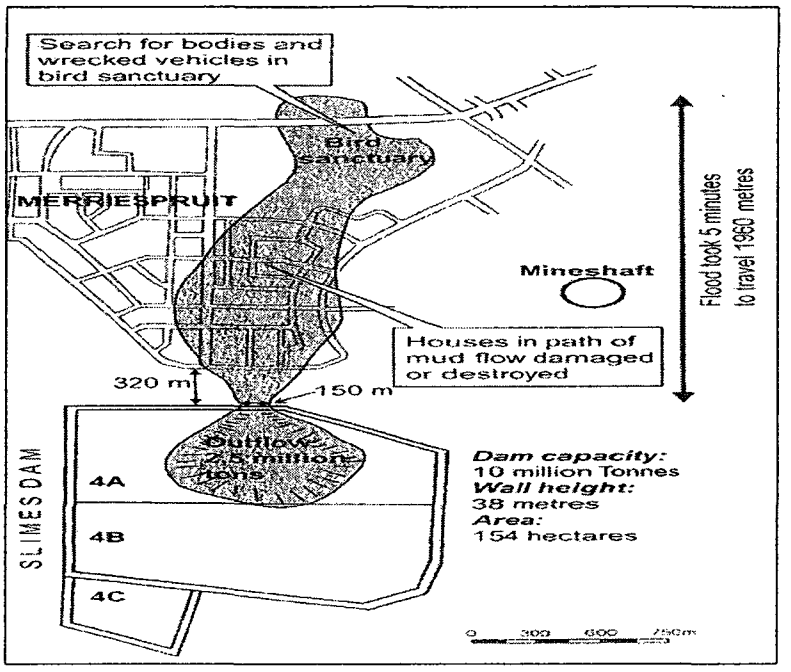

Figure 26. The Flow Path of Merriespruit from Van Niekerk and Viljoen (2005)

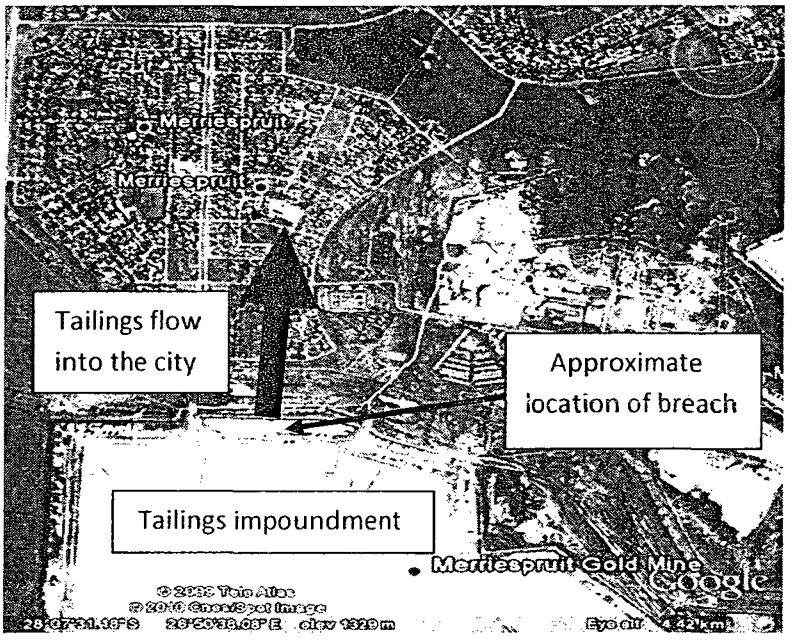

Figure 27. View of Merriespruit city and the tailings dam in the south from above (Google Earth, 2010)

The model calibration which was performed previously, demonstrated the capacity of the simulation tool to model a situation in which a relatively viscous fluid would flow as a result of a sudden break in its confining environment and would come to a rest when

the effects of active driving and resisting forces reach equilibrium. It also provided the information on how the changes in fluid parameters in the simulation tool affect the outcome and therefore, paved the way for implementation of the case studies' environment and properties of tailings in the simulation tool in order to be modeled.

The following sections provide a detailed description of modeling the case studies mentioned in the previous section. The necessary considerations in modeling incidents are considered first, followed by an account of scene creation and value assignment, and the results.

6.3 Considerations in Model Implementation

To create the models as akin to the physical incidents as possible, there were two key parameters which had to be imported in the software as precisely as possible, as they would greatly influence the outcome of the simulation. The two parameters were the terrain and the properties of tailings.

6.3.1 The Terrain

In case of a failure in a tailings dam structure resulting in the flow of tailings in the area behind the dam, the terrain has an important role. The characteristics of the terrain influence the manner in which tailings run out and advance. The aspects on which the terrain can have influence include the velocity at which the tailings travel, the direction of the flow, the run out distance and the area the tailings cover both longitudinally and in width. The terrain's roughness and the existing irregularities influence the velocity of

tailings. It serves as a resisting force against the tailings' advancement which eventually, as time passes its constant value becomes greater than the values of the driving forces, which decrease over time, resulting in the tailings flow coming to a rest after traveling a certain distance. Depending on their sizes, the irregularities of the terrain can affect the direction of the flow by acting as obstacles in the flow path, the velocity at which the tailings flow by introducing slopes with various angles to the path and finally, the distance the tailings flow by trapping the tailings in pits or accelerating the movement by introducing rather steep slopes.

To increase the accuracy of the models and maintain the three dimensional method of modeling, Digital Elevation Models (DEM), digital maps producing the elevation of a specific terrain (Figure 28), were selected as the objects representing the terrain. The area in which the dam failures in the case studies had occurred were located on the DEMs which were later cropped and prepared based on the longitude and latitude of the area where the physical incidents occurred, to be utilized in the modeling tool using MICRODEM (Guth, 2009), a mapping software which merges and displays models and maps.

6.3.2 Tailings Properties

Tailings properties are among the factors that affect the simulations most. The distance, up to which the tailings travel, apart from the effects of the terrain, depend on parameters such as the viscosity and density of the tailings. The more viscous the tailings are, the greater driving forces they need to travel longer distances; therefore, under the same circumstances tailings with higher viscosity and density come to rest in

a shorter distance from the impoundment. The same reason is valid for the run out time of the tailings. As the viscosity increases, due to the lower tendency in the particles to become separated from the body of the flow, the time in which the tailings travel a specific distance also increases. Moreover, the shape and the uniformity of the flow could be controlled by assigning various values to the special factors representing the properties of the tailings in the simulation tool such as internal and external pressures.

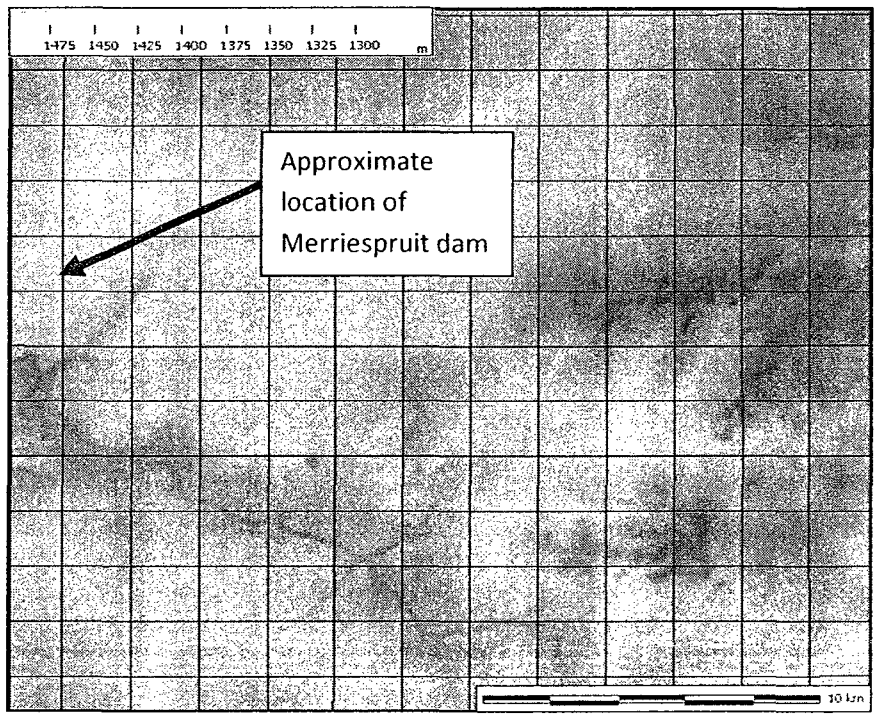

Figure 28. Sample of a DEM of South Africa (NASA)

The information regarding creation of the scene and the environment of each of the case studies and results of the simulations are included in the following section.

6.4 Model Creation

This section includes the data regarding modeling tailings dam failures to be implemented in the simulation tool and for the results to be compared with the physical incidents. The incidents include Tapo Canyon and Merriespruit tailings dam failures.

6.4.1 Tapo Canyon Tailings Dam Failure

Based on the information provided in 'Case Studies' section and according to Harder and Stewart (1996), the data regarding Tapo Canyon tailings dam failure is provided in the following table:

Table 6. Data regarding Tapo Canyon tailings dam

Dam Height (m)	Breach Length (m)	Run Out Distance (m)	Tailings' State
24	60	180	Highly Viscous

After the incident, a major part of the tailings had not travelled a relatively long distance and had come to rest at a distance of 180m from the south western part of the tailings dam. This implied that considering the parameters defining the characteristics of the terrain, such as friction and roughness, a high value had to be selected as the run out distance was rather short in comparison to Merriespruit tailings dam failure. The DEM did not include any vegetation or other potential obstacles or changes in the

terrain, therefore, the dimension of the terrain in the '*z*' direction which represented the height of the object, was increased to amplify the irregularities of the terrain and the effects of them on the flow.

When the correct dimensions and characteristics were applied to the terrain, the dam had to be created and located on the terrain. The dam had a shape similar to a triangle with two 270m long sides and the third side being 300m in length. Having created the model dam using cube objects in different sizes, knowing that the breach was developed close to the south western wall, to create the breach in the model a separate retaining cube was used which would be removed at the beginning of the simulation to let the tailings flow out of the impoundment. In order for the model dam to resemble the real dam and for the simulation to represent the real incidents the sides of each square in the RealFlow grid were taken as 30 meters on which the whole model and scene were based. The location of the dam on the terrain was found according to the irregularities of the terrain using 'Google Earth'.

As it was reported after model calibration the material modeled was paste-like tailings and therefore, large values had been assigned to parameters such as viscosity and density. According to Harder and Stewart (1996), the tailings retained behind the dam were highly viscous and as a result, in addition to traveling a short distance from the dam, they formed a slope from the breach to the point they came to rest. Thus, the value assigned to the viscosity of the tailings was much greater than the values used in the calibration experiment. For the same reason there was a low tendency among the particles to leave the continuum and therefore a greater value was assigned to the external pressure in relation to the internal pressure. This resulted in fewer particles leaving the body of the flow and as a result the decreasing the chance of splash

occurrences which was more similar to a paste-like tailings flow. A high density value was chosen for the tailings representing the almost paste- like character of the tailings with high viscosity. However, in order to protect the system from collapsing while the simulation was in progress and the motion of the particles was calculated, the resolution was decided not to have a high value.

6.4.2 Merriespruit Tailings Dam Failure

In accordance with the provided information in the 'Case Studies' section and according to Van Niekerk and Viljoen (2005) and Blight and Fourie (2005), the following table contains the information regarding Merrie Spruit tailings dam failure some of which can also be seen in Figure 26:

Table 7. Data regarding Merriespruit tailings dam

Dam Height (m)	Breach Length (m)	Run Out Distance (m)	Approximate Run Out Time (min)	Tailings' State
38	150	1960	5	Low Viscosity

The DEM was not inclusive of all the irregularities in the area. It also did not contain the vegetation and the structures in the flow path. Therefore, the scale of the terrain along the 'z' axis, which represented the height of the model, was increased to compensate for the shortcomings of the created environment.

The dam had five sides with the longest side (the western wall) being approximately 1687 meters. Since the dam was a very large structure retaining the tailings in more than one tailings impoundment pond covering a vast area, only the northern part of the dam, where the breach developed, was included in the simulation. To form the breach, a retaining cube was embedded in the part of the dam were the breach was developed and was removed at the beginning of the simulation when the area behind the dam was filled with water. In order for the model dam to resemble the real dam and for the simulation to represent the real incidents the sides of each square in the RealFlow grid was taken as 75m on which the whole model and scene were based. The location of the dam on the terrain was found in the same way as Tapo Canyon's according to the irregularities of the terrain using 'Google Earth'.

According to Van Niekerk and Viljoen (2005), the entire incident, from the time the tailings dam failed and the tailings flowed along the valley and into the town to the time the tailings came to a rest, occurred in approximately 5 minutes. Moreover, the distance the tailings traveled to finally come to a rest, as demonstrated in figure 26, was 1960 meters which is a rather long distance. Owing to the facts about the tailings flow in this incident, it was concluded that relatively low values had to be assigned to the parameters representing the characteristics of the terrain, friction and roughness.

Regarding the properties of the tailings, given that excessive rain contributed to failure of the dam (Van Niekerk and Viljoen, 2005), which resulted in the dam losing its free board and the development of the breach, it was concluded that the tailings behind the dam had been mixed with a great amount of water and therefore the characteristics of the tailings were up to some extent similar to characteristics of water. Thus, the values assigned to the parameters representing the characteristics of tailings were considerably

lower than the assigned values in calibration tests modeling tailings paste which was considerably denser and more viscous. This fact can also be verified by a comparison between the run out distances and their corresponding time of Merriespruit tailings dam failure and the calibration tests. This also implies the assignment of a density value closer to the density of water for the tailings. Since the nature of the tailings in this incident was not 'paste-like', a lower value was assigned to external pressure in comparison to the previous model. Thus, the flow of the material would be more similar to water since the possibility of the particles' leaving the body of the flow easily, existed. However, this value was still larger than the internal pressure's to prevent experiencing unnecessary splashes. To protect the simulation tool from collapsing during the simulation of the large amount of tailings in this model, a low value was assigned to resolution.

6.5 Results and Discussion

The following sections present the results of modeling Tapo Canyon and Merriespruit tailings dam failures. Several models of each of the mentioned incidents were processed with the values assigned to the parameters representing the terrains and the tailings differing from model to model. The data presented in the following sections are the results of the closest models to the physical incidents.

The values assigned to each parameter in each model and the results are shown in the following tables and diagrams.

6.5.1 Tapo Canyon Tailings Dam Failure

The values assigned to the tailings and the terrain parameters in the model which best resembled the Tapo Canyon incident are presented in Table 8.

Table 8. Data for Tapo Canyon tailings dam failure modeling

Resolution	Density (kg/m^3)	Viscosity	Friction and Roughness	External Pressure	Bounce
5	4000	110	0.98	3	0.1

The tailings retained behind the Tapo Canyon dam had a paste-like characteristic, which resulted in the tailings behind the dam traveling a short distance and also forming a slope from the breach to the point it came to rest. The value assigned to viscosity was the highest value that could be assigned without the simulation tool's collapsing. In addition to the value assigned to viscosity, the run out distance also influenced the assigned value to friction and roughness. The value was selected to be quite great in order to resist the flow of the tailings and thus bring the tailings to a rest in a relatively short distance from the dam. In the case of Tapo Canyon's tailings, the material's paste-like nature implied a uniform flow with a minimum number of particles leaving the body of the flow and also observing fewer splashes throughout the flow. In order to achieve such behavior the external pressure was selected to be three times greater than the internal pressure.

Given that there was no report of the terrain's, on which the tailings flowed in the physical incident, demonstrating bouncy characteristic; the value assigned to bounciness of the terrain was relatively small.

Figure 29 represents the result of the Tapo Canyon tailings dam failure modeling which is consisted of the distance the tailings flow has covered over time and its corresponding velocity. The non-linear trend of the tailings flow over time demonstrates that as the time passed the tailings needed more time to advance and cover more land whereas in the first minutes of the incident due to the tailings' great head behind the dam more areas were covered in a short time. There is also a part of the distance over time diagram where there is an accumulation of points. It has to be noted that due to the existence of higher velocities at the beginning of the incident, more observing points were taken in order to observe the first minutes of the flow more precisely and facilitate plotting a more accurate diagram.

The velocity, as shown in Figure 28, experiences a great rise in the first minutes of the incident as the obstacle blocking the tailings' path (the wall of the dam) was removed in the form of a breach and the existing head of the tailings behind the dam drove the tailings out of the dam where the velocity reached the maximum value of approximately 0.4 (m/s). As the head fell and the driving forces started to weaken, the effects of the terrain's friction and roughness could be observed more clearly which resulted in a rapid decline in the velocity. The non-linear trend of the reduction in the tailings flow's velocity can be observed in the velocity diagram.

The flow of the tailings which was observed in the simulation tool was up to a great extent similar to the process that Harder and Stewart (1996) had described. The flow demonstrated the characteristics of thick, paste-like tailings and only a few signs of

turbulence were observed, and finally at a distance of 180m from the dam where the velocity had been decreased significantly in relation to the mentioned maximum value, the tailings formed a slope with its starting point being at the breach.

Despite all the similarities between the physical incident and the model, there was one factor which did not completely satisfy the resemblance condition. As it is demonstrated in Figure 29, even though the tailings did not come to a rest at the distance of 180m from the breach, the velocity at that point decreased considerably in comparison to the maximum velocity. This shortcoming of the model was to a considerable degree due to the lack of details on the terrain. As the tailings flowed on the terrain, the only resisting factors against the flow of the tailings were the terrain's irregularities, friction and roughness, whereas in the physical incident natural and man-made obstacles and even the changes in the shape of the terrain caused over the time by the mining and extracting activities also contributed to the process of stopping the tailings from moving forward.

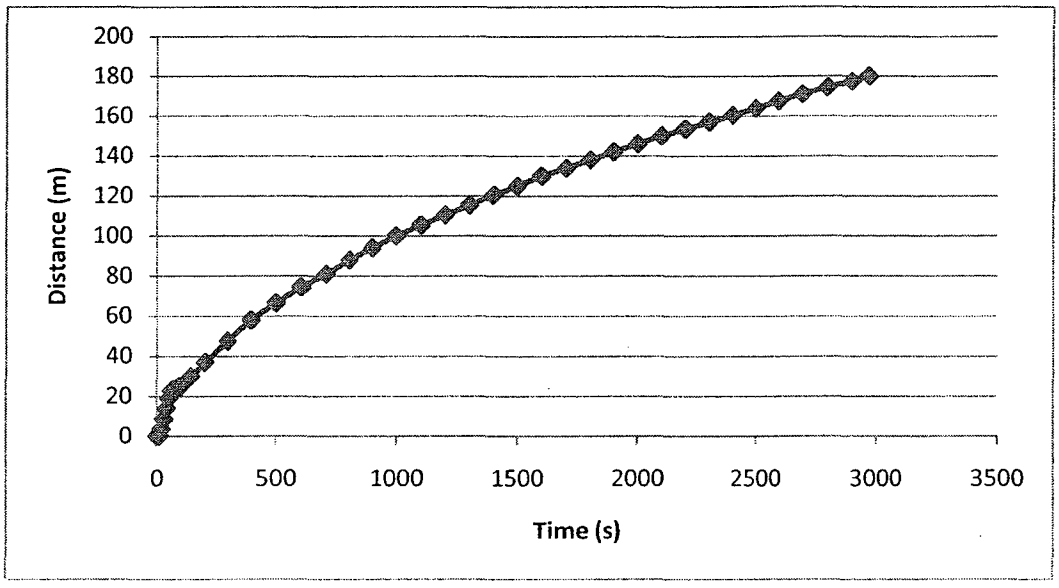

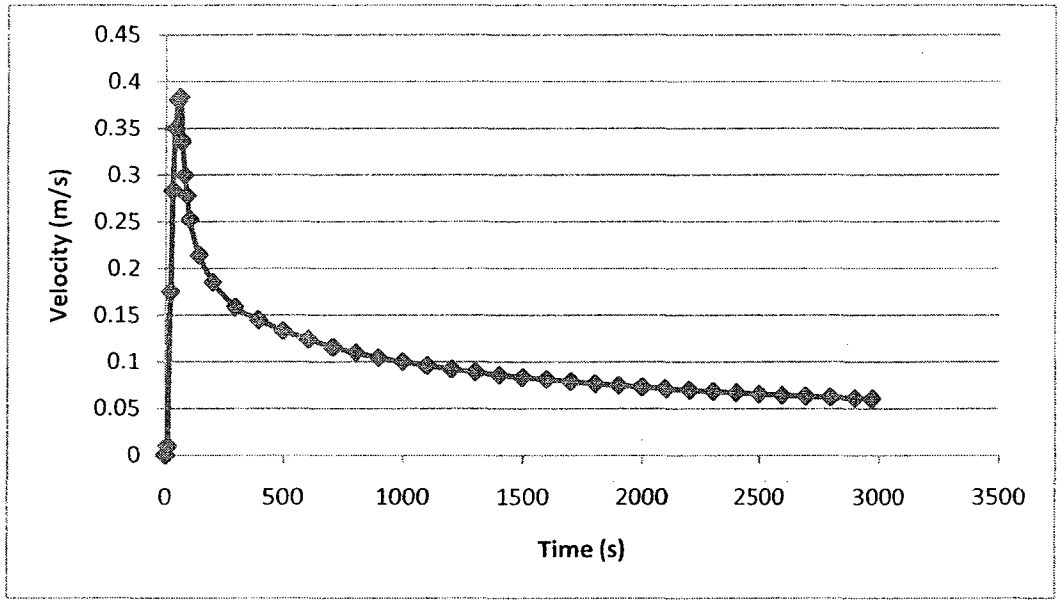

Figure 29. Diagrams demonstrating run out distance and velocity versus time for Tapo Canyon tailings dam failure modeling

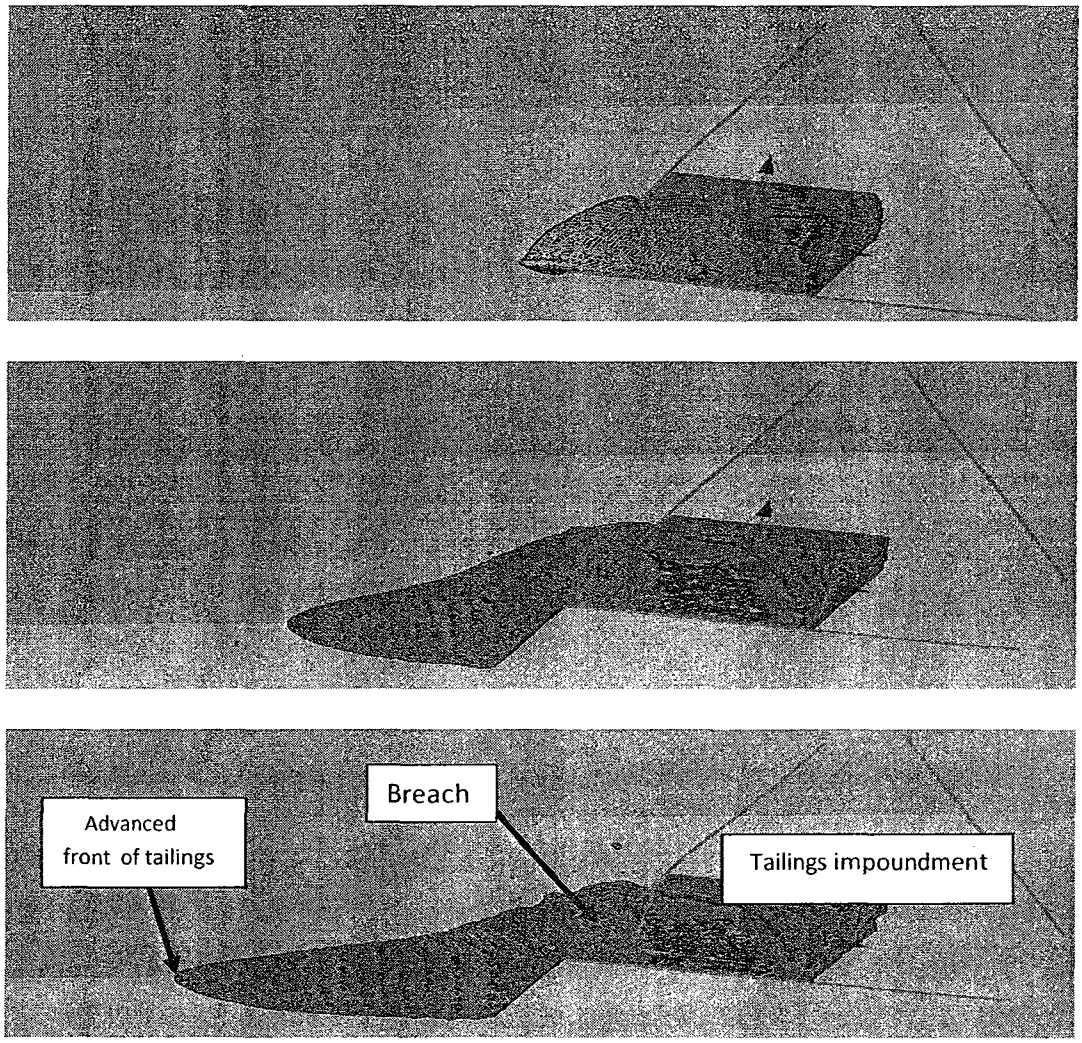

Figure 30. Scenes of modeling Tapo Canyon tailings dam failure demonstrating tailings at 25m, 120m and 180m distance from the dam

6.5.2 Merriespruit Tailings Dam Failure

The values assigned to the tailings and the terrain parameters in the model, which best resembled the Merriespruit incident, are presented in Table 9.

Table 9. Data for Merriespruit tailings dam failure modeling

Resolution	Density (kg/m^3)	Viscosity	Friction and Roughness	External Pressure	Bounce
5	1100	3	0.0001	1.5	0.1

As Van Niekerk and Viljoen (2005) mentioned, the area in which Merriespruit tailings dam is located experienced a heavy rain fall hours before the dam failure occurred which resulted in the dam's losing its free board. Thus, it was concluded that there was a considerable amount of water added to the tailings behind the dam and therefore, the tailings had characteristics almost similar to water. In addition to the large amount of tailings behind the dam due to its great dimensions, low viscosity also influenced the rather long distance the tailings traveled to come to a rest. Based on this fact, a relatively small value was assigned to viscosity of the tailings behind the Merriespruit tailings dam. Due to the low viscosity of the tailings, the particles could move and slide past one another much easily and therefore could advance up to a farther point than more viscous tailings under the same circumstances. Given that due to the rain a considerable amount of water had been introduced to the retained tailings behind the dam the density of the tailings was not great in value; therefore a value close to the density of water was assigned to the density of tailings in this model.

After the breach was developed, the tailings had flowed out of the impoundment and started to move toward the city. The tailings had traveled a distance of 1960m in approximately 5 minutes which is indicative of its high velocity and also some

properties of the terrain. For the tailings to travel the relatively long distance in such a relatively short time, the roughness and friction of the terrain had to be assigned a considerably small value. Hence, the resistance against the movement of the flow created by the terrain's friction and roughness would not affect the movement as greatly as it did in Tapo Canyon's case.

As the particles in tailings with very low viscosity and density have more tendency to leave the body of the flow and the flow has a more turbulent nature, the value assigned to external pressure was reduced to be slightly greater than the internal pressure. While this value provided the possibility of observing a more turbulent flow, by being slightly greater than the default value assigned to internal pressure (1) it still caused the tailings particles to act different from water particles. Given that there was no data in the literature with regards to bounciness of the terrain, the value assigned to bounciness of the terrain was considerably small.

Figure 31 represents the result of the Merriespruit tailings dam failure modeling which is consisted of the distance the tailings flow has covered over time and its corresponding velocity.

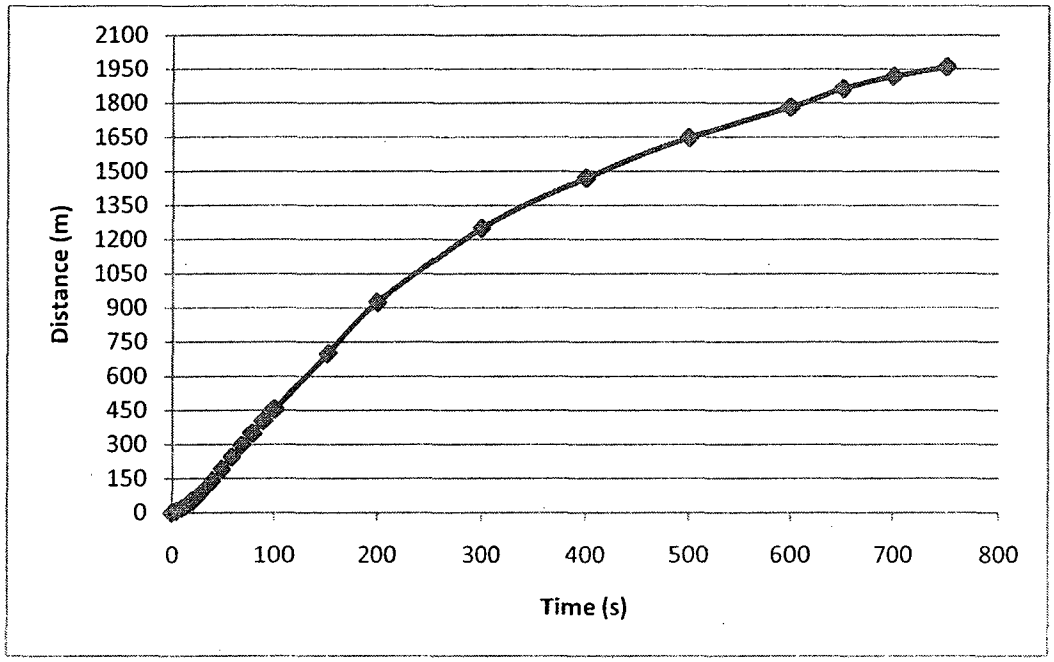

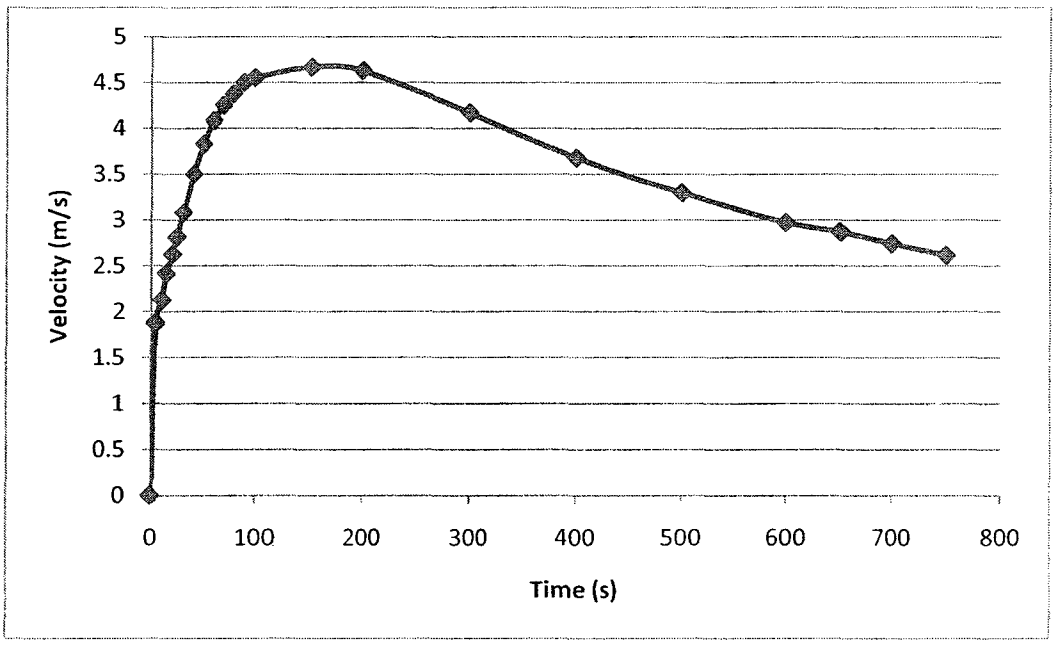

Figure 31. Diagrams showing run out distance and velocity versus time for Merriespruit tailings dam failure modeling

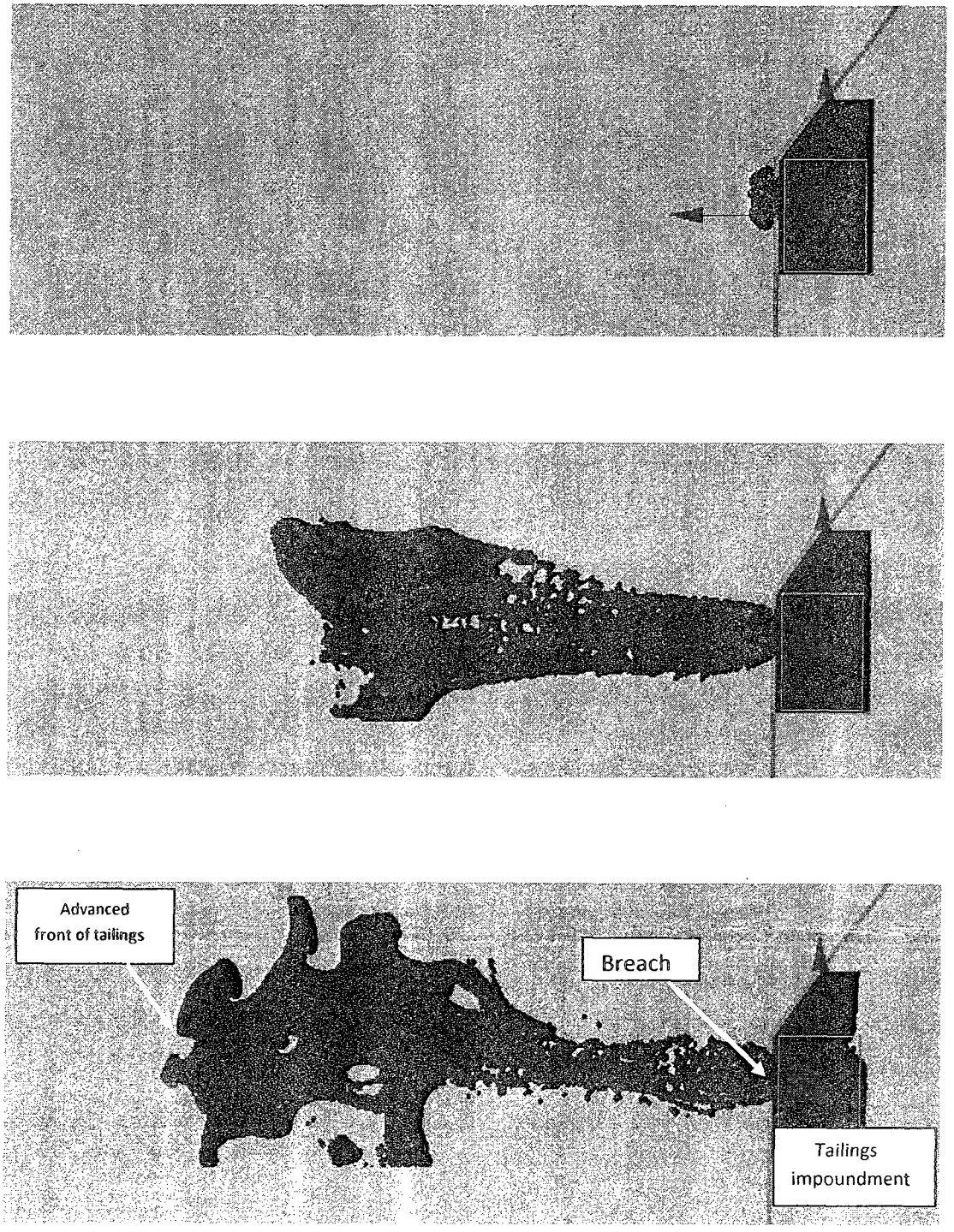

Figure 32. Scenes of modeling Merriespruit tailings dam failure showing tailings at 80m, 1650m and 1960m distance from the dam

According to the diagrams in Figure 31, in the first hundred seconds the tailings flow advanced rapidly and the velocity increased continuously. It was observed that during approximately the first hundred and fifty seconds of the incident, the velocity, due to the head of the tailings behind the dam and under gravity, continued to increase. However, as the time passed, the driving effects of gravity and the head started to decrease the flow speed rapidly, after it had reached a maximum value of approximately 4.7(m/s). The effects of friction and roughness of the terrain and also its irregularities became greater in value than the effects of the driving forces as they started to weaken and therefore; there is a decline in the velocity.

Even though the selected model resembled the physical incident by having approximately the same shape as the physical tailings flow and also reaching the same point as the tailings in the incident, none of the models for Merriespruit reached zero velocity at the end of the simulation. One of the most important reasons for observing such behavior in the model is that most of the factors in modeling the incident and running the simulations were tried to be the closest possible to the real physical properties and factors of the physical incident; however, there were several parameters such as dimensions of the terrain, the head of the retained tailings behind the dam or the values assigned to the tailings properties were decided by trial and error based on the data collected from the calibration tests. Therefore, even the slightest deviation from the exact conditions of the incident might result in a different output.

The second explanation for the behavior of the model is the condition of the imported terrain in the simulation tool:

a. The terrain itself was made by converting a Digital Elevation Model into a triangulated geometry. To be able to have the most accurate result out of the

simulations, having the same irregularities on the terrain as the ones which were present at the time of the incident was necessary. This also applies to the case of Tapo Canyon modeling. The process of building the dam and also mining included stripping some parts of the rocks and the mountains and therefore, the geometry of the area was not exactly represented by the terrain used in the simulations. One other important point on this matter is the quality of the terrain object. In order to be able to locate a mining area or a dam on a DEM the possibility of zooming with regards to its quality is of great importance. In the case of the quality of the map's not permitting zooming in to the area over a specific degree depending on the scale of the selected area, the larger the modeling area is, the fewer details will be presented in the model and placing the model dam in the correct location with the correct dimensions would be more difficult.

b. DEM maps provide the user with only the elevation of a region excluding all the other types of data such as the vegetation and structures. In the incident of Merriespruit tailings dam, the gigantic structure was built approximately three hundred meters to the south of the city and therefore the breach in the wall facing the city caused a colossal amount of tailings flow in the residential area. After the distance between the dam and the city was traveled, there should have been the shape of the city, the buildings and the streets that directed the flow. The width of the streets and the distance between the structures ought to have controlled the speed and the run out distance of the tailings. Moreover, in presence of such factors the width of the flow would have been controlled, the movement of the tailings would have faced more obstacles as a result of which

the tailings would have come to a rest and finally altering the dimensions of the terrain would not have been necessary. However, these factors were not present on the terrain during the modeling process and this fact must have greatly influenced the tailings' shape, run out distance and coming to a rest.

c. The fluid parameters were not as precise as they have to be in the simulation tool. The values assigned to most of the parameters defining the behavior of the fluid, in this case tailings, were not representative of the physical values such parameters might have. This fact necessitated the calibration of the simulation tool and therefore the values corresponding to the parameters had to be assigned by trial and error.

d. The elevation of the terrain had been increased in order to observe the effects of the irregularities on the flow. Therefore, some of the parameters such as the viscosity of the tailings and the friction of the terrain not only had to be set based on the incident but also based on the terrain with new dimensions. Moreover, the change in the scale of the irregularities changed the intensity of the effects of such factors on the tailings flow.

The simulation result for Tapo Canyon shows that the direction of the flow is quite similar to the real incident. The tailings flowed into the valley to the south and the velocity significantly decreased after traveling 180 meters from the dam and before reaching either the creek or the city.

As for the Merriespruit, as it is mentioned in segment 'd' above, the model suffered greatly from the lack of the structures present in the way of the flow. However, the flow showed the tendency toward moving in the same direction as in the incident and later when almost three quarters of the distance was covered due to the same reason the

tailings were spread over the other parts of the city as well. Moreover, the presence of the structures would have confined the tailings to some extent and would have given the tailings a greater depth during the flow and could result in the simulation being finished faster than the current one which would have decreased the run out time in the model to be in the range of the physical run out time. Figures 33 to 35 show the final results of modeling both case studies.

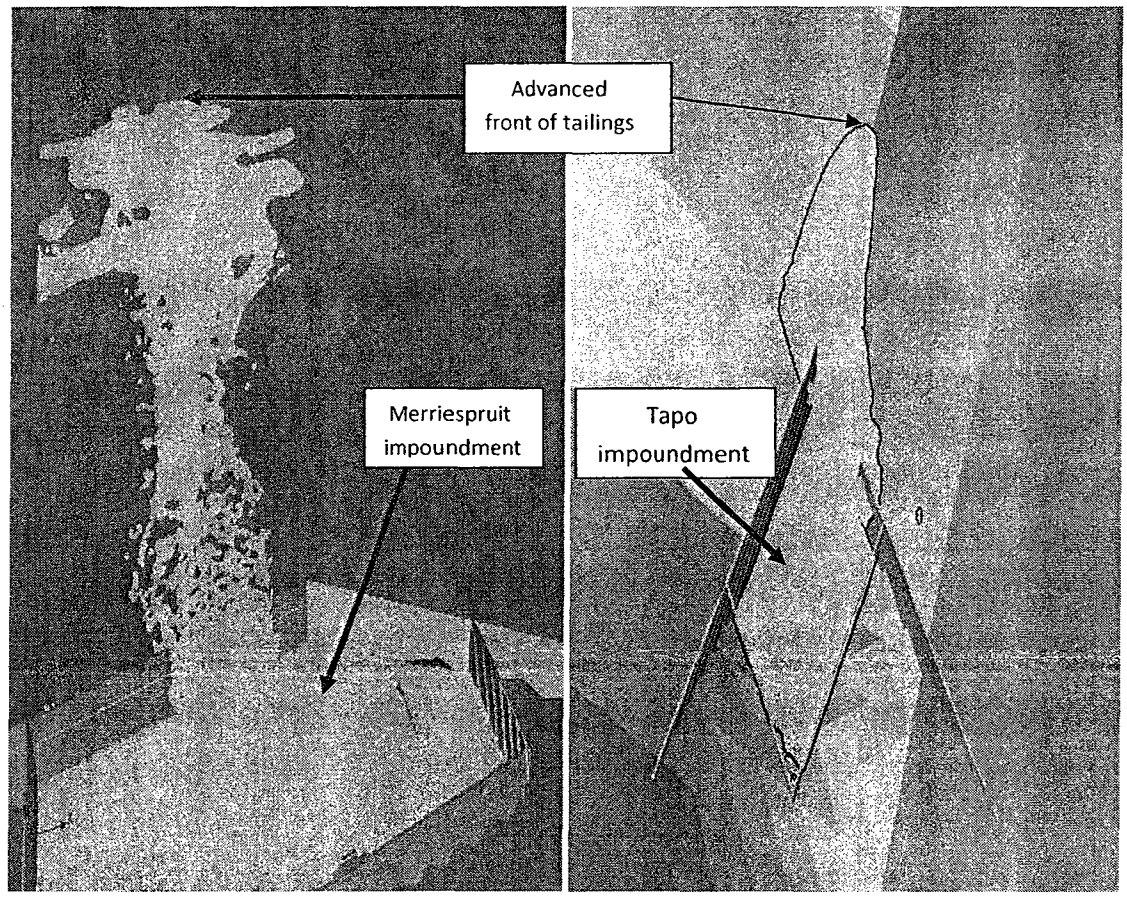

Figure 33. Prespective views of the Merriespruit and Tapo Canyon tailings dams failure model demonstrating the tailings at a 1960m (Merriespruit) and a 180m (Tapo Canyon) distance from the dam

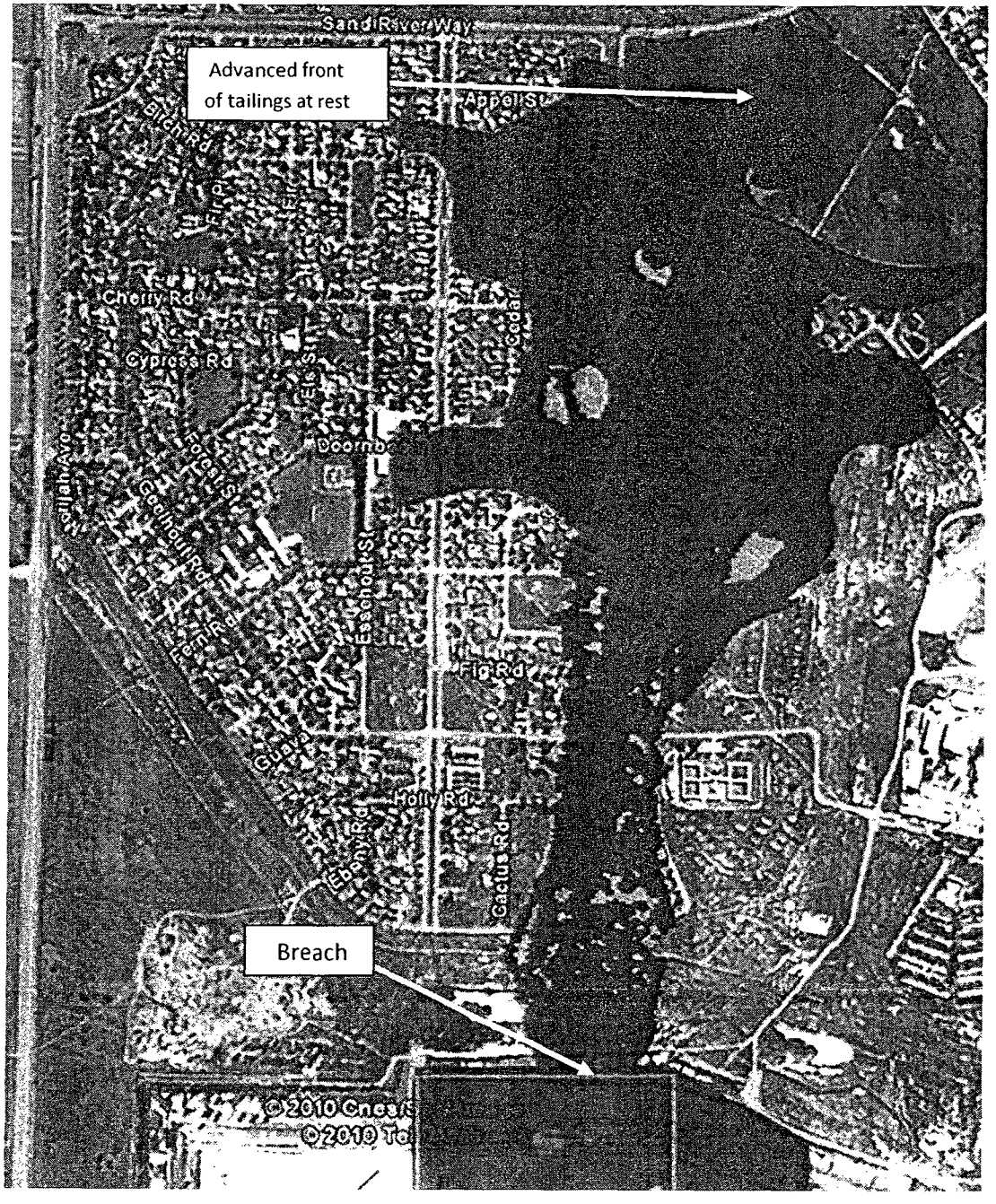

Figure 34. The result of Merriespruit tailings dam failure modeling projected on the map (Google Earth, 2010) of the area

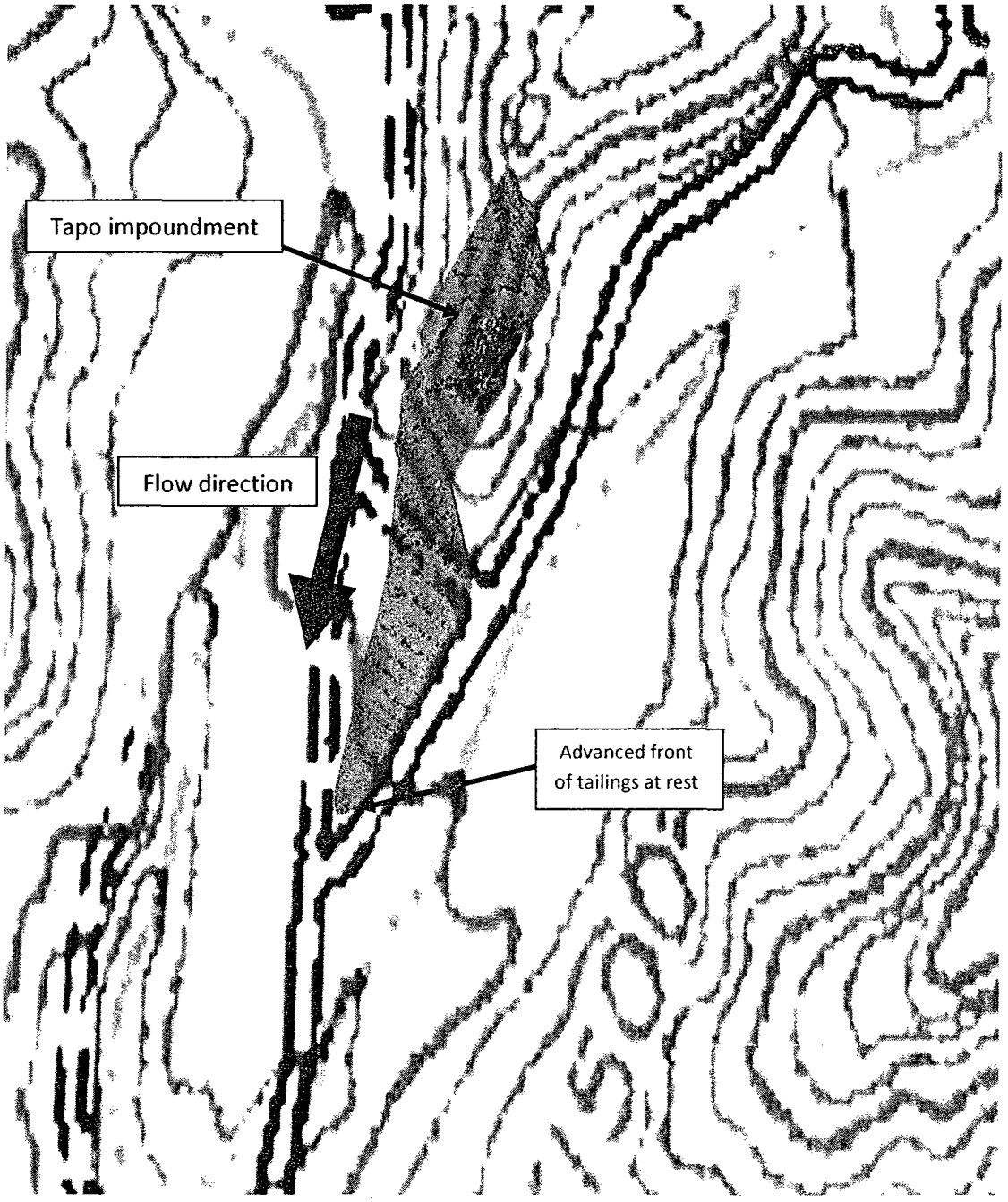

Figure 35. The result of Tapo Canyon tailings dam failure modeling projected on the topographic map of the area

Chapter Seven: Conclusion and Recommendations

Conclusion and Recommendations

7.1 Conclusion

This research focused on using data provided by observations performed by other researchers, such as Van Niekerk and Viljoen (2005), Harder and Stewart (1996), Blight and Fourie (2005) and Crowder (2004), of tailings flow and tailings dam failures to determine the possibility of utilizing a simulation tool to model the flow of tailings as Non-Newtonian fluids in the case of a dam failure. Performing the modeling using Smoothed Particle Hydrodynamics (SPH) method was the basis of this study.

Several simulations based on the laboratory tests performed by Crowder (2004) were performed to calibrate the simulation tool based on tailings flow. The modeling of Crowder's flume test experiments revealed that although the values assigned to a number of the parameters defining the characteristics of the tailings and the plane on which the tailings flow in the simulation tool, are not representative of physical values, a calibration of such kind could be a means to adjust the values with the data provided in the physical incidents.

Having calibrated the simulation tool, Tapo Canyon and Merriespruit tailings dam failures were modeled using Digital Elevation Models (DEMs). Tapo Canyon tailings dam failure included thick, high viscosity, 'paste-like' tailings with a long run out length, whereas the Merriespruit tailings dam failure consisted of thin, low viscosity tailings with a relatively short run out distance. The results of the tests demonstrated

the simulation tool's ability to simulate tailings dam failures. It revealed that even though the general shape of flow and the distance covered resembled the physical incidents to a great extent, there were shortcomings with regards to the velocity of the tailings flow after traveling the expected run out distances. However, these problems can be solved by using more accurate DEMs while sufficient data regarding the tailings' and the terrain's characteristics is provided.

Hence, the results of this study revealed that the idea of modeling the flow of tailings in the case of dam failure by means of the mentioned simulation tool (where sufficient data and accurate maps are provided) has the potential to be performed. It could be used to predict distribution of tailings in the case of a dam failure in order to take necessary actions to reduce the potential damages and losses. Modeling tailings flow could also be considered in the preliminary phase of a tailings dam construction, and based on the results, location of the dam and suitable environmental and urban damage prevention methods can be determined.

This research was performed to provide a new perspective in modeling tailings flow by introducing the application of a simulation tool, thus generating a basis for prevention of future disasters caused by dam failures.

7.2 Recommendations

With regards to the enhancement of modeling tailings flow in the case of dam failures there are a number of issues that require further research:

- Lack of data concerning the tailings dam failures such as the data regarding the characteristics of tailings and the terrain, the volume of tailings retained behind the dam, the volume of the tailings which flowed out of the impoundment through a breach and the viscosity of the tailings, requires further research on the tailings incidents in order for a comprehensive set of data to be provided for the desired incident.
- With the availability of data to create a tailings dam failure model, steps to modeling possible future tailings dam failures (or the possible failure of existing dams) can be taken in order to prevent possible damages and losses.
- The Digital Elevation Models (DEMs) used in the simulation tool as the terrain on which the tailings traveled, were not sufficient to create the incidents' scenes due to their poor quality (when focusing on a specific area) and the absence of structures and vegetation in the model, which had important impacts on the events in the physical incidents.
- In the case of predicting the run out distance of tailings caused by a possible failure of a future dam, studies can be performed on possibility of making changes in the topography of the area in a way to reduce the flow length in order to control the flow.
- The results of modeling the previously occurred tailings dam failures produced by utilizing RealFlow 4 as the simulating tool can be compared to the results produced by other tools such as SPHysics in order to determine the most accurate simulation tool.

References

References

1. Abulnaga, B., Major, K., and Wells, P. (2002). *Selection and sizing of slurry lines, pump boxes, and launders.* In A. Mular, D. Halbe, D. Barrat (Eds.), *Mineral processing plant design, practice, and control: Proceedings.* Colorado, USA: Society for Mining, Metallurgy, and Exploration (SME).

2. Babayean-Koopaei, K., Valentine. E.M., and Ervine, D.A. (2002). Case study on hydraulic performance of Brent reservoir siphon spillway. *Journal of Hydraulic Engineering, 128(6),* 562-567.

3. Barnes, H.A. (1999). The yield stress -a review- everything flows? *Journal of Non-Newtonian Fluid Mechanics, 81,* 133-178.

4. Bartrum, J., Bowler, A., and Butcher, G. (1987). SAG mill operations at Kidston gold mines. *Mineral and Metallurgical Processing, 3(2),* 96-104.

5. Bauer, W.F. (1958). The Monte Carlo method. *Journal of the Society for Industrial and Applied Mathematics, 6(4),* 438-451.

6. Blight, G., and Steffen, K. (1979). Geotechnics of gold mine waste disposal. *Current Geotechnical Practice in Mine Waste Disposal,* ASCE, New York, 1-53.

7. Botella, B.L., Alix, J.M., Mora, L.M., and Stasiuk, M. (2006). *RF4 user guide v1.1.* Spain: Next Limit S.L.

8. Carter, R. A. (2005). Robinson copper re-awakens. *Journal of Engineering and Mining, 206(2),* 26-29.

9. Chalaturnyk, R.J., Scott, J.D., and Ozum, B. (2002). Management of oil sands tailings. *Journal of Petroleum Science and Technology, 20(9),* 1025-1046.

10. Chhabra, R.P. (2007). *Bubbles, drops, and particles in non-newtonian fluids.* U.S.A.: Taylor & Francis Group.

11. Colagrossi, A., and Landrini, M. (2003). Numerical simulation of interfacial flows by smoothed particle hydrodynamics. *Journal of Computational Physics, 191,* 448-475.

12. Crowder, J.J. (2004). *Deposition, consolidation, and strength of a non-plastic tailings paste for surface disposal.* Ph.D. Thesis. Department of Civil Engineering, University of Toronto, Toronto.

13. Crespo, A.J.C., Gomez-Gesteira, M., and Dalrymple, R.A. (2008). Modeling dam break behavior over a wet bed by a SPH technique. *Journal of Waterway, Port, Coastal and Ocean Engineering, 134(6),* 313-320.

14. *Crushing of ore and minerals.* (2008). Retrieved May 25, 2008, from http://www.metsominerals.com/inetMinerals/mm_home.nsf/FR?ReadForm&ATL=/inetMinerals/mm_segments.nsf/WebWID/WTB-041221-2256F-ECCB6

15. Daniel, M.L., Frost, R.L., and Zhu, H.Y. (2008). Laponite supported titania photocatalysts. *Journal of Colloid and Interface Science, 322(1),* 190-195.

16. Davies, M.P. (2001). Impounded mine tailings: what are the failures telling us?. *The Canadian Mining and Metallurgical Bulletin, 94,* 53-59.

17. Dobrzinski, I. (1997). Beverly and Honeymoon uranium prospects. *MESA Journal, 5,* 9-11.

18. El-Shall, H., and Zhang, P. (2004). Process for dewatering and utilization of mining wastes. *Journal of Mineral Engineering, 17,* 269-277.

19. Environment Canada, Mining, Mineral and Metallurgical Processes Division. (1987). *Mine and mill waste water treatment.* Report: EPS2/MM/3.

20. Ergun, L., and Ersayin, S. (2002). Studies on pinched sluice concentration. part 1: the effects of operating variables and sluice geometry on the performance of pinched sluices. *Minerals Engineering, 15,* 423-435.

21. Fournier, B., Rupin, N., Bigerelle, M., Najjar, D., and Iost, A. (2006). Application of the generalized lambda distributions in a statistical process control methodology. *Journal of Process Control, 16,* 1087-1098.

22. Gesteira, M.G., Rogers, B.D., Dalrymple, R.A., Crespo, A.J.C., Narayanaswamy, M. (2008). *User guide for the SPHysics code.* Retrieved February 17, 2009 from http://wiki.manchester.ac.uk/sphysics/index.php/SPHYSICS_Home_Page

23. Graebel, W. P. (2001). *Engineering fluid mechanics, International Student Edition.* New York: Taylor & Francis Publishers.

24. Google Inc. (2009). Google Earth (Version 5.1.3533.1731) [Software]. Retrieved January 28, 2010 from http:/earth.google.com

25. Guth, P. (2009). MICRODEM (Version 2009.8.5.1) [Software]. Retrieved 15 October, 2009 from http://www.usna.edu/Users/oceano/pguth/website/microdem/microdemdown.htm

26. Hamel, J., and Gunderson, J. (1973). Shear strength of Homestake slimes tailings. *Journal of Soil Mechanics and Foundation Division, ASCE, 99(SM5),* 427-431.

27. Harder Jr., L.F., and Stewart, J.P. (1996). Failure of Tapo Canyon tailings dam. *Journal of Performance of Constructed Facilities, 10(3),* 109-114.

28. Headrick, T.C., and Mugdadi, A. (2006). On simulating multivariate non-normal distributions from the generalized lambda distribution. *Computational Statistics & Data Analysis, 50,* 3343-3353.

29. Henriquez, J.A. (2008). *Dynamic imaging and modeling of gold paste tailings flows.* M.A.Sc. Thesis. Department of Civil Engineering, Carlton University, Ottawa.

30. Henriquez, J., and Simms, P. (2009). Dynamic imaging and modeling of multi layer deposition of gold paste tailings. *Journal of Minerals Engineering, 22(2),* 128-139.

31. Kasperski, K.L. (1992). A review of properties and treatment of oil sands tailings. *AOSTRA Journal of Research, 8,* 11-53.

32. Knecht, J., and Patzelt, N. (2004). *High pressure grinding rolls-applications for the platinum industry.* International Platinum Conference 'Platinum Adding Value'. South Africa: The South African Institute of Mining and Metallurgy.

33. Kuang, Y.L., Xie, J.X., and Ou, Z.S. (2004). Properties of a jigging bed analyzed with a high speed analyzer (part 2): A series of motion equations of the water in the jig. *International Journal of Coal Preparation and Utilization, 24(5),* 297-309.

34. Kwak, M. (2004). *Flow characteristics of tailings paste for surface disposal.* M.A.Sc. Thesis. Department of Civil Engineering, University of Toronto, Toronto.

35. Kwak, M., James, D. F., and Klein, K.A. (2005). Flow behaviour of tailings paste for surface disposal. *International Journal of Mineral Processing, 77(3),* 139-153.

36. Larson, R.G. (1999). *The structure and rheology of complex fluids.* U.S.A.: Oxford University Press.

37. Lidell, P.V., and Boger, D.V. (1996). Yield stress measurements with the vane. *Journal of Non-Newtonian Fluid Mechanics, 63(2-3),* 235-261.

38. Liu, K.F., and Mei, C.C. (1989). Slow spreading of a sheet of Bingham fluid on an inclined plane. *Journal of Fluid Mechanics, 207,* 505-529.

39. Lynch, A.J., and Rowland, C.A. (2005). *The history of grinding.* USA: Society for Mining, Metallurgy, and Exploration (SME).

40. MacKinnon, M.D. (1989). Development of the tailings pond at Syncrude's oil sands plant: 1978-1987. *AOSTRA Journal of Research, 5,* 109-133.

41. Matthews, B.W., Fletcher, C.A.J., Partridge, A.C., and Vasquez, S. (1999). Computations of curved free surface water flow on spiral concentrators. *Journal of Hydraulic Engineering, 125(11),* 1126-1139.

42. Monaghan, J.J. (1989). On the problem of penetration in particle methods. *Journal of Computational Physics, 82,* 1-5.

43. Monaghan, J.J. (1994). Simulating free surface flows with SPH. *Journal of Computational Physics, 110,* 399-406.

44. Monaghan, J.J. (1997). SPH and Riemann solvers. *Journal of Computational Physics, 136,* 298-307.

45. Mpofu, P., Addai-Mensah, J., and Ralston, J. (2003). Influence of hydrolysable metal ions on the interfacial chemistry, particle interactions, and dewatering behavior of kaolinite dispersions. *Journal of Colloid and Interface Science, 261(2),* 349-359.

46. NASA. *South Africa* [DEM]. Retrieved November, 11, 2009 from http://www2.jpl.nasa.gov/srtm/

47. Nielsen K., and Kristiansen J. (1995). Can blasting enhance grindability of ores? *IMM Transactions, 104,* 144-148.

48. Pastor, M., Quecedo, M., Panturoiu, C., Gonzalez, E., Fernandez, J., and Mira, P. (1999). *Numerical modeling of debris flows.* Aussios, France: 11th Alert Graduate School.

49. Pettibone, H., and Kealy, C. (1971). Engineering properties of mine tailings. *Journal of Soil Mechanics and Foundation Division, ASCE, 97(SM9),* 1207-1225.

50. Pinarbasi, A., and Imal, M. (2005). Viscous heating effects on the linear stability of Poiseuille flow of an inelastic fluid. *Journal of Non-Newtonian Fluid Mechanics, 127(2-3),* 67-71.

51. Ripley, E., Redman, R., and Maxwell, J. (1978). *Environmental impact of mining in Canada.* Canada: Centre for Resource Studies, Queens University.

52. Rodriguez-Paz, M., and Bonet, J. (2003). A corrected smooth particle hydrodynamics method for the simulation of debris flows. *Journal of Numerical Methods for Partial Differential Equations, 20(1),* 140-163.

53. Rubinstein, J.B. (1995). *Column flotation: processes, design, and practices.* Switzerland: Gordon and Breach Science Publishers.

54. Shatalov, V.V., Fazlullin, M.I., Ramashkevich, R.I., Smirnova, R.N., and Adosik, G.M. (2001). Ecological safety of underground leaching of uranium. *Atomic Energy Journal, 91(6)*, 1009-1015.

55. Simms, P. (2007). On the relation between laboratory flume test and deposition angles of high density tailings. *Proceedings of the Tenth International Seminar on Paste and Thickened Tailings*. Perth, Australia, 329-335.

56. Soderberg, R., and Busch, R. (1977). *Design guide for metal and nonmetal tailings disposal.* U.S. Bureau of Mines Information Circular 8755.

57. Sofra, F., and Boger, D.V. (2001). Slope prediction for thickened tailings and pastes. *Tailings and Mine Waste '01: Proceedings of the 8th International Conference*, Fort Collins, Colorado, U.S.A., 15-18 January 2001. A.A. Balkema, Rotterdam, The Netherlands, 75-83.

58. Sofra, F., and Boger, D.V. (2002a). *Planning*, design and implementation strategy for thickened tailings and pastes. *Proceedings of 9th International Conference on Tailings and Mine Waste 02*, Fort Collins, Colorado, USA 27-30 January, 129-138.

59. Sofra, F., and Boger, D.V. (2002b). Rheology for waste minimization in the minerals industry. *Chemical Engineering Journal, 86(3)*, 319-330.

60. Swegle, J.W., Hicks, D.L., and Attaway, S.W. (1995). Smoothed particle hydrodynamics stability analysis. *Journal of Computational Physics, 116*, 123-134.

61. Taylor, G., Farrington, V., Woods, P., Ring, R., and Molloy, R. (2004). *Review of the environmental impacts of the acid in situ leach uranium mining process.* CSIRO Land and Water Client Report, EPA. Retrieved June 25, 2008, from http://www.epa.sa.gov.au/pdfs/isl_review.pdf

62. Tome, M.F., and McKee, S. (1994). Gensmac: a computational marker and cell method for free surface flows in general domains. *Journal of Computational Physics, 110*, 171-186.

63. U.S. Environmental Protection Agency, Office of Solid Waste, Special Waste Branch. (1994). *Design and evaluation of tailings dams.* Technical Report EPA530-R-94-038. Washington DC: U.S. Environmental Protection Agency.

64. U.S. Environmental Protection Agency. (1995). *Ap42, fifth edition compilation of air pollutant emission factors, volume 1: stationary point and area sources.* Triangle Park, NC: Environmental Protection Agency.

65. U.S. Environmental Protection Agency. (2001). Bunker Hill mine water management remedial investigation/feasibility study. Prepared by CH2M Hill for U.S. Environmental Protection Agency.

66. Van Niekerk, H.J., and Viljoen, M.J. (2005). Causes and consequences of the Merriespruit and other tailings dams failures. *Journal of Land Degradation and Development, 16,* 201-212.

67. Vick, S.G. (1983). *Planning, design, and analysis of tailings dams.* Canada: Wiley-Interscience.

68. Wagener, F. (1997). The Merriespruit slimes dam failure: overview and lessons learnt: technical paper. *Journal of South African Civil Engineering, 39(3),* 11-15.

69. Wahler, W.A., and Associates. (1973). *Analysis of coal refuse dam failure: Middle Fork Buffalo Creek, Saunders, West Virginia.* Washington D.C.: United States department of the Interior, Bureau of Mines.

70. Watson, J.H.P. (1999). High temperature superconducting permanently magnetized discs and rings: prospects for use in magnetic separation. *Journal of Minerals Engineering, 12(3),* 281-290.

71. Wright, P.G. (1977). The variation of viscosity with temperature. *Physics Education, 12,* 323-325.

72. Yuhi, M., and Mei, C.C. (2004). Slow spreading of fluid mud over a conical surface. *Journal of Fluid Mechanics, 519,* 337-358.

Appendix

Table 10. Values assigned to the parameters in Monte Carlo simulations

RESOLUTION				DENSITY				VISCOSITY				FRICTION & ROUGHNESS				DISTANCE	ANGLE OF REPOSE(degree)
Random Number	Mean Value	Deviation	X_i	Random Number	Mean Value	Deviation	X_i	Random Number	Mean Value	Deviation	X_i	Random Number	Mean Value	Deviation	X_i		
0.520888	10	3	10.156	0.340168	4000	500	3795.351	0.197885	22.5	6.25	17.21498	0.160211	0.5	0.15	0.351436	1.3	2.202
0.81136	10	3	12.63816	0.096668	4000	500	3350.053	0.544727	22.5	6.25	23.19708	0.440458	0.5	0.15	0.477691	1.215	2.592
0.421514	10	3	9.410183	0.647322	4000	500	4187.785	0.512595	22.5	6.25	22.69591	0.873735	0.5	0.15	0.671293	1.084	3.168
0.755967	10	3	12.06929	0.912606	4000	500	4678.352	0.691093	22.5	6.25	25.59903	0.79233	0.5	0.15	0.621633	1.119	3.069
0.367619	10	3	8.992417	0.906091	4000	500	4658.176	0.79976	22.5	6.25	27.73222	0.560052	0.5	0.15	0.522501	1.1	3.226
0.382683	10	3	9.110878	0.495297	4000	500	3994.149	0.671745	22.5	6.25	25.26168	0.170025	0.5	0.15	0.357388	1.222	2.811
0.131661	10	3	6.651641	0.72454	4000	500	4296.473	0.17662	22.5	6.25	16.71929	0.334408	0.5	0.15	0.436252	1.29	2.441
0.046538	10	3	4.949955	0.10677	4000	500	3378.774	0.242415	22.5	6.25	18.15673	0.92459	0.5	0.15	0.715596	1.113	3.086
0.11988	10	3	6.479326	0.978125	4000	500	5012.416	0.342172	22.5	6.25	19.97586	0.148593	0.5	0.15	0.344065	1.2	2.624
0.416004	10	3	9.368153	0.888456	4000	500	4608.344	0.614068	22.5	6.25	24.29951	0.540366	0.5	0.15	0.515093	1.14	3.013
0.140813	10	3	6.771396	0.720199	4000	500	4290.016	0.094102	22.5	6.25	14.28007	0.306851	0.5	0.15	0.42475	1.4	2.127
0.164646	10	3	7.083094	0.810696	4000	500	4438.464	0.766908	22.5	6.25	27.03153	0.582977	0.5	0.15	0.531203	0.942	3.887
0.109402	10	3	6.315559	0.000615	4000	500	2402.296	0.251308	22.5	6.25	18.3326	0.742283	0.5	0.15	0.597026	1.269	2.707
0.778253	10	3	12.28792	0.606981	4000	500	4134.78	0.354106	22.5	6.25	20.17656	0.584348	0.5	0.15	0.531727	1.28	2.237
0.934168	10	3	14.52744	0.006445	4000	500	2752.5	0.394829	22.5	6.25	20.84447	0.606695	0.5	0.15	0.540323	1.342	2.347
0.105551	10	3	6.252503	0.215104	4000	500	3607.412	0.79709	22.5	6.25	27.67281	0.304	0.5	0.15	0.423534	1.09	3.255
0.991303	10	3	17.16304	0.837047	4000	500	4489.591	0.682028	22.5	6.25	25.43987	0.007942	0.5	0.15	0.136894	1.582	1.774
0.928611	10	3	14.39966	0.559712	4000	500	4074.577	0.598234	22.5	6.25	24.0439	0.13319	0.5	0.15	0.33366	1.33	2.368
0.825498	10	3	12.79942	0.769445	4000	500	4366.677	0.748585	22.5	6.25	26.66531	0.78774	0.5	0.15	0.619242	1.15	2.937
0.38697	10	3	9.14432	0.433495	4000	500	3916.861	0.064118	22.5	6.25	12.98219	0.700237	0.5	0.15	0.578281	1.38	2.116
0.846975	10	3	13.06157	0.126622	4000	500	3429.89	0.88502	22.5	6.25	29.9915	0.174531	0.5	0.15	0.360046	1.163	2.953
0.97922	10	3	16.13942	0.840596	4000	500	4496.882	0.378688	22.5	6.25	20.58253	0.707995	0.5	0.15	0.581638	1.312	2.313
0.204014	10	3	7.528774	0.262095	4000	500	3683.316	0.281153	22.5	6.25	18.89981	0.549102	0.5	0.15	0.518375	1.205	2.851
0.025184	10	3	4.10643	0.58816	4000	500	4110.616	0.245811	22.5	6.25	18.22429	0.488115	0.5	0.15	0.495563	1.26	2.726
0.330916	10	3	8.696344	0.695206	4000	500	4253.755	0.291869	22.5	6.25	19.09597	0.083278	0.5	0.15	0.292493	1.436	2.153
0.734157	10	3	11.86578	0.798489	4000	500	4416.31	0.667886	22.5	6.25	25.19542	0.257559	0.5	0.15	0.402901	1.206	2.848
0.57026	10	3	10.52729	0.3109	4000	500	3754.891	0.768605	22.5	6.25	27.06625	0.140075	0.5	0.15	0.338408	1.175	2.874
0.542483	10	3	10.31775	0.426024	4000	500	3907.416	0.168389	22.5	6.25	16.51718	0.747739	0.5	0.15	0.59957	1.34	2.222
0.072892	10	3	5.633562	0.739332	4000	500	4318.872	0.812412	22.5	6.25	28.02061	0.682029	0.5	0.15	0.570557	0.972	3.943
0.414811	10	3	9.359034	0.3853	4000	500	3855.217	0.359194	22.5	6.25	20.26137	0.064516	0.5	0.15	0.272054	1.376	2.123